# STUDY ON ELECTROCHEMICALLY TREATED CARBON ELECTRODES FOR PHENOL, α-NAPHTHOL AND THEIR SELECTED DERIVATIVES DETECTION

BY

**MUHAMMAD AZEEM AKBAR RANA**

A Dissertation Presented to the

DEANSHIP OF GRADUATE STUDIES

**KING FAHD UNIVERSITY OF PETROLEUM & MINERALS**

DHAHRAN, SAUDI ARABIA

In Partial Fulfillment of the

Requirements for the Degree of

# DOCTOR OF PHILOSOPHY

In

**CHEMISTRY**

**DECEMBER 2017**

KING FAHD UNIVERSITY OF PETROLEUM & MINERALS

DHAHRAN- 31261, SAUDI ARABIA

**DEANSHIP OF GRADUATE STUDIES**

This dissertation, written by **Muhammad Azeem Akbar Rana** under the direction of his dissertation advisor and approved by his dissertation committee, has been presented and accepted by the Dean of Graduate Studies, in partial fulfillment of the requirements for the degree of **DOCTOR OF PHILOSOPHY IN CHEMISTRY.**

Dr. Abdel-Nasser Kawde
(Advisor)

31/12/2018

Dr. Abdulaziz A. Al-Saadi
Department Chairman

Dr. Anvarhusein A. Isab
(Member)

Dr. Salam A. Zummo
Dean of Graduate Studies

Dr. Basheer Chanbasha
(Member)

7/2/18

Date

Dr. M. A. Morsy
(Member)

Dr. Saviour A. Umoren
(Member)

Dedicated to my beloved parents who always prays for my success in life.

Dedicated to my beloved brothers, wife, and son.

# ACKNOWLEDGMENTS

All hymns and thanks to Allah Almighty, the most gracious, the merciful and worthy of all praises, who guides the way and gives the courage to complete the tasks. All respect and love for Hazrat Muhammad (Peace be Upon Him) who enabled us to recognize our creator and to understand philosophy of the Life.

This acknowledgement is not simply an expression of formal duty, but all the emotional associations I have with the persons who have helped me, during my research and make this report presentable.

I am grateful to King Fahd University of Petroleum and Minerals for offering me scholarship for my Ph.D. Studies. I would like to acknowledge the noble guidance and skilled advice of chairman, Department of Chemistry. It is my foremost obligation to express my sincere gratitude to my respected, highly learned, gracious and revered research supervisor Dr. Abdel Nasser Kawde, who contributed significantly to the scholarly merit of this work and helped me to formulate my research ideas and critically reviewed my experimental designs and results. I would like to express my special gratitude to my Ph.D. committee members Dr. Anvarhusein A. Isab, Dr. Basheer Chanbasha, Dr. M. A. Morsy and Dr. Saviour A. Umoren for their extended suggestions whenever needed. I would also like to offer my admiration to all respected faculty members and lab fellow who always remain available for all sort of support.

Finally, I owe appreciations to the individuals who mean a lot to me, my Mother and Father for their altruistic love, care and sacrifice to mold my life. I would never be able to pay back the love and tenderness lavished upon by my parents. It's my fortune to appreciatively acknowledge the support of my wife for her continued and infallible love, support, and understanding during my pursuit of Ph.D. degree that made the completion of dissertation possible. I recognize my little boy Ibrahim with gratitude for showing forbearance during my dissertation write up and enduring my ignorance. I believe myself the luckiest individual in the world to have such an adorable and caring family with unconditional support.

Muhammad Azeem Akbar Rana

# CONTENTS

# LIST OF TABLES

# LIST OF FIGURES

# LIST OF ABBREVIATIONS

| | | |
|---|---|---|
| EIS | : | Electrochemical impedance spectroscopy |
| GCE | : | Glassy carbon electrode |
| GCE-ox | : | Oxidized glassy carbon electrode |
| PYR | : | Pyrogallol |
| SPCE | : | Screen-printed carbon electrode |
| HQ | : | Hydroquinone |
| CA | : | Catechol |
| NPPy/SDS | : | Nano polypyrrole-sodium dodecyl sulfate film |
| GPE | : | Graphite pencil electrode |
| α-NAP | : | α-Naphthol |
| PGPE | : | Pretreated graphite pencil electrode |
| DNA | : | Deoxyribose nucleic acid |
| EDCs | : | Endocrine disrupting compounds |
| BDDE | : | Boron doped diamond electrode |
| ET | : | Estrone |
| ABP | : | Aminobiphenyl |
| AN | : | Aminonaphthalene |

| | | |
|---|---|---|
| HPLC | : | High performance liquid chromatography |
| BD-NCD | : | Boon doped nanocrystalline diamond |
| XPS | : | X-ray photoelectron spectroscopy |
| 4-NP | : | 4-Nitrophenol |
| CV | : | Cyclic voltammetry |
| pCGPE | : | Pre-charged graphite pencil electrode |
| S/N | : | Signal to noise ratio |
| PGPE-NHNA | : | NaOH and sodium acetate pretreated graphite pencil electrode |
| 4-CNP | : | 4-Chloro-1-Naphthol |
| AuNP | : | Gold nanoparticle |
| USEPA | : | United State Environmental Protection Agency |
| SWV | : | Square wave voltammetry |
| PB | : | Phosphate buffer |
| PBS | : | Phosphate buffer saline |
| PAH | : | Polyaromatic hydrocarbon |
| TLC | : | Thin layer chromatography |
| MWCNT | : | Multi walled carbon nanotubes |

| | | |
|---|---|---|
| EDTA | : | Ethylenediaminetetraacetic acid |
| AB | : | Acetate buffer |
| CPE | : | Carbon paste electrode |
| LSASV | : | Linear sweep anodic stripping voltammetry |
| SWASV | : | Square wave anodic stripping voltammetry |
| Ep | : | Peak potential |
| ip | : | Peak current |
| RSD | : | Relative standard deviation |
| PtNP | : | Platinum nanoparticles |
| PAO | : | Poly (acridine orange) |
| HIF | : | High-index facet |
| HNCMS | : | Hollow nitrogen-doped carbon microsphere hybrids |
| β-CD | : | β-cyclodextrin |
| PtNPs/GNs | : | Platinum Nanoparticles/Graphene Nanohybrids |
| PGPE-PH | : | KOH pretreated graphite pencil electrode |
| PGPE-HA | : | HCl pretreated graphite pencil electrode |
| PGPE-SA | : | $H_2SO_4$ pretreated graphite pencil electrode |

PGPE-NH : NaOH pretreated graphite pencil electrode

PGPE-NA : $CH_3COONa$ pretreated graphite pencil electrode

PGPE-$N_2P$ : $Na_2HPO_4$ pretreated graphite pencil electrode

PGPE-NP : $NaH_2PO_4$ pretreated graphite pencil electrode

PGPE-PH$N_2P$ : KOH and $Na_2HPO_4$ pretreated graphite pencil electrode

PGPE-PHNP : KOH and $NaH_2PO_4$ pretreated graphite pencil electrode

PGPE-PHNA : KOH and $CH_3COONa$ pretreated graphite pencil electrode

PGPE-LP : $LiClO_4$ pretreated graphite pencil electrode

PGPE-PBS : Phosphate buffer saline pretreated graphite pencil electrode

PGPE-NHLP : NaOH and $LiClO_4$ pretreated graphite pencil electrode

PGPE-NHPBS: NaOH and Phosphate buffer saline pretreated graphite pencil electrode

PGPE-NHNA : NaOH and $CH_3COONa$ pretreated graphite pencil electrode

NiDMG : Nickel(II) dimethylglyoxime

RGO : Reduced graphene oxide

ITO : Indium tin oxide

AA : Ascorbic acid

# ABSTRACT

Full Name : Muhammad Azeem Akbar Rana

Dissertation Title : Study on electrochemically treated carbon electrodes for phenol, α-naphthol and their selected derivatives detection

Major Field : Chemistry

Date of Degree : December 2017

Phenol, α-naphthol and their derivatives are compounds that are omnipresent to our surroundings and categorized as environmental pollutant. Higher concentration of these contaminants regarded to be a major environmental and occupational health problem. The quantification of these toxins is crucial for analysis of biochemical operation as well as for development of analytical instruments used in water quality, environmental regulation or laboratories. Direct oxidation of phenols and naphthols at the electrode surface leads to fouling of electrode due to the formation of polymers on its surface. Novel electrochemically treated carbon electrodes were utilized to detect target species and eliminate the drawbacks of the conventional electrodes, such as low sensitivity, poor selectivity, and passivation of electrode surface. Electrochemical pretreatment offers an acceptable alternate method to modify the surface of carbon electrodes, rather than use of complex modification methods. The electrochemical pretreatment process produces such transducers that display undistorted, well-define and reproducible signals. The pretreated carbon electrodes also resolve the signal of close peaks with good signal-to-background characteristics as compared to untreated and modified electrodes. The present work reports the preparation of pretreated electrodes from graphite pencil electrode. For characterization of developed surfaces, such as capacitance measurement, electroactive area, and electron transfer ability; cyclic voltammetry and electrochemical impedance spectroscopy (EIS) were used. Fundamental studies have been done to understand the changes occurring during the electrochemical treatment and the effects of nature of supporting electrolytes on the detection capability of electrodes. The inexpensive and simple electrodes presented fantabulous sensibility, selectivity, duplicability, broad linear range and staggeringly low limit of detection.

# ملخص الرسالة

**الاسم الكامل**: محمد عظيم اكبر رنا

**عنوان الرسالة: دراسة عن أقطاب الكربون المعالجة كهروكيميائياً وإستخدامها في تقدير الفينول، الفا-نافثول ومشتقاتهما المختارة.**

**التخصص: كيمياء**

**تاريخ الدرجة العلمية: ديسمبر 2017**

الفينول، الفا-نافثول ومشتقاتهما هي مركبات منتشرة في كل مكان لمحيطنا وصُنفت على أنها ملوثات بيئية. التركيز العالي من هذه الملوثات حيث أن مشكلة صحية بيئية ومهنية رئيسية. القياس الكمي لهذه السموم هو أمر حاسم لتحليلات عملية كيمو-حيوية وكذلك لتطوير الأجهزة التحليلية المستخدمة في نوعية المياه، الأنظمة البيئية أو المختبرات. ان الأكسدة المباشرة من الفينولات والنافثولات على سطح القطب يؤدي إلى اتساخ القطب بسبب تشكيل البوليمرات على سطحه. تم استخدام أقطاب كربونية جديدة معالجة كهروكيميائياً للكشف عن الأنواع المستهدفة والقضاء على السلبيات من الأقطاب التقليدية، مثل الحساسية المنخفضة ، فقر الانتقائية، والكساء من سطح القطب. المعالجة الكهروكيميائية تقدم طريقة بديلة مقبولة لتعديل سطح أقطاب الكربون، بدلا من استخدام طرق التعديل المعقدة. عملية المعالجة الكهروكيميائية تنتج مثل هذه المحولات التي تعرض إشارات غير مشوهة، واضحة المعالم وقابلة للتكرار. الأقطاب الكربون سابقة المعالجة أيضاً حل إشارة القمم القريبة بخصائص جيدة إشارة-إلي-الخلفية مقارنةً مع الأقطاب غير المعالجة والمعدلة. العمل الحالي تقارير إعداد أقطاب معالجة مسبقاً من قلم رصاص الجرافيت. لتوصيف الأسطح المتقدمة، مثل قياس السعة، المنطقة الكهربائية النشطة، و قدرة نقل الإلكترون، فولتامتري الدائري ومطيافية المعاوقة الكهروكيميائية تم استخدامها. أجريت دراسات أساسية لفهم التغييرات التي تحدث أثناء المعالجة الكهروكيميائية وآثار طبيعة دعم الشوارد على القدرة على الكشف من الأقطاب. تقوم الدراسة الحالية قطب بسيط وغير المكلفة مع مزيد من الحساسية، الانتقائية، إعادة إنتاج، نطاق خطي واسع والحد من الكشف بشكل مذهل.

# Chapter 1

## Introduction

From last five decades till now electrochemistry is mainly based on electrodes made up of solid materials. Major characteristics required for a material to be selected as electrode includes; high electrical conductivity, electrochemical stability, fast electron transfer and show reproducible electrical and chemical features [1]. Electrodes showing low background current and fast electron transfer rate with highly reproducible physiochemical characteristics are denoted as ‘active’ or ‘electrode in activated state’. The electrode can be activated by targeting its surface morphology and structure at the molecular scale in the process of pretreatment [2]. As a result, required characteristics, i.e. fast reaction kinetics and low background current can be achieved. There are various factors that influence the reaction kinetics like nature, surface purity, electrical features and microstructure of electrode material [3–5] The nature of particular redox system determines the extent of the effect produced by factors affecting reaction kinetics.

The electrode cannot be used directly for trace analysis of any sort of analyte as it is received from manufacturer or lab storage because its surface interacts with a different type of matter and air. The particulate matter from surroundings or leftover of the redox system under study block the active sites of the transducer. While the interaction of air under ambient or potential induced conditions with electrode materials, especially carbon electrodes, oxidize the surface. Oxidized surface shows a great affinity towards polar molecular adsorption due to the presence of polar oxygen-containing functional groups and higher wettability [6]. Consequently, electrode completely or partially blocked and

show low reaction rate and less reproducible results for a specific analyte. If analyte under study is not removed properly from the electrode surface, it can make its way to next measurement and affect the results. Due to these reasons pretreatment of the electrode surface is very important. Pretreatment not only cleans the surface of the electrode but also change the surface chemistry and microstructure that in long run affect the sensitivity of electrode towards target analyte [7].

## 1.1 Techniques for the pretreatment of carbon electrodes

Various techniques have been established to activate the electrode through pretreatment and get highly reproducible and sensitive results. As carbon-based electrodes are widely used for electroanalysis, that is why our focus will remain limited to the techniques utilized for pretreatment of carbon material based electrodes.

1.1.1 Mechanical polishing and solvent cleaning

1.1.2 Vacuum heat treatment

1.1.3 Laser-based thermal treatment

1.1.4 Microwave plasma treatment

1.1.5 Radio-frequency plasma treatment

1.1.6 Electrochemical pretreatment

### 1.1.1 Mechanical polishing and solvent cleaning

Before any sort of pretreatment, the mechanical polishing is done to remove adsorbed particles from the surroundings or leftovers of the past use to get a fresh surface. Usually, mechanical polishing is not an independent way of pretreatment but the first step of any pretreatment procedure [8,9]. Another simple way that usually utilized in conjunction with mechanical polishing is solvent cleaning. In this pretreatment process

one or more solvents are applied for 20-30 min. Consequently, contaminants are removed by dissolution or desorption of contaminants from the surface of the electrode. For this purpose, highly pure organic solvent like dichloromethane, acetonitrile, isopropanol, toluene, etc. can be used [10].

### 1.1.2 Vacuum heat pretreatment

Heat treatment is done under high vacuum ($10^{-6}$ torr) or in the presence of the inert gas to remove the contaminants and chemically bind oxygen chemically from the surface. Oxygen is present in the form of functional groups, that is why for the decomposition of these oxygen-containing functional groups on the surface of electrode minimum of 500$^{o}$ C temperature is required. The electrode is treated with heat for 10-30 min to desorb all the contaminants and oxygen to get a clean surface [11,12]. Some precautions are needed while doing heat treatment of electrode.

- Heat treatment should be done under vacuum or in the presence of inert gas because the presence of oxygen can oxidize and corrode the surface.
- Temperature control is very crucial because temperature lower than 500$^{o}$ C could not decompose the oxygen-containing functional groups as a result active site will not vacant and electrochemical measurements will not show reproducible and sensitive signals for the target analyte.
- Cleaned surface of the electrode will deactivate if shortly come into contact with oxygen present in surroundings, that is why the cleaned surface of the electrode must be used for the electrochemical assay as soon as possible after heat treatment to get best outcomes.

### 1.1.3 Laser pretreatment

Laser treatment is another way to pretreat the electrode surface by directing highly intense and short pulse of laser light. If the power density of the incident pulse is lower than 50 MW $cm^{-2}$ then no structural changes occur like heat treatment surface temperature of the electrode increase. Consequently electrode surface is activated due to the remotion of adsorbed toxins and chemisorbed oxygen from the electrode surface. On the other hand, incident power density 50 MW $cm^{-2}$ or more change the microstructure and produce new active edge plane sites. This process not only cleans the surface to expose the existing active sites of the electrode but also create new active sites, depending on the applied conditions [13].

### 1.1.4 Microwave plasma pretreatment

To ensure removal of oxygen-containing functional groups, a pretreatment technique very similar to vacuum heat treatment is employed called microwave plasma treatment or hydrogen plasma treatment. Atomic hydrogen present in plasma interact with the electrode surface and replace the chemisorbed terminal oxygen. This process not only removes the oxygen from electrode surface but also the formation of strong C – H bond stabilized the surface and minimize the chance of oxidation when it comes in contact with environmental oxygen. Consequently, the oxygen-depleted surface is obtained [14].

### 1.1.5 Radio frequency plasma pretreatment

Another strategy to remove the oxygen from bare or chemically modified electrode surface is by exposing the surface to the argon plasma at very low pressure, i.e. 0.1 Torr. The plasma is produced by passing the argon gas through a high-energy radio

frequency coil. In this process, highly energetic argon ions are sputtered on the electrode surface that results in the removal of oxygen. This technique also roughened the surface and oxygen content also decrease. To produce plasma oxygen can also be used, when this plasma is directed to electrode surface oxygen is introduced on the electrode. Factors like radio frequency power, the pressure of the gas, nature of gas and pretreatment time determine the resultant nature of electrode [15].

### 1.1.6 Electrochemical pretreatment

As compared to the pretreatment techniques discussed above, electrochemical pretreatment shows most dramatic effect on the surface microstructure and features of electrodes. Electrochemical pretreatment not only cleans the electrode surface but also produce new active edge plane sites [16]. The newly produced active sites carry a high density of electronic states and a large amount of oxygen-containing functional groups. The high density of the electronic states shows the presence of unique double-layer structure, that causes a huge potential drop and quick electron transfer kinetics [17,18]. On the other hand, if suitable oxygen-containing functional groups for a redox system is incorporated on the surface of the electrode, they act as a catalyst for the rate of electron transfer. During this process, anodic or cathodic (fixed or cyclic) potential is applied to a certain limit of time in the presence of a suitable electrolyte. The extent to which pretreatment effect electrode surface depends on the quantity of charge passed at the particular potential [19–21].

The mechanism of formation of edge plane active site during electrochemical pretreatment can be divided into two major steps [22,23];

i. Firstly, graphene sheets got separated due to penetration of molecules and ions of solvents between the layer of the electrode structure.

ii. Secondly, due to intercalation of ions microstructure strains started to increase to such an extent that fracture graphene sheet exposing new edge planes.

## 1.2 Electrochemical pretreatment parameters for carbon electrodes

The parameters that poses prominent effect on the surface of carbon electrodes are as follows.

### 1.2.1 Nature of pretreatment solution

Nature of solvent or electrolytes and ionic strength of solution used for pretreatment play a vital part in ion penetrations and separation of graphene sheet. The outstanding increase is observed in reaction kinetics when the pretreatment of the carbon electrode surface is done in aqueous media [24,25]. Pretreatment of carbon electrode surface resulted in the introduction of electroactive oxygen-containing functional groups. The specificity and ultra-sensitivity of electrode surface majorly depend on the nature of solution employed for the pretreatment of carbon electrode surfaces [26]. Conventionally available electrodes display poor electron transfer kinetics and absorption reaction, while electrochemical pretreatment with suitable solution dramatically increases the signal for the target analytes and selectivity of the electrode surface [27,28].

### 1.2.2 Effect of pH on pretreated carbon electrodes

The rate of electron transfer for a particular redox system directly correlated with the number of oxygen-containing functional groups on the surface of the pretreated electrode. The oxygen-containing functional groups provide active sites on the surface of the electrode for particular redox system and also help proton or electron exchanging for

redox system. Consequently, reaction kinetics are affected in a positive way. The oxygen-containing functional groups also increase the density of electronic states and also impact the electric double layer. Interaction of water with edge plane site which attaches oxygen-containing functional group is different from hydrophobic basal plane [19,20]. Some of the functional groups formed during electrochemical pretreatment did not show any electrochemical activity, due to their acidic nature the ionize to release protons. As a result, the surface of electrode shows pH-dependent electrochemical behavior and carry a large amount of charge. The carboxylic acid is an example of an acidic oxygen-containing functional group that deprotonates and increase the -ve charge on the surface of electrode [29].

### 1.2.3 Potential applied for pretreatment

There are various well-developed methods for electrochemical pretreatment of electrode surface involving galvanostatic, potentiostatic and potentiodynamic methods. For the electrochemical pretreatment controlled potential should be applied according to the requirement of redox system under study because it plays crucial role in determining structural features and amount of oxygen-containing functional groups, e.g. if anodic pretreatment is done under applied potential below 1.0 V results in mild pretreatment and cause small variations in microstructure, whereas treatment is done at applied potential higher than 1.5 V cause major changes in electrode surface structure and large amount of oxygen-containing groups incorporated [30–32]. Electro-oxidation or electro-reduction pretreatment have their own advantages and disadvantages for a particular analyte. Thorough oxidation of glassy carbon electrode ensued in the establishment of tightly condensed film of oxide, that revealed inferior sensitivity but greater stability for

epinephrine. Whereas a permeable oxide film is raised when a reduction potential is employed for pretreatment of the glassy carbon electrode. In contrast with the outcomes obtained from the oxidized surface, the reduced porous film electrode present greater sensitivity for epinephrine but low stability and could not attenuate the interferences from ascorbic acid. To overcome the disadvantages and utilize the salient features of the pretreated surface, partially reduced GCE-ox surface was designed by monitoring the reduction time and potential. The resultant GCE-ox-red surface exhibited advanced sensitivity, selectivity, and remarkable stability when employed for recognition of epinephrine [33].

## 1.3 Pretreated carbon electrodes for detection of phenol, α-naphthol, and other water pollutants

A variety of chemical compounds are used for different purposes including industrial production, food processing or healthcare needs. Due to vast applications, there has been a growing interest to study their route in our environment and effect on living organisms. The contamination of water bodies by these widespread pollutants are of great concern. These pollutants include phenols, naphthol, metal ions and micro-organic contaminants. Due to their toxic nature lot of efforts have been made to detect them at trace level in order to save the water resources and their ecosystem.

### 1.3.1 Phenol and derivatives

The Pyrogallol (PYR) is phenol derivative showing antioxidant activity and majorly used in plastics, cosmetics, and pharmaceuticals. Due to its widespread use also expose the living organisms to these toxic compounds. To closely monitor the trace amount of PYR in environmental water samples pretreated screen-printed carbon

electrode (SPCE) was employed. The anodically activated SPCE displayed higher resistance towards the interferences ranging from inorganic salts to phenol derivatives [34]. In another work, two positional isomers of dihydroxybenzene Hydroquinone (HQ) and catechol (CA) were detected simultaneously by anodically pretreated SPCE [35]. The SPCE pretreated potentiodynamically utilized for simultaneous detection of isomers of aminophenol. Pretreatment enhances the catalytic activity of the SPCE by producing a positive effect on the heterogeneous electron transfer rate [36]. The modified surface of a carbon electrode can also be selectively activated for analytes. A nano polypyrrole-sodium dodecyl sulfate film (NPPy/SDS) was deposited on the surface of GCE. Electrochemical pretreatment of the modified electrode was done in 0.1 M phosphate buffer solution to enhance the electrocatalytic activity of electrode surface towards target analytes. Surface characterization revealed the appearance of nano-cracks, a decrease of hydrophilic character and higher electron transfer rate of NPPy/SDS polymer film after pretreatment [37].

### 1.3.2 α-Naphthol and derivatives

In our recent work, disposable graphite pencil electrode (GPE) was pretreated in NaOH aqueous solution to get a transducer with good sensitivity for α-NAP. The higher electrocatalytic activity of the pretreated GPE was attributed to the introduction of oxygen-containing functional groups or the graphite oxide film formed during pretreatment. The PGPE displayed linear response between 0.01 – 2.0 μM with a detection limit of 1.5 nM. The developed PGPE was successfully applied for detection of α-NAP in real water samples [26]. Zhao et al. used anodically activated GCE as a platform for the acid-denatured DNA to get DNA/GCE(ox). The modified sensor

dramatically enhances the peak current for α-naphthol (α-NAP) by ten folds. There was also a prominent peak for oxidation of guanine and adenine residue. However, it decreases by increasing the concentration of α-NAP. The DNA based sensor proved to be very sensitive with 5 nM limit of detection [38].

### 1.3.3 Electrochemical detection of endocrine disrupting compounds

The endocrine disrupting compounds (EDCs) enter the water bodies through human activities such as water treatment plants and agricultural activities. High level of exposure to EDCs resulted in complexities in development and reproduction. A cathodically polarized BDDE was formulated to detect the Estrone (ET) in environmental samples [39]. The genotoxic Aminobiphenyl (ABP) and Aminonaphthalene (AN) are difficult to detect simultaneously by utilizing electrochemical methodology. The anodically activated BDDE employed for the 1-AN, 2-AN, 2-ABP and 4-ABP in a quaternary solution. the analytes first pass through HPLC for separation and then anodically pretreated BDDE act as a detector. The proposed HPLC-BDDE method was successfully applied to azo dyes with detection limit up to nanomolar level [40]. Nurhayati and coworkers applied dynamic electrochemical activation to boron-doped nanocrystalline diamond BD-NCD electrode for simultaneous detection of Pb (II), Cu (II) and Hg (II) in aqueous samples. The surface characterization of BD-NCD by XPS revealed that pretreatment resulted in cleaner surface and higher electrocatalytic activity towards the individual or tertiary solution of metals [41].

**Table 1.1. Electrochemically treated electrodes for detection of water pollutants**

| Sr# | Electrode | Treatment medium/pH | Treatment potential (V) | Treatment time/cycles | Analyte | Technique | Medium/pH | Linear range (µM) | LOQ (µM) | LOD (µM) | Application | Ref. |
|---|---|---|---|---|---|---|---|---|---|---|---|---|
| 1. | DNA/GCE(ox) | 0.1 M PBS/ pH 5.0 | +1.75 | 300 sec | α-NAP | DPV | 0.1 M AB/ pH 5.0 | 0.01 – 1.1 | 0.01 | 0.005 | Untreated Natural Water | [38] |
| 2. | GPE | 0.8M NaOH | 1.3 – 1.9 | 50 cycles | α-NAP | LSV | 0.1 M PB/ pH 6.0 | 0.01 – 2.0 | 0.01 | 0.0015 | Sea water, swimming pool water, tap water and drinking water | [26] |
| 3. | NPPy/SDS/GCE | 0.1 M PB/ pH 7.0 | -1.3 - +0.8 | - | 4-NP | SWV | 0.1 M PB/ pH 7.0 | 0.0001 - 100 | 0.0001 | 0.0001 | Tap water | [37] |
| 4. | BDD | - | - | - | ET | DPV<br>SWV | 0.25 M $H_2SO_4$ | 0.2 – 2.0<br>0.1 – 2.0 | 0.2<br>0.1 | 0.2<br>0.1 | Tap and lake water | [39] |
| 5. | BDD | 0.1 M $HNO_3$ | +2.4 | 60 sec | 2AB<br>4AB<br>1-AN<br>2-AN | DPV | - | 0.0075 – 1 | 0.0075 | 0.014<br>0.011<br>0.0049<br>0.0046 | Sunset Yellow | [40] |
| 6. | BD-NCD | 0.1 M $Na_2SO_4$ | -1.5 - +2.5 | 1 cycle | Pb (II)<br>Cu (II)<br>Hg (II) | LSV | 0.2 M AB/ pH 5.0 | 1.0 – 22.5<br>1.0 – 22.5<br>1.0 – 10 | 1.0<br>1.0<br>1.0 | 1.39<br>0.102<br>0.666 | Lake water | [41] |
| 7. | SPCE | 0.1 M PB/ pH 7.0 | +1.7 | 100 sec | PYR | CV | 0.1 M PB/ pH 7.0 | 10 – 1000 | 10 | 0.33 | Tap water and lake water | [34] |
| 8. | SPCE | 0.1 M PB/ pH 7.0 | +2.0V | 900 sec | HQ<br>CA | SWV | 0.1 M PB/ pH 7.0 | 0.1 – 50<br>0.1 – 70 | 0.1<br>0.1 | 0.05<br>0.05 | River water | [35] |
| 9. | SPCE | 0.1 M PB/ pH 7.0 | -0.6 - +1.6 | 40 cycles | 2AP<br>3AP<br>4AP | NPV | 0.1 M PB/ pH 7.0 | 0.2 – 100<br>3.0 – 200<br>0.2 - 200 | 0.2<br>3.0<br>0.2 | 0.07<br>0.16<br>0.05 | River water | [36] |

In this dissertation, different types of electrodes were prepared by utilizing electrochemical pretreatment such as pCGPE, PGPE, PGPE-NHNA and AuNP-PGPE. The characterization of developed electrodes was done by cyclic voltammetry (CV) and electrochemical impedance spectroscopy (EIS). To confirm the presence of charge stored on surface of electrodes cyclic voltammetry was employed. For the measurement of electron kinetics of electrodes before and after electrochemical activation, EIS method was used. The electroactive areas of electrodes were calculated by using the CV at different scan rates. All the work done is categorized in chapters

**Chapter 2** describes the Open-circuit electrochemical polymerization for the sensitive detection of phenols. The method developed here is simple, sensitive, rapid, and overcomes the well-documented surface fouling of carbon electrodes by phenols. It was demonstrated that electrochemical pretreatment of GPE store charge on its surface. The charge on GPE surface allows the formation of phenol polymer under open-circuit conditions and detection was done in an aqueous buffer solution. A pre-charged disposable graphite pencil electrode (pCGPE) was found to be useful for both phenol sampling and sensing. Phenol sampling was accomplished by immersing the pCGPE into a phenol solution. This method permitted phenol detection with a detection limit of 4.17 nM (0.39 ppt).

**Chapter 3** presents an electrochemically treated graphite pencil electrode (PGPE) for direct and indirect determination of α-naphthol. For in-situ detection of α-naphthol, pretreatment of GPE surfaces is conducted in 0.8 M NaOH by cycling the potential between 1.3 and 1.9 V at a scan rate of 100 $mVs^{-1}$. The influence of the pretreatment is studied extensively, and optimum conditions are obtained. Based on the constructed

calibration curve, a linear range of 0.01 µM to 2.0 µM with a detection limit of 1.5 nM (S/N=3) is obtained.

The indirect determination of α-naphthol was done by targeting the polymer peak. For this purpose, the electrochemical pretreatment of GPE surface was conducted in 1.0 M KOH by the potential +1.6 V for 200 sec. The calibration curve displayed a linear range of 0.02 µM (20 nM) and 0.3 µM (300 nM) with a detection limit of 8.9 nM (S/N=3). the developed method was successfully employed for the indirect determination of trace amount of α-naphthol in real samples.

**Chapter 4** pronounces synergetic effect of mixture of sodium hydroxide and sodium acetate to get electrochemically treated graphite pencil electrodes for trace detection of 4-chloro-1-naphthol. Cyclic scanning between certain potential range of graphite pencil electrode (GPE) in mixture of NaOH and sodium acetate (NHNA) solution resulted in activation of electrode surface. Synergistic effect of both supporting electrolytes was manifested. Formulated pretreated graphite pencil electrode (PGPE-NHNA) expressed high sensitivity and selectivity towards oxidation of 4-CNP. The oxidation peak current against 4-CNP concentration at PGPE-NHNA displayed linearity between 0.01 µM to 1.0 µM with equation $I(\mu A) = 540.07\ C_{4\text{-CNP}(\mu M)} + 33.028$ and regression constant ($R^2$) of 0.9986. The PGPE-NHNA afforded very low detection limit of 0.00157 µM or 1.57 nM (S/N=3) for 4-CNP quantification. The PGPE-NHNA showed high immunity for spiked concentration of different interfering compounds.

**Chapter 5** depicts the simple and sensitive detection of 4-nitrophenol in real water samples by utilizing gold nanoparticles modified pretreated graphite pencil electrode. The PGPE electrode alone displayed distinct electrocatalytic properties while reducing 4-

nitrophenol (4-NP). Reduction current against 4-NP concentration at PGPE displayed linearity between 0.01 µM to 0.8 µM. The PGPE was further modified by AuNP to increase the working range of PGPE for sensing 4-NP. The Developed PGPE and AuNP-PGPE could be employed to vast concentration range of 4-NP varying between 0.01 – 100 µM. The modified electrodes were aimed at different amounts of 4-NP varying form low concentration 0.2 µM to high concentration, i.e. 25 µM in water models.

**Chapter 6** includes the concluding remarks and future prospects for electrochemically treated electrodes

For our knowledge, the presented outcomes were the first analytical application of electrochemically activated graphite pencil electrodes for sensing phenol, α-naphthol and their selected derivatives. The activated surface successfully applied for trace level detection of pollutants in real life samples due to their high electrocatalytic activity. The electrochemically treated surfaces also utilized as stable platform to deposit gold nanoparticles. the pretreated graphite pencil electrodes show higher sensitivity, selectivity, and low detection limit. These characteristics will be exploited for developing the environment friendly sensors with applications in real life samples.

The results reported in this Ph.D. dissertation have been published in ISI quoted journals, as follows:

- Open-circuit electrochemical polymerization for the sensitive detection of phenols. (Electroanalysis: I.F. 2.851)
- Novel electrochemically treated graphite pencil electrode surfaces for the determination of trace α-naphthol in water samples. (Journal of the Chinese Chemical Society: I.F. 0.935)

One patent is filed

- Open Circuit Electrochemical Polymerization for Sensitive Detection of Phenol. (Filed Application Ref # 458306US)

The manuscripts under review:

- Synergetic effect of mixture of sodium hydroxide and sodium acetate to get electrochemically treated graphite pencil electrodes for trace detection of 4-chloro-1-naphthol in real water samples. (Submitted to Electroanalysis)
- Simple and sensitive detection of 4-nitrophenol in real water samples by utilizing gold nanoparticles modified pretreated graphite pencil electrode. (Submitted to Journal of Electroanalytical Chemistry)
- Novel electrochemical method for sensitive determination of α-naphthol in water and urine samples by aiming poly(α-naphthol) formed on the surface of treated graphite pencil electrode.

# Chapter 2

## Open-circuit Electrochemical Polymerization for the Sensitive Detection of Phenols

### 2.1 Introduction

Phenolic compounds are common and ubiquitous environmental pollutants [42,43]. Because most phenols cause serious health problems [44–46], phenol detection is recognized as an important capability. Phenols are classified as hazardous wastes and virulent pollutants by the United State Environmental Protection Agency [47,48]. Phenols can adversely affect human health by promoting weight loss and weariness. In severe cases of exposure, phenols can cause respiratory cancer, cardiac problems, and the suppression of the immune system [49,50]. Hence, the detection of phenols in trace quantities is crucial.

A variety of analytical techniques have been developed for the detection of phenols, including spectrophotometry [51–59], chromatography [60–63], and electroanalytical methods [64–67]. Most of these methods are time-inefficient and costly because the samples require pretreatment, extraction, and surface adsorption [68,69]. Electrochemical methods are attractive phenol detection methods because they are low-cost, simple, and rapid [64]. Nevertheless, the formation of a strongly adhesive semipermeable layer on the surfaces of the solid electrodes rendered the phenol detection process unmanageable [70]. A variety of studies have examined the process by which oxidized phenolic layers form on a solid electrode surface [70,71]. The phenols are irreversibly electro-oxidized at an electrode surface, then subsequently hydrolyzed to

produce hydroquinone and catechol ortho and para oxidation products. These products are then reversibly oxidized and adsorb onto the electrode surface [72].

A variety of efforts have been applied toward preventing electrode surface fouling by phenols. For example, glassy carbon electrodes [73], boron-doped diamond electrodes [74], and porous copper-modified graphite pencil electrodes [75] have been tested in electrochemical phenol detection devices. A new approach to determining the presence or quantity of phenol in a water sample has been developed. A working electrode, such as a GPE, is charged using an electrochemical treatment. The charge stored on the surface of the GPE facilitated electropolymerization when dipped into the phenol solution without application of a potential. The formation of the electropolymer was monitored using square wave voltammetry.

## 2.2 Experimental

### 2.2.1 Materials

All chemicals were analytical reagent grade and were used without further purification. Phenol, sodium hydroxide, hydrochloric acid, monosodium phosphate, monopotassium phosphate, disodium phosphate**,** sodium chloride, potassium chloride, 4-bromophenol, 2,4-dichlorophenol, ascorbic acid, uric acid, glucose, fructose, 4-aminbenzoic acid and cadmium sulfate were obtained from Sigma Aldrich® (USA). Cobalt chloride was received from BDH Limited Poole England, and calcium chloride was obtained from BAKER ANALYZED Reagent. Hi-polymer graphite pencil HB black leads were obtained from Pentel (Japan). All leads had a total length of 60 mm and a diameter of 0.5 mm and were used as received.

### 2.2.2 Apparatus

A mechanical pencil was used as a holder for both the uncharged and charged graphite pencil leads. Electrical contact with the lead was achieved by soldering a copper wire to the metallic part that held the lead in place inside the pencil. The pencil was fixed vertically with 15 mm of the pencil lead extending outside of the pencil, and 10 mm of the lead were immersed in the solution. This length corresponded to a geometric electrode area of 16.10 $mm^2$. CHI 660C (CH instruments, USA) was used for all electrochemical work. The electrochemical cell contained a pre-charged graphite pencil electrode (pCGPE) as a working electrode, a Pt wire counter electrode and an Ag/AgCl (Sat. KCl) reference electrode.

### 2.2.3 Graphite pencil electrode (GPE) charging

The 10-mm length of the extruded GPE from pencil, an Ag/AgCl reference, and Pt counter electrodes were immersed into a cell containing different concentrations of NaOH. Cyclic voltammetry was applied to charge the GPE surface. Other conditions included a 1.3–1.9 V potential range, 50 CV segments, and a 100 mV/s scan rate. Next, the prepared charged pCGPE was gently dipped twice in deionized water to wash the electrode. All electrochemical measurements were performed immediately after preparing the charged electrodes.

### 2.2.4 Open circuit electropolymerization of phenol

The pCGPE was dipped into a phosphate buffer (PB) solution (0.1 M, pH 7.2) containing a certain concentration of phenol. The phenol was open-circuit electropolymerized over 120 seconds with stirring.

### 2.2.5 Electrochemical detection

Square wave voltammetric (SWV) measurements of phenol were performed under optimized electrochemical conditions in phosphate buffer saline (PBS) (0.1 M, pH 7.2). The pCGPE with polyphenol on its surface was connected in a three-electrode electrochemical cell setup and allowed a 10-s rest period under quiescent conditions.

### 2.2.6 Drinking water sample preparation

Tap, bottled and vending drinking water samples were collected and filtered through a 0.45 μm membrane to remove any precipitation. Into 5.0 mL of each of these water samples were spiked 0.5 μM phenol.

## 2.3 Results and discussion

### 2.3.1 Evaluation of GPE charging solution

The phenol detection strategy described here relies on charging the graphite pencil electrode surface through electrochemical treatment.

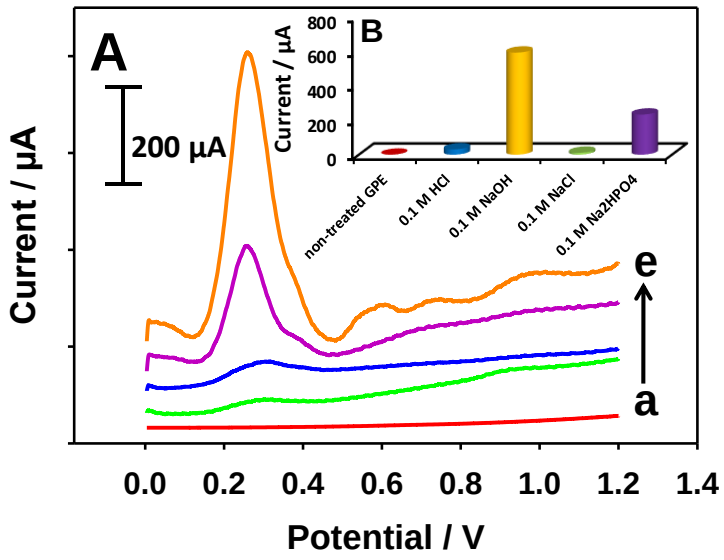


**Figure 2. 1. SWVs obtained from a 2mM phenol solution in 0.1M Phosphate buffer, pH 7.2, in the presence of the uncharged a) and charged GPEs in various 0.1M media: b) NaCl, c) HCl, d) $Na_2HPO_4$, and e) NaOH solutions. Working conditions: the charging potential was 1.3–1.9 V, 50 charging CV segments were used, the charging scan rate was 100 mV/s, the frequency was 50 Hz, the amplitude was 0.06 V, the polymerization time was 60 sec, and the polymerization medium was phosphate buffered at pH 7.2. (B) The corresponding histogram.**

The open-circuit electropolymerization of phenol on the surface of the pre-charged electrode is performed simply by dipping the electrode into a phenol solution. In this way, phenol detection is achieved in a suitable medium. The coupling between the electrochemically charged electrode and the phenol yields highly specific and sensitive electronic detection. Figure 2.1 shows square wave voltammograms (SWVs) of phenol (2 µM) in the presence of the pCGPE. Charging was performed using different solutions. Well-defined oxidation peaks corresponding to the phenol polymer may be distinguished. The electrochemical oxidation current of the phenol polymer on the surface of the pCGPE charged in 0.1 M NaOH was ≈ 2.54, ≈ 19.1, or ≈ 54.2 times the values obtained using pCGPEs charged in 0.1 M $Na_2HPO_4$, 0.1 M HCl, or 0.1 M NaCl respectively.

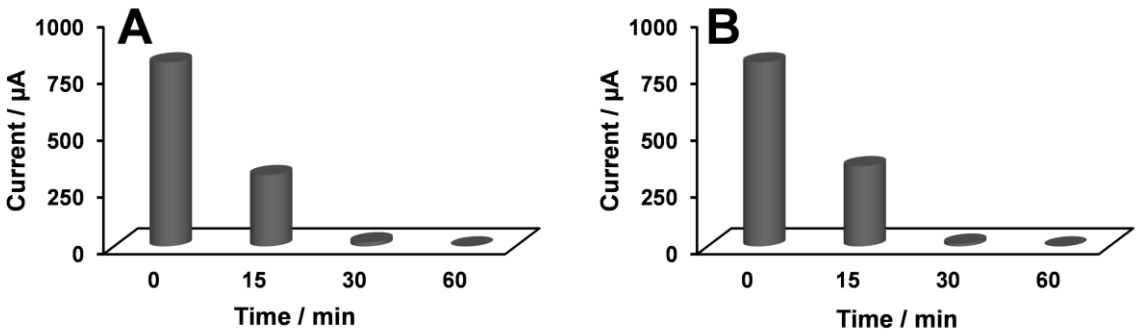


**Figure 2. 2. The corresponding histograms of the discharging rate of Pre-charged GPEs stored in A) air and B) PB, pH 7.2 for 0, 15, 30 and 60 min. Open circuit polymerization was followed in 50 µM Phenol in 0.1 M phosphate buffer solution, pH 7.2 for 2 min.**

The results revealed that the electrode charged in 0.1 M NaOH yielded a higher peak current in the presence of phenol. The pre-charged graphite surfaces stored in air, water, or phosphate buffer were found to discharge within one hour as shown in Figure 2.2.

The electropolymerized phenol film that formed on the pCGPE from either a 50 µM or 2 µM phenol solution retained its electroactivity for three days or three hours, respectively, when stored in air, water or buffer (data not shown).

### 2.3.2 Detection medium and pH

Figure 2.3 shows that the pH of the detection medium (PBS) prominently affected the peak current and the peak position. These results revealed that a pH of 7.0 in the detection medium was optimal for detecting phenols.

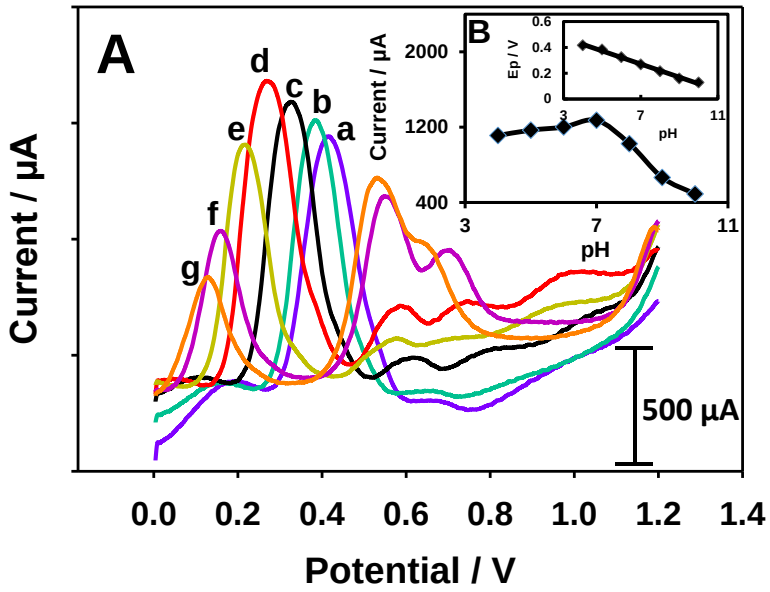


**Figure 2. 3. (A) SWVs of 2 mM phenol in 0.1M PBS, pH 7.0, at the following pH values: a) 4, b) 5, c) 6, d) 7, e) 8, f) 9, and g) 10. The charging solution was 0.1M NaOH. Other working conditions were the same as those presented in Figure 1. (B) Corresponding plot of the peak current (mA) vs. pH. The inset shows a plot of the peak potential (V) vs. pH.**

The effect of the polymerization time on the measured peak current in the SWVs was monitored using a charged electrode in PBS, pH 7.2, containing 2 µM phenol. As the polymerization time increased, the peak current increased up to 120 sec, after which it leveled out to a constant value as shown in Figure 2.4. This effect led us to set 120 sec as the optimal polymerization time for phenol.

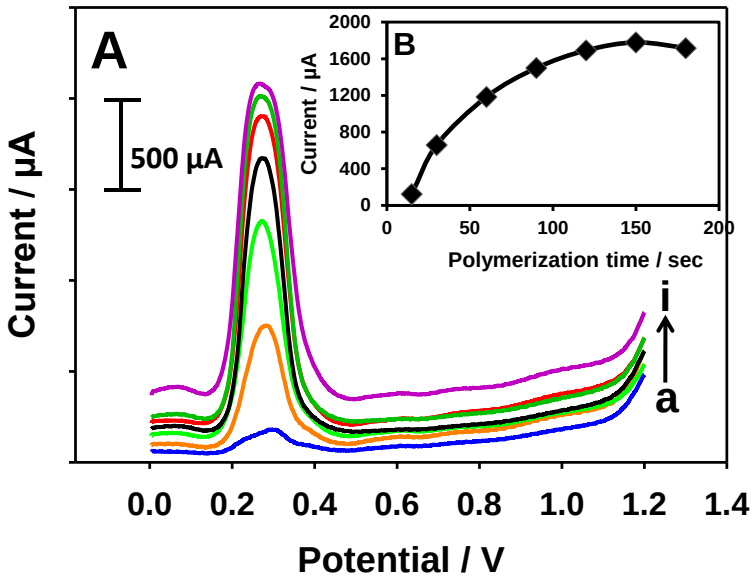


**Figure 2. 4. (A) SWVs of 2 mM phenol in 0.1M phosphate buffer saline, pH 7.0 after different open circuit polymerization time: a) 15, b) 30, c) 60, d) 90, e) 120, f) 150 and g) 180 sec. Pretreatment solution 0.1M NaOH, other working conditions were same as in Figure 2. 1. (B) The corresponding plot of peak current ip (mA) vs polymerization time.**

### 2.3.3 Characterization of pre-charged GPE

The interesting performance of the pCGPE could be attributed to the fact of that the electrochemical pretreatment of carbon-based electrodes leads to an increase in the number of surface oxygen-containing groups and/or formation of graphite oxide films [76]. Thus, it is possible that an active layer is formed on the pCGPE surface, e.g., an oxygen-containing groups/graphite oxide film, or active species generated during the electrochemical processes, e.g., oxygen and radicals generated during water oxidation, that could be themselves adsorbed on the porous graphite carbon material, and act as oxidant or polymerization initiator, once contacted by phenols. Figure 2.5 A shows a comparison between the cyclic voltammetric behavior in 6 M NaOH solution at a slow scan rate of 2 $mVs^{-1}$ for GPE surfaces before (a), and after (b) its electrochemical pretreatment in 0.1M NaOH. The specific capacitance for both surfaces calculated according to Eqn. 2.1 [77], and based on the integrated area under the corresponding CV

curves were 187.51 F/g and 5734.81 F/g for GPE, and pCGPE, respectively. The dramatic increase in the specific capacitance of the GPE surface after its electrochemical treatment may be behind its gained capabilities to complete the electrochemical polymerization under an open circuit condition.

$$C = Q/ \Delta E \, . \, m \qquad 2.1$$

Where Q is the voltammetric charge, m is the weight of the electrode and ΔE is the working potential window used for the CV. Moreover, Figure 2.5 B shows the Nyquist plots of GPE (a) and pCGPE (b) electrodes in 0.1M KCl solution containing a mixture of 5 mM each of $K_4[Fe(CN)_6]$ and $K_3[Fe(CN)_6]$ with a frequency range of 100 kHz to 0.01 Hz. The plot obtained at GPE is composed of a semicircle and a straight line, where only a straight line for the pCGPE was obtained. Since the semicircle at higher frequency region is attributed to the charge transfer process at the electrode/electrolyte interface, the straight line at lower frequency region is ascribed to the diffusion process in solid [78]. Thus, the electrochemical reaction resistance at pCGPE electrode is comparatively much smaller. In addition, the straight line at lower frequency region for pCGPE used is sloppier than that for the GPE used, suggesting that the former is more capacitive than the later. These outcomes are in correspondence with the voltammograms shown in Figure 5A.

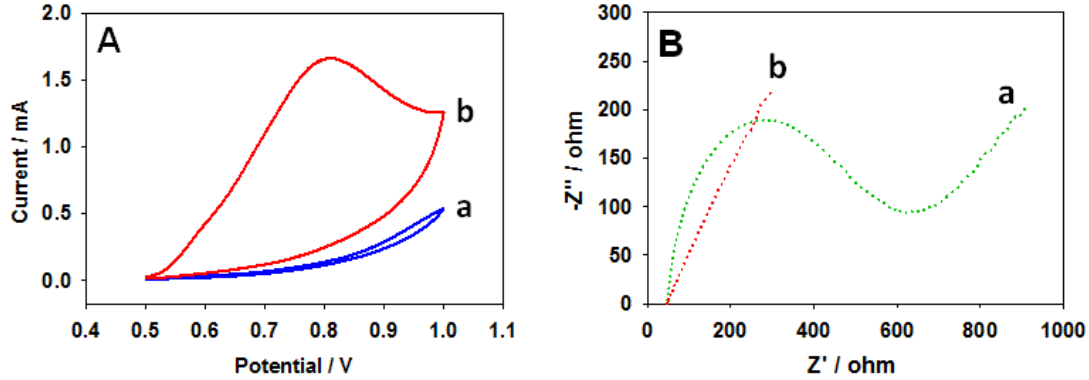


**Figure 2. 5. CVs in 6 M NaOH electrolyte at 2 mV/sec scan rate (A), and Nyquist plots in 0.1M KCl solution containing a mixture of 5 mM $K_4[Fe(CN)_6]$ and 5 mM $K_3[Fe(CN)_6]$ (B) of uncharged (a), and charged (b) GPE.**

To confirm the pseudo capacitor performance of the electrochemically treated graphite carbon electrode, a discharging experiment was completed for the pre-charged GPE in the absence (a), and presence (b) of 100 mM phenol in PBS (0.1 M, pH 7.0) as shown in Figure 6. In the absence of phenol, the electrode discharge was linear and lasted for over 100 min (Figure 2.6 a), where in the absence of phenol it got discharged quickly in a matter of few minutes (Figure 2.6 b). This could be attributed to the charge consumption in the electropolymerization of phenol.

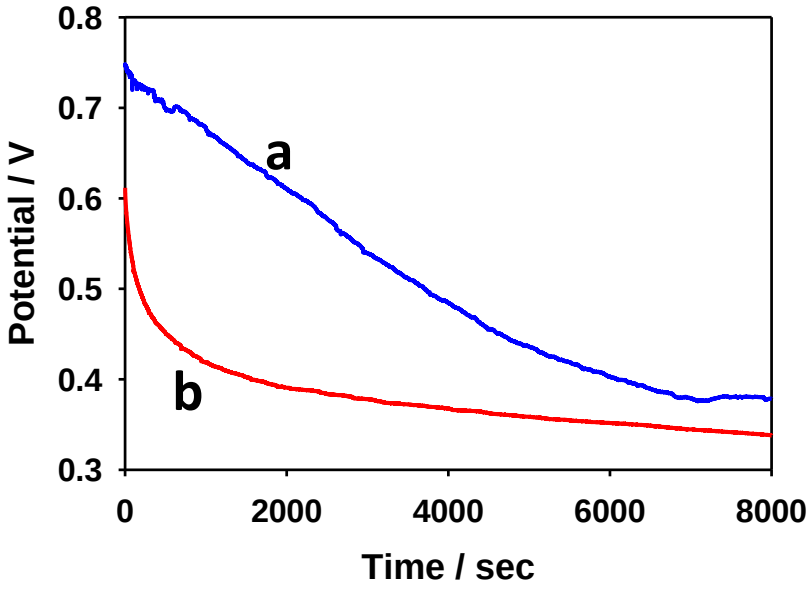


**Figure 2. 6. Open circuit potential curves in absence (a), and presence (b) of 100 mM phenol in PBS (0.1 M, pH 7.0) at the pre-charged GPE.**

### 2.3.4 Calibration

A calibration curve was recorded as a function of the phenol concentration by plotting the peak maxima of the SWVs. Increasing the concentration of phenol clearly increased the peak current, as shown in Figure 2.7, and a linear relationship was observed with a correlation coefficient of r = 0.9998 and a linear range of 0.05 – 1.0 µM. The detection limit for phenol was 4.17 nM (S/N=3).

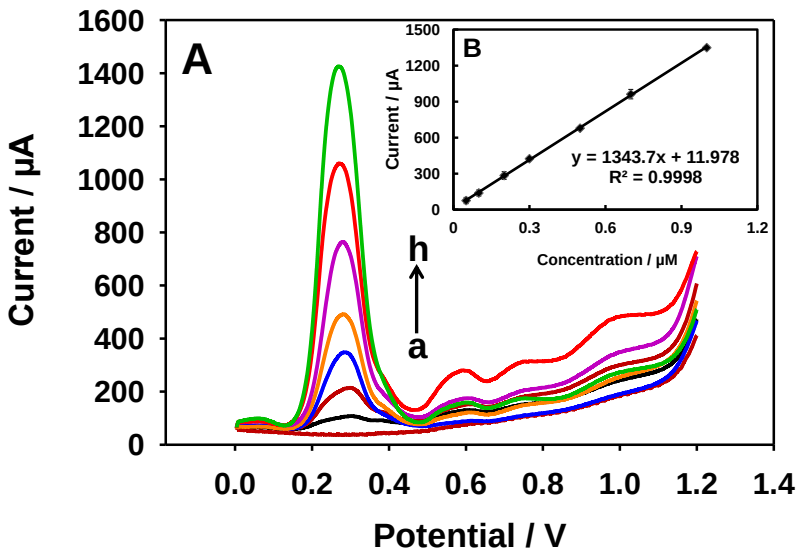


**Figure 2. 7. Square wave voltammograms at the charged GPE in a 0.1M PBS solution, pH 7.0 containing different phenol concentrations: a) 0, b) 0.05, c) 0.1, d) 0.2, e) 0.3, f) 0.5, g) 0.7, or h) 1.0 mM. The conditions included a charging solution of 0.1 M NaOH, a polymerization time of 120 sec, and all other working conditions were the same as those listed in Figure 2. 1. The inset shows the corresponding calibration curve.**

### 2.3.5 Reproducibility and Interferences

The reproducibility of the phenol detection process was tested by electrochemically oxidizing the phenol polymer using 6 newly fabricated electrodes. The results demonstrated an acceptable reproducibility, with a relative standard deviation of 3.76%. The possibility of detecting phenol in actual samples was also investigated. The phenol content in actual water samples is typically present at concentrations lower than the detection limit of the present method and, therefore, is undetectable. For this reason, 0.5 µM phenol was added to the water samples. A calibration curve was used to calculate the recovery of phenol at the pCGPE, revealing the presence of 99.25, 107.07, and 110.93% phenol in drinking water collected from the filtration plant at the university, tap water, and commercial drinking water respectively. The effects of various interferents on the peak current corresponding to phenol oxidation were studied. We found that the

addition of 0.5 µM 4-bromopheonl, 2, 4-dichlorophenol, ascorbic acid, uric acid, fructose, or a mixture of metals ($Co^{+2}$, $Cu^{+2}$, $Ca^{+2}$, $Na^{+}$, and $K^{+}$) shifted the signal obtained from 0.5 µM phenol by +2.65, +11.74, –5.89, +9.53, +0.72, and –7.96%, respectively, as shown in Figure 2.8.

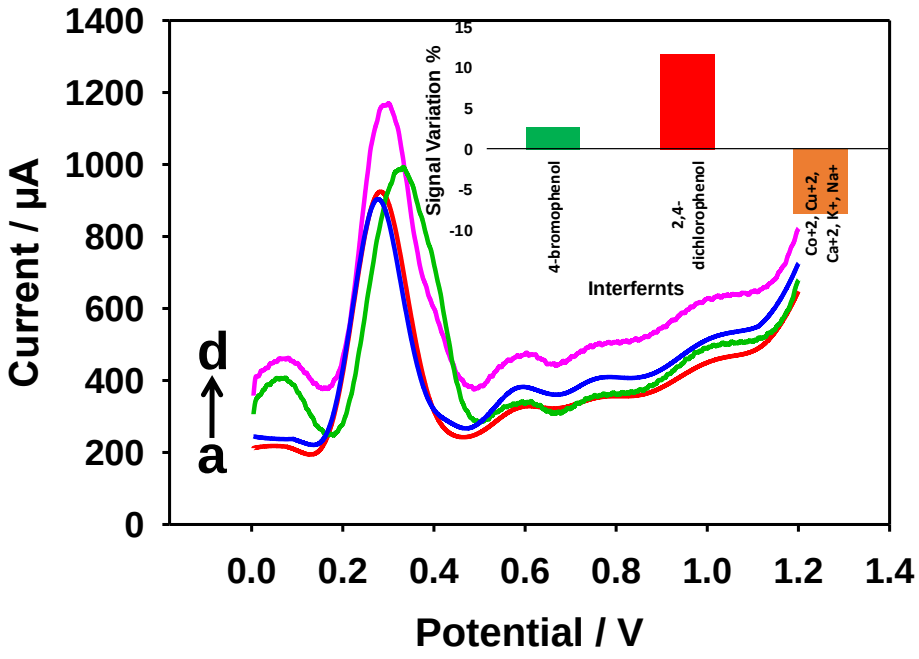


**Figure 2. 8. SWVs of open-circuit polymerized 0.5 µM phenol in 0.1 M PB, pH 7.0 at the pre-charged GPE in absence (a), and presence of 0.5 µM (b) each of $Co^{+2}$, $Cu^{+2}$, $Ca^{+2}$, $K^{+}$ and $Na^{+}$ mixture, (c) 4- bromophenol, and (d) 2,4-dichlorophenol. Inset is the corresponding histogram.**

These experimental results reflected the good sensing sensitivity, selectivity, and stability of the phenol polymer formed at the fabricated pCGPE.

## 2.4 Summary

We successfully fabricated a novel, extremely low-cost, disposable, and easily fabricated phenol sensor using the electrochemically charged surface of a GPE. The highly reproducible sensor exhibited remarkable electrocatalytic activity, synthesizing a phenol polymer layer through oxidation. The detection limit, analytical selectivity,

sensitivity, and stability of the technique were very good. The performance of the novel pCGPE proved to be excellent and was found to be suitable for the analytical determination of various phenol concentrations.

# Chapter 3

## Electrochemically treated graphite pencil electrode surfaces for the determination of trace α -naphthol in real life samples

### 3.1 Direct detection of α -naphthol

#### 3.1.1 Introduction

α-naphthol is a polyaromatic hydrocarbon (PAH) that are components of the organic aerosols and show mutagenic and carcinogenic properties [79–82]. Increased concentration of PAH considered to be a major environmental and occupational health problem [83,84]. These compounds are not degradable so they can stay longer in environment [85]. PAH compounds are volatile in nature and measurement of these compounds helps to determine extent of exposure and the amount of PAH compounds in body [86]. Now-a-days the individual detection of PAH is of great interest so α-naphthol is selected as analyte, and it is considered to be highly toxic as compare to its isomer 2-naphthol [87].

On exposure to naphthalene the concentration of α-naphthol increase because bioactivation of naphthalene by human enzyme P450 produce α-naphthol [88,89] as shown in Figure 3. 1. α-naphthol presence in body cause severe effects on human organs like liver, kidney, skin, and eyes [90–92]. The problems associated in severe case are crampy abdominal pain, nausea, vomiting, and sometimes convulsions. Intestinal or percutaneous absorption may lead to severe nephritis, liver injury, and acute hemolytic anemia [79] and retinal changes have been described in literature.[93–96]

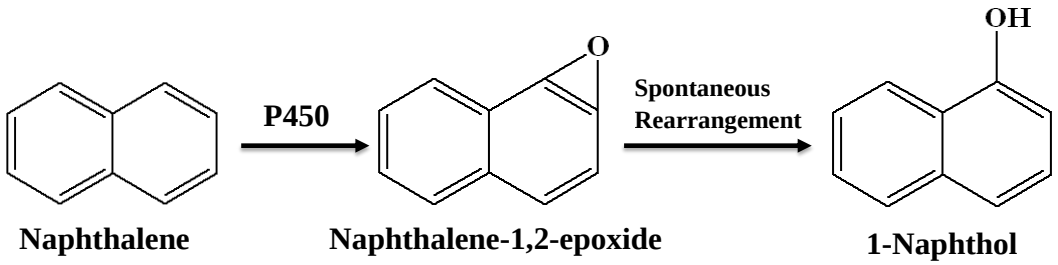


**Figure 3. 1. Mechanism of conversion of naphthalene to α-naphthol inside human body.**

The analytical techniques for determination of α-naphthol in various samples include capillary zone electrophoresis [97], resonance Rayleigh scattering spectrometry [98], spectrophotometry [99], high performance liquid chromatography (HPLC) [100], Synchronous scanning fluorescence [101], and thin layer chromatography (TLC) [102]. They are expensive and complex methods that require highly qualified personals, significant labor, and analytical resources.

Electrochemical methods are frequently used in analytical chemistry due to their high sensitivity, low cost, fast response, simple instrumentation and portability [103,104]. The poor electrocatalytic properties of conventional electrodes, however, limit their use in measuring α-naphthol trace concentrations. These electrocatalytic properties of electrodes for detection of α-naphthol can be improved by electrochemical pretreatment [105], modifying the electrode with a suitable electrocatalyst or electron mediator [106]. For detection of α-naphthol various modified electrodes have been constructed and used such as poly (acridine orange) film modified electrode [107], G-DNA modified gold electrode [108], high-index facet $SnO_2$ modified electrode [106], gold nanoparticles/hollow nitrogen-doped carbon microsphere hybrids functionalized with SH-β-cyclodextrin modified electrode [109], carbon nanotubes network joined by Pt-nanoparticles modified electrode [110], ß-Cyclodextrin-platinum nanoparticles/graphene

nanohybrids modified electrodes [111], Nano-$TiO_2$/MWNTs composite film modified electrode [112], and multiwall carbon nanotubes modified electrode [113]. Despite of the selectivity of these voltammetric techniques, inexpensive, more sensitive and selective methods are still needed to detect α-naphthol. Electrochemical pretreatment of graphite pencil electrode seems to be a simple, less time consuming and more applicable strategy in comparison to other procedures. Moreover, this strategy eliminates the use of toxic compounds required in modification of the electrode surface [114–118].

In the present study, a simple electroanalytical detection method based on the electrochemically treated graphite pencil electrode (PGPE) is described for the detection of trace concentration level of α-naphthol in water samples. The analytical performance was evaluated by linear sweep anodic stripping voltammetric technique, and all findings are reported in the following sections.

## 3.1.2 Experimental

### 3.1.2.1 Reagents

All chemicals were analytical reagent grade and used without further purification. α-naphthol, lithium chlorate, sulfuric acid, Tris-borate EDTA buffer (pH 9.0), Tris-buffered saline (20nM Tris, pH 7.4), Tris-EDTA buffer solution (10 mM Tris-HCl; 1 mM EDTA, pH 7.4) and sodium acetate buffer (AB) solution (3.0 M, pH 5.2) were obtained from Sigma Aldrich® (USA). The nitric acid was obtained from AnalaR® (England). Glassy carbon electrode (GCE), Pt disc and Au-disc electrodes were obtained from CH instruments® (USA). All other chemicals are same as state in 2.1.1.

### 3.1.2.2 Apparatus

The identical apparatus was utilized as in 2.1.2.

### 3.1.2.3 Preparation of phosphate buffer

The 4 – 8 pH values of phosphate buffer were obtained by adding calculated volumes of 1.0 M $NaH_2PO_4$ and 1.0 M $Na_2HPO_4$ in 100 ml flasks, upto the mark with double distilled water.

### 3.1.2.4 Pretreatment of GPE

The pretreatment of GPE was done in similar way as mentioned in 2.1.3.

### 3.1.2.5 Water sample preparation

Certain amount of water sample from tap water in the laboratory, sea water in local district, swimming pool water in the university, and drinking water were firstly filtered through a 0.45 μm membrane to remove any precipitation and then precisely diluted with 0.1 M PB. For electrochemical detection, 20 μL water samples solution was transferred into 10 mL 0.1 M PB solution.

## 3.1.3 Results and discussion

### 3.1.3.1 Electrode materials and pretreatment medium evaluation

The electrocatalytic properties of different transducers towards the electrochemical detection of α-naphthol were assessed using SWASVs (Figure 3.2 A). Glassy carbon (GC), graphite pencil (GP), carbon paste (CP), Pt disc and Au disc electrodes were tested. The obtained results showed that except GPE other four electrodes (GC, CP, Pt, and Au) did not respond well to α-naphthol at the 5 μM

concentration level, GPE gave a well-defined α-naphthol response. However, the highest signal was obtained at the GPE as shown in the histogram of Figure 3. 2 B.

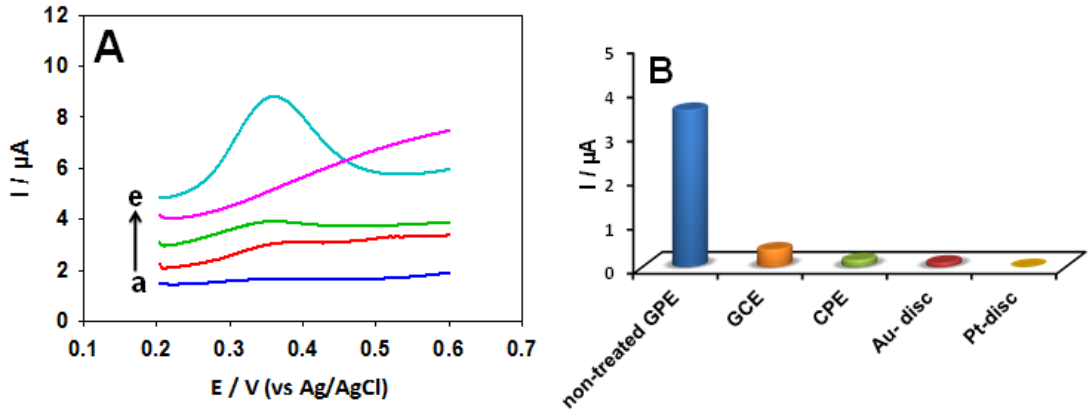


**Figure 3. 2. (A) Square wave anodic stripping voltammograms (SWASVs) of 5 µM α-naphthol at different electrodes: a) Au electrode, b) CPE, c) GCE, d) Pt electrode and e) GPE. Working conditions: deposition potential 0.2 V, deposition time 60 sec, frequency 15 Hz and amplitude 0.025 V. (B) showing corresponding histograms.**

The effect of the GPE surface pretreatment medium was evaluated including NaOH, $LiClO_4$, $HNO_3$, $H_2SO_4$, HCl, AB solution and phosphate buffer (PB) solution. Fifty pretreatment segments within a potential range of 1.3 to 1.9 V of cyclic voltammetry (CV) was performed and followed by the detection of α-naphthol. The pretreatment of the graphite pencil electrode (GPE) in AB, $HNO_3$, $H_2SO_4$, and HCl did not show any enhancement in the α-naphthol, while in PB and NaOH prominently increased the peak current of α-naphthol. Since a high electrochemical redox signal is essential for the fabrication of any ultrasensitive electrochemical sensor, NaOH was chosen as a medium for the GPE treatment, for the electroanalytical determination of α-naphthol (Figure 3. 3 B).

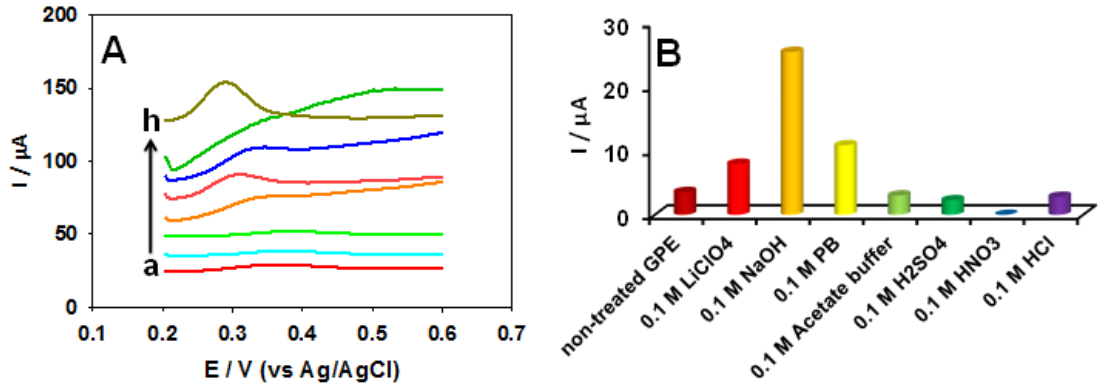


**Figure 3. 3. (A) SWASVs of 5 µM α-naphthol at unpretreated (a) and pretreated GPEs in various 0.1 M media: b) acetate buffer, c) HCl, d) $H_2SO_4$, e) phosphate buffer, f) LiClO4, g) $HNO_3$ and h) NaOH solutions. Working conditions: Pretreatment potential 1.3 to 1.9 V, pretreatment segments 50, pretreatment scan rate 100 mV/s, deposition potential 0.2 V, deposition time 60 sec, frequency 15 Hz and amplitude 0.025 V. (B) corresponding histogram.**

The main constituent of graphite pencil electrode is graphite (65%), clay (30%) and only 5% is electro-inactive polymer as a binder. Thus, pencil lead is mainly consist of graphite, a form of carbon in which each atom is connected together by weak bonds. Clay is naturally occurring aluminosillicate showing the ion exchange properties. However, the graphitic part of pencil in contact with the pretreatment solution (i.e. NaOH) is cleaned and various oxygen containing functional groups are attached. The α-naphthol enhancement in signal of GPE after pretreatment can be attributed to the increased oxygen containing groups on the electrode surface or to the formation of graphite oxide film.

In order to determine the effect of the concentration of the pretreatment solution (NaOH) on the GPE, GPE was pretreated in different concentrations of NaOH ranging from 0.1 M to 1.2 M in potential range of 1.3 to 1.9V; scan rate was fixed at 100 $mVs^{-1}$. Then pretreated electrode was used for determination of α-naphthol. Figure 3. 4 A shows Linear sweep anodic stripping voltammograms (LSASVs) obtained using these electrodes in phosphate buffer (0.1M, pH 7.0). with increasing the concentration, the

peak current for 5 µM α-naphthol also change and show maximum peak current at 0.8M NaOH as in Figure 3.4 B.

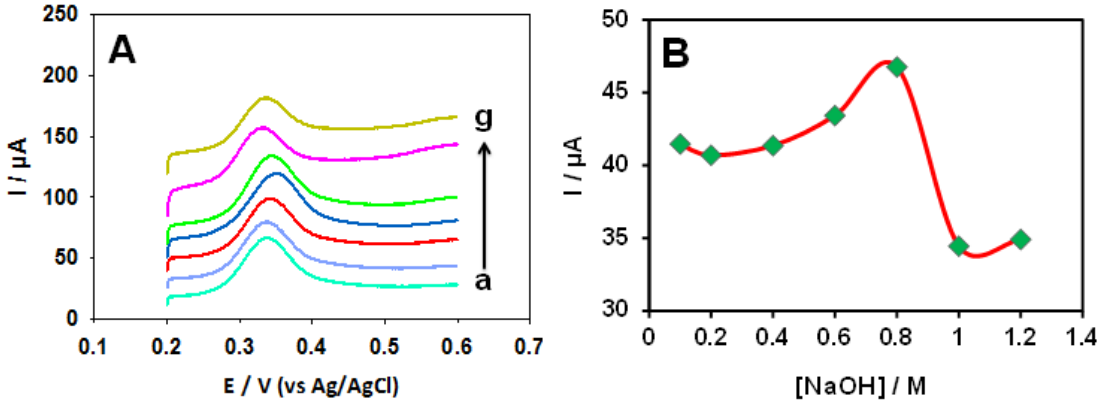


**Figure 3. 4. (A) Linear sweep anodic stripping voltammograms of 5 µM α-naphthol in 0.1 M phosphate buffer solution, pH 7.0 at GPE surfaces pretreated in NaOH solutions of different concentrations: a) 0.1, b) 0.2, c) 0.4, d) 0.6, e) 0.8, f) 1.0 and g) 1.2 M. Working conditions: Pretreatment potential 1.3 to 1.9 V, pretreatment segments 50, pretreatment scan rate 100 mV/s, deposition potential 0.2 V, deposition time 60 sec, scan rate 0.1 V/s and sample interval 0.001 V. (B) The corresponding plot of peak currents ip (µA) vs concentration of NaOH.**

### 3.1.3.2 Optimizing the electrochemical treatment parameters

In order to evaluate the number of peak segments, the potentiodynamic pretreatment of the GPE carried out by scanning with different number of segments between 1.3 – 1.9V and with a scan rate of 100 mV $s^{-1}$. Based on obtained results (Figure 3. 5 A) the maximum ip was observed with 50 pretreatment scan numbers. Therefore, number of pretreatment scans that was considered to be optimum was 50.

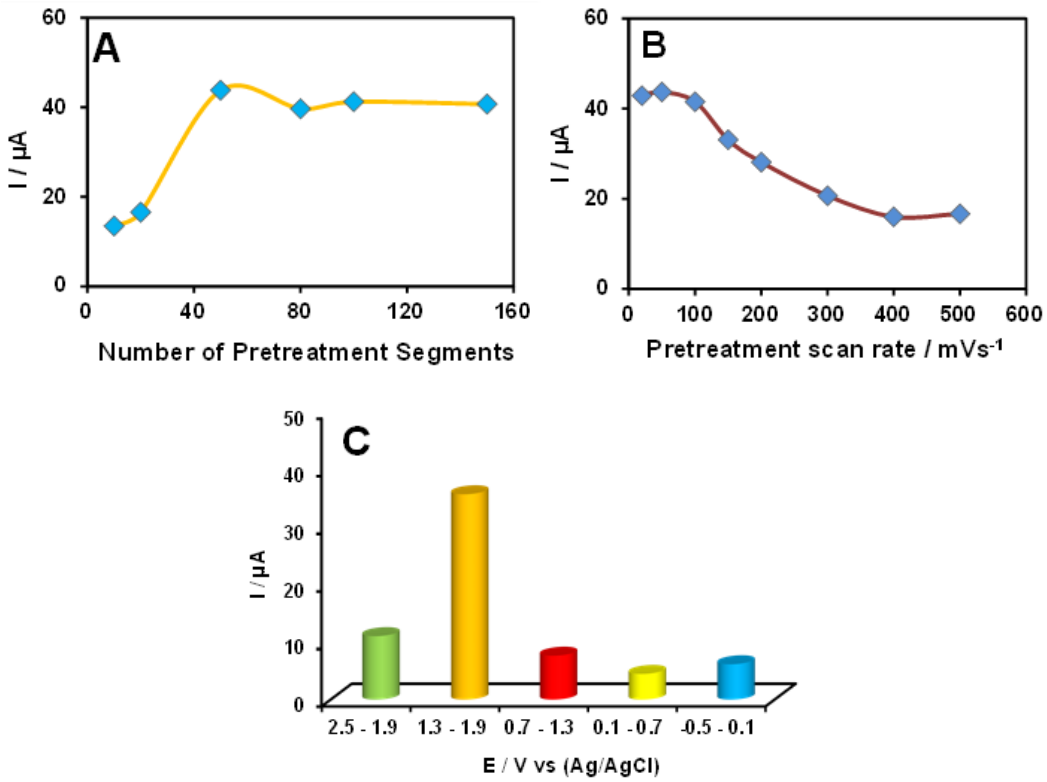


**Figure 3. 5. Plot of peak current vs number of pretreatment segments (A), pretreatment scan rate (B) and pretreatment potential C of LSASVs of 5 µM α-naphthol in 0.1 M phosphate buffer solution, pH 7.0 Pretreatment solution 0.1 M NaOH, other working condition were the same as in Figure 3. 4.**

To obtain best pretreatment scan rate, the GPE pretreatment was done between 1.3 – 1.9V at 50 pretreatment segments and scan rate was varied from 20 – 500 $mVs^{-1}$. Outcomes (Figure 3. 5 B) showed that ip for scan rates of 20, 50 and 100 was almost same. To get best results in short time, 100 $mVs^{-1}$ was optimum scan rate for pretreatment.

Finally, the effect of scan potential range on GPE was studied. Histogram 3. 5 C depicts the influence of scanning potential range used during the GPE pretreatment on LS peak currents for a 0.1 M solution of phosphate buffer (pH 7.0) containing 5 µM α-naphthol. It was observed that potential range of 1.3 – 1.9V show highest peak current. The optimal CV pretreatment parameters are summarized in Table 3. 1.

**Table 3. 1. Optimal pretreatment parameters for α-naphthol determination by the linear sweep anodic stripping voltammetry method using a pretreated electrode.**

| Electrode | Pretreatment media | Pretreatment potential range (V) | Pretreatment scan rate (mV/s) | Number of pretreatment CV segments |
|---|---|---|---|---|
| GPE | NaOH (0.8M) | 1.3 to 1.9 | 100 | 50 |

### 3.1.3.3 Detection technique, medium, and pH

Firstly, in order to determine the effect of voltammetric technique suitable for detection of α-naphthol different voltammetric techniques were applied. Including differential pulse, square wave, differential normal pulse, linear sweep, stair case and normal pulse voltammetry, the results (Figure 3. 6) revealed that Linear sweep voltammetry give highest peak current for same concentration of α-naphthol.

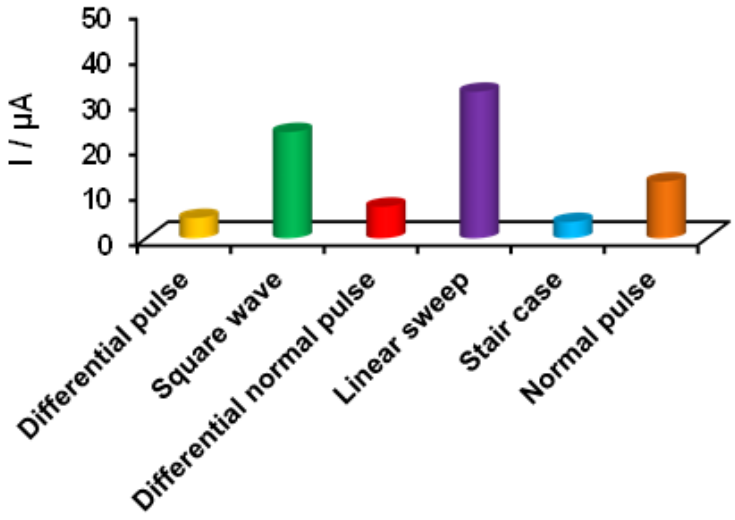


**Figure 3. 6. The corresponding histogram showing effect of voltammetric techniques on 5 µM α-naphthol in 0.1 M phosphate buffer solution, pH 7.0. Pretreatment solution 0.1 M NaOH, other working conditions were the same as in Figure 3. 4.**

In order to use the best detection medium for α-naphthol various solutions were used like, HCl, NaOH, AB, PB, tris-EDTA buffer, tris-buffered saline, tris-borate EDTA buffer and phosphate buffer saline. All the solutions were with same concentration, i.e. 0.1M (all buffer used in this study were of same pH, i.e. 7.0). NaOH, tris-EDTA buffer and HCl show no peak for 5 µM α-naphthol. However, AB, PB, tris-buffered saline, tris-borate EDTA buffer and phosphate buffer saline give well defined peaks (Figure 3. 6 A). It was observed that peak current for α-naphthol was highest in 0.1M phosphate buffer (Figure 3. 7 B), so for further optimization phosphate buffer was used.

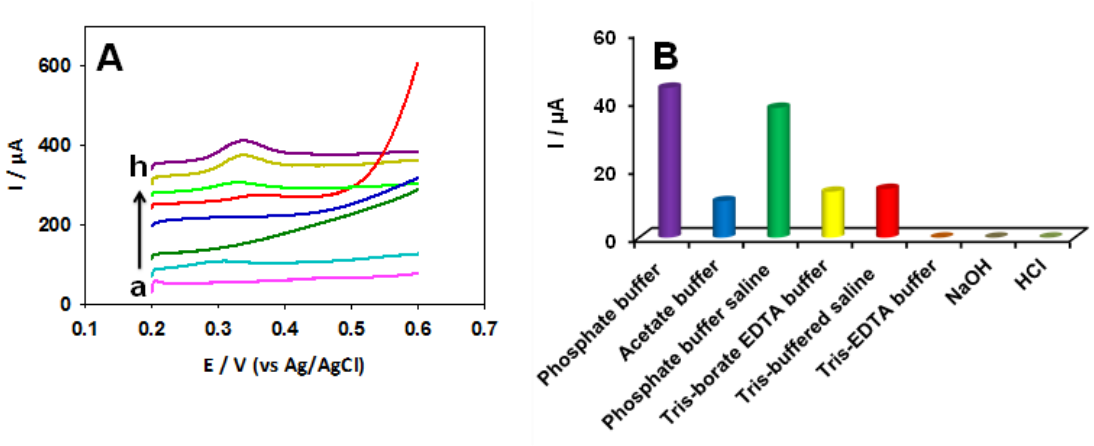


**Figure 3. 7. (A) LSASVs of 5 µM α-naphthol in different supporting electrolytes. a) 0.1M HCl, b) 0.1M acetate buffer, c) 0.1M NaOH, d) 0.1M tris-EDTA buffer, e) 0.1 M tris-borate EDTA buffer, f) 0.02 M tris-buffered saline, g) 0.01 M phosphate buffer saline and h) 0.1 M Phosphate buffer solution. Pretreatment solution 0.8 M NaOH, other working conditions are same as mentioned in Figure 3.4. (B) The corresponding histogram.**

The pH value of the detection buffer, as well as the LSASV parameters, greatly influence the detection limit of α-naphthol. Thus, the effect of pH and the optimization of LSASV parameters for α-naphthol electro-oxidation on PGPE were analyzed. The effect of pH on the LSV response to the electrooxidation of a 5 µM α-naphthol in phosphate buffer at pretreated GPE was systematically studied over the pH range of 4.0 to 8.0. As the pH increased, the electro-oxidation peak potential (Ep) of α-naphthol became less

positive (Figure 3. 8 B inset), Figure 3. 8 B shows that the highest electro-oxidation signal was obtained at pH 6.0. Since pH 6.0 was the optimum pH.

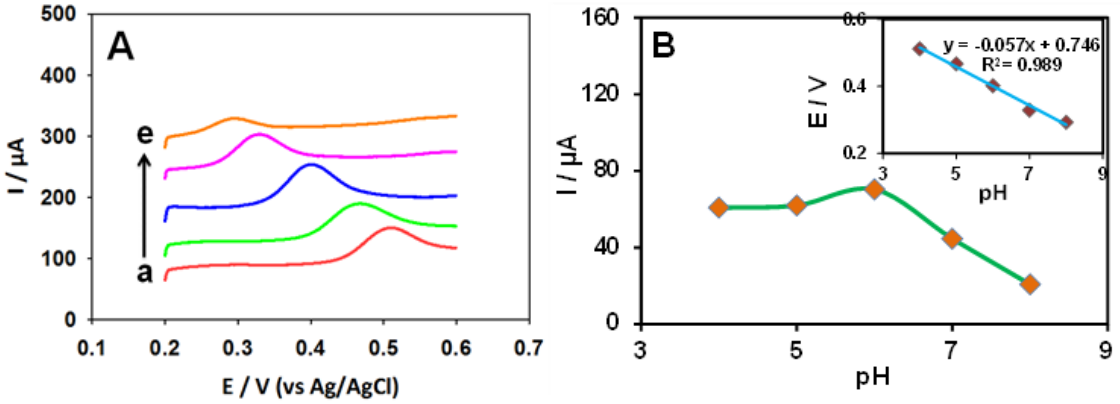


**Figure 3. 8. (A) LSASVs of 5 µM α-naphthol in 0.1 M phosphate buffer at different pH: a) 4.0, b) 5.0, c) 6.0, d) 7.0 and e) 8.0. Pretreatment solution 0.8 M NaOH, other working conditions are same as mentioned in Figure 3. 4. (B) The corresponding plot of pH vs peak current and inset is the plot of pH vs peak potential.**

### 3.1.3.4 Optimization of LSASV parameters

In order to determine the effect of scan rate variation on the activity of PGPE, detection of α-naphthol was carried out at different scan rate values. Corresponding histogram obtained show a prominent variation in peak current. By increasing scan rate the peak current also increase upto 6000 $mVs^{-1}$ as show in Figure 3. 9 A.

Afterward, in order to determine the effect of sample interval on the activity of PGPE different sample intervals were applied for detection of 5 µM α-naphthol by keeping all the parameters constant (same as Figure 3. 4 A). Highest peak current was obtained when 0.003V sample interval was applied (Figure 3. 9 B). So, 0.003V was regarded to be optimum sample interval for α-naphthol detection.

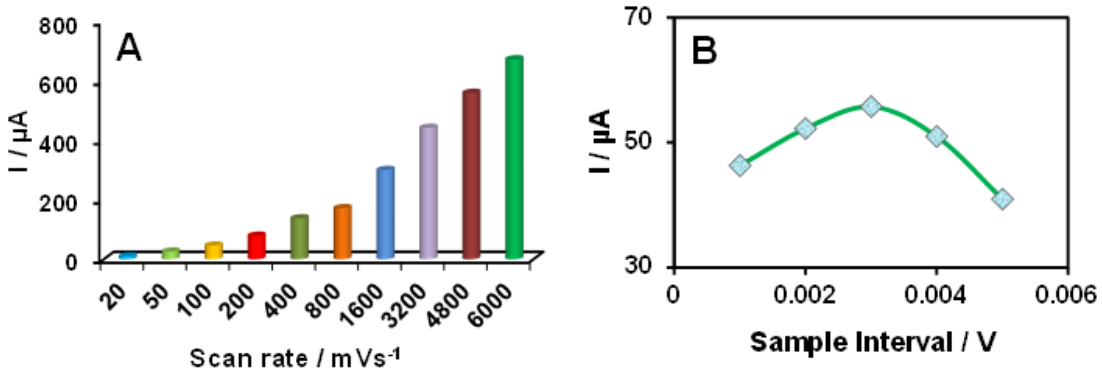


**Figure 3. 9. plot of peak current vs scan rate (A) and sample interval (B) of LSASVs of 5 µM α-naphthol in 0.1 M phosphate buffer solution, pH 7.0, pretreatment solution 0.8 M NaOH, other conditions are described in Figure 3. 4.**

Optimization of deposition time was done for detection of α-naphthol by PGPE. Time was varied from 0 to 300 seconds, with increase in deposition time the peak current also increases up to 180 sec after that it became nearly constant as mentioned in Figure 3. 10 inset B.

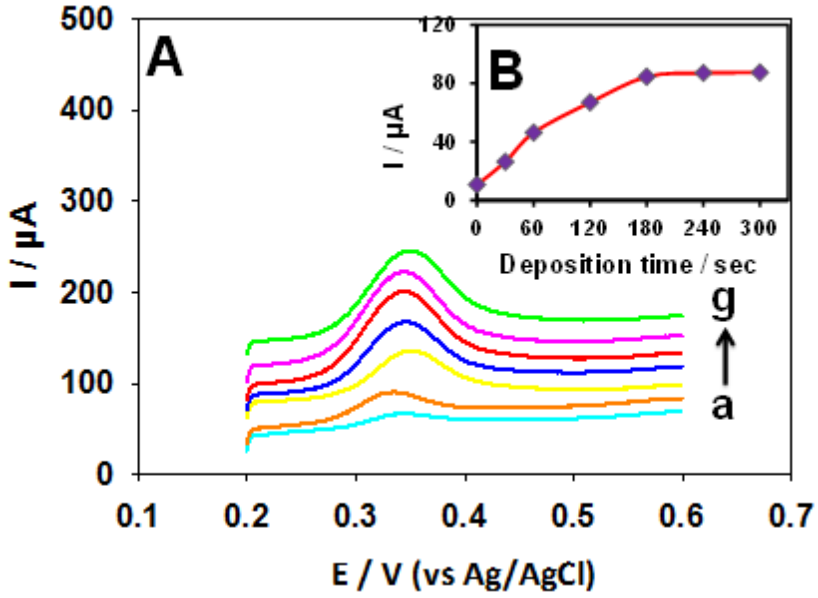


**Figure 3. 10. (A) LSASVs of 5 µM α-naphthol in 0.1 M phosphate buffer solution, pH 7.0 at different deposition times a) 0, b) 30, c) 60, d) 120, e) 180, f) 240 and g) 300 sec. Pretreatment solution 0.8 M NaOH, other conditions are described in Figure 3. 4. Inset (B) is the corresponding plot of ip vs deposition time.**

Finally, deposition potential was optimized for 5 µM α-naphthol at PGPE. Deposition potential was varied from -0.5 V to 0.5 V, the peak current was highest for the -0.1 V deposition potential as mentioned in Figure 3. 11 A and B. The optimal LSASV parameters are summarized in Table 3. 2.

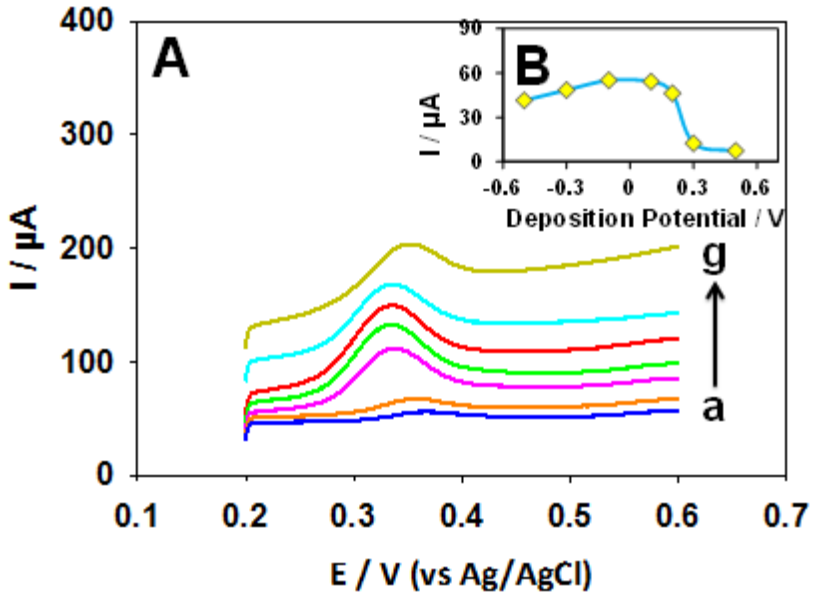


**Figure 3. 11. (A) LSASVs of 5 µM α-naphthol in 0.1 M phosphate buffer solution, pH 7.0 at different deposition potentials a) 0.5, b) 0.3, c) 0.2, d) 0.1, e) -0.1, f) -0.3 and g) -0.5 V. Pretreatment solution 0.8 M NaOH, other conditions are described in Figure 3. 4. (B) The corresponding plot of ip vs deposition potential.**

**Table 3. 2. Optimal detection parameters for α-naphthol by the linear sweep anodic stripping voltammetry method using a pretreated electrode.**

| Sensing media | Technique | Detection sample interval (V) | Detection scan rate (mV/s) | Deposition potential (V) | Deposition time (sec) |
|---|---|---|---|---|---|
| 0.1M Phosphate buffer (pH 6.0) | Linear sweep anodic stripping voltammetry | 0.003 | 6000 | -0.1 | 180 |

### 3.1.3.5 Reproducibility

To check for reproducibility, five LSASVs of 0.5 µM α-naphthol was assessed at five new PGPE surfaces under the optimum conditions (data not shown). The mean ± standard deviation peak current was 307.56 ± 4.056 µA, with an RSD of 1.32 %.

### 3.1.3.6 Interference study

The selectivity of PGPE was investigated in the presence of variety of organic compounds in 0.7 µM α-naphthol solution. The oxidation current of α-naphthol with the presence of different other analytes was repetitively measured three times, and the average current values were evaluated. The results showed no prominent interference was observed for the same quantity of the following compounds 3,4-dichlorophenol, phenol, 4-bromophenol, 4-nitrophenol, 2,3-dichlorophenol, ascorbic acid, hydrazine, glucose, fructose and 4-aminobenzoic acid. Results are mentioned in table 3. 3.

**Table 3. 3. Effect on peak current of 0.7 µM α-naphthol electro-oxidation at GCPE electrodes under optimum conditions in the presence of various contaminants (0.7 µM).**

| Potential interference | Signal change % | Potential interference | Signal change % |
|---|---|---|---|
| 3,4-Dichlorophenol | -2.87 | Hydrazine | -4.11 |
| Phenol | -10.30 | Glucose | -8.45 |
| 4-Bromophenol | +2.30 | Fructose | -6.22 |
| 4-Nitrophenol | -1.24 | Ascorbic acid | -20.02 |
| 2,3-Dichlorophenol | +5.71 | 4-Aminobenzoic acid | -6.37 |

### 3.1.3.7 Calibration

Dependence of α-naphthol peak currents on its concentration presented in Figure 3. 11. Under optimum conditions as mentioned in table 1 and 2 the peak currents were linearly proportional to the α-naphthol concentration in the range of 0.01 to 2.0 µM with $R^2$ = 0.999 (Figure 3. 12, inset A) and low concentration plot of ip vs [α-naphthol] 0.01 to 0.1 µM with $R^2$ = 0.997 (Figure 3. 12, inset B). So the limit of quantification is 0.01 µM, and limit of detection is 1.5 nM (based on S/N=3) for α-naphthol by PGPE.

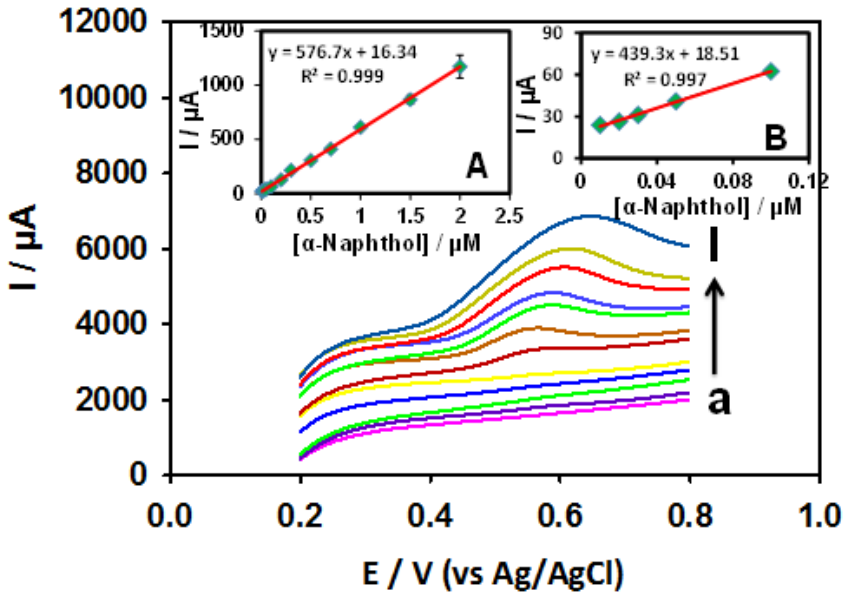


**Figure 3. 12. Linear sweep anodic stripping voltammograms at the pretreated GPE in 0.1 M phosphate buffer solution, pH 6.0 containing different α-naphthol concentrations: a) 0, b) 0.01, c) 0.03, d) 0.05, e) 0.1, f) 0.5, g) 1.0, h) 1.5, i) 2.0, j) 3.0, k) 5.0 and l) 10.0 µM. The other working conditions were as mentioned in Table 3. 1. The inset (A) shows the corresponding calibration curve, and inset (B) show the calibration curve corresponding to low concentration 0.01 – 0.1 µM.**

### 3.1.3.8 Determination of α-naphthol in water samples

Detection of α-naphthol in water samples by non-pretreated GPE is impossible due to low electroactivity. The ability of the PGPE was investigated to detect low concentrations of α-naphthol in water samples. Table 4 displays the promising outcomes gained from the PGPE for added amount of α-naphthol.

**Table 3. 4. Concentration of α-naphthol spiked in water was measured by PGPE.**

| S. No. | Water samples | Added concentration (µM) | Detected by PGPE method (µM) | % Recovery of electrochemical method |
|---|---|---|---|---|
| 1 | Sea water | 0.7 | 0.657 | 93.95 |
| 2 | Swimming pool water | 0.7 | 0.641 | 91.69 |
| 3 | Tap water | 0.7 | 0.638 | 91.27 |
| 4 | Drinking water | 0.7 | 0.609 | 87.13 |

(where n=3)

When we compare present strategy with previously developed methods, it shows comparable results (table 3. 5).

**Table 3. 5. Comparison of analytical performance of some electrochemical sensors for α-naphthol.**

| Technique | Sensing materials | Sensing media (pH) | Linear range (µM) | Limit of detection (nM) | Limit of quantification (µM) | Ref. |
|---|---|---|---|---|---|---|
| Linear sweep anodic stripping voltammetry | Pretreated GPE | 0.1 M PB (pH 6.0) | 0.01 – 2.0 | 1.5 | 0.01 | This work |
| Linear sweep voltammetry | PtNPs/CNTs modified GCE | 0.1 M AB (pH 5.8) | 1.0 – 800 | 500 | 11 | [118] |
| Cyclic voltammetry | PAO film modified GCE | PBS (pH 7.4) | 0.2 – 3.2 | 80.0 | 0.2 | [119] |
| Differential pulse voltammetry | Nano-$TiO_2$/MWNTs Composite Film Modified GCE | 0.1 M AB (pH 5.57) | 0.83 – 10 | 350 | 0.83 | [112] |
| Amperometry | MWNTs Modified GCE | – | 1 – 3000 | 400 | 1 | [113] |
| Differential pulse voltammetry | HIF $SnO_2$ modified GCE | 0.1 M $Na_2SO_4$ | 0.02 – 0.4 | 5.0 | 0.02 | [106] |
| Differential pulse voltammetry | Denatured DNA-Modified Pretreated GCE | 0.10 M AB (pH 5.0) | 0.01 – 1.1 | 5.0 | 0.01 | [38] |
| Electrochemical impedance spectroscopy | G-DNA modified gold electrode | 0.02 M Tris-$ClO_4$ buffer (pH=7.4) | 0.001 – 100 | 0.1 | 0.001 | [108] |
| Differential pulse voltammetry | HS-β-CD/AuNPs/HNCMS modified GCE | 0.1 M PBS (pH 7.4) | 0.002 – 0.15 | 1.0 | 0.002 | [109] |
| Differential pulse voltammetry | β-CD-PtNPs/ GNs modified GCE | 0.1 M PBS (pH 7.4) | 0.0008 – 0.22 | 0.23 | 0.0008 | [111] |

## 3.2 Indirect detection of α-naphthol

### 3.2.1 Introduction

Polyaromatic hydrocarbons (PAHs) are widely existent and one of most structurally variable class of organic compounds. They are ever-present to our surroundings and categories as pollutants [119,120]. Majorly, combustion of fossil fuels is one of the bigger source of PAHs in environment, although plants and microorganisms

also contribute to concentration of PAHs in our surroundings [121,122]. Increased concertation of PAHs believed to be a prominent environmental and occupational health problem. Currently separate recognition of PAH is of excessive curiosity. α-naphthol (α-NAP) is usually utilized as biomarker to determine the extent of contact of PAH [123]. α-NAP is widely used for manufacturing of dyes, pigments, and pharmaceuticals. Existence of α-NAP in human body can cause liver, excretory organ and tegument problems. In severe cases, α-NAP can cause hemolytic anemia and cancer [124]. The above-mentioned issue made the close monitoring of α-NAP very important.

Different kinds of analytical procedures have been formulated for the espial of α-NAP, which include spectrophotometry [125], chromatography [126], and fluorescence [127]. Most of methodologies are time-inefficient and expensive due to the samples pretreatment and extraction is required. Electrochemical methods are attractive for quantification of α-NAP as they are inexpensive, uncomplicated, and quick. Various sort of attempts have been utilized for detection of α-NAP on modified electrode surfaces. For example, $SnO_2$ modified glassy carbon electrode [106] Poly (acridine orange) film modified glassy electrode [128], multiwall carbon nanotubes modified glassy carbon electrode [113], amino-functionalized, SBA-15-carbon paste electrode [129], and electrochemically treated graphite pencil electrode [26] have been tested for electrochemical determination of α-NAP.

A novel attempt to determine the existence or amount of α-NAP in water and urine samples has been originated. For this purpose, poly(α-naphthol) (p(α-NAP)) is targeted as sign of existence of α-NAP in sample solution. As a result of electrochemical process, α-naphthol has capability to form polymer on the surface of electrode [130].

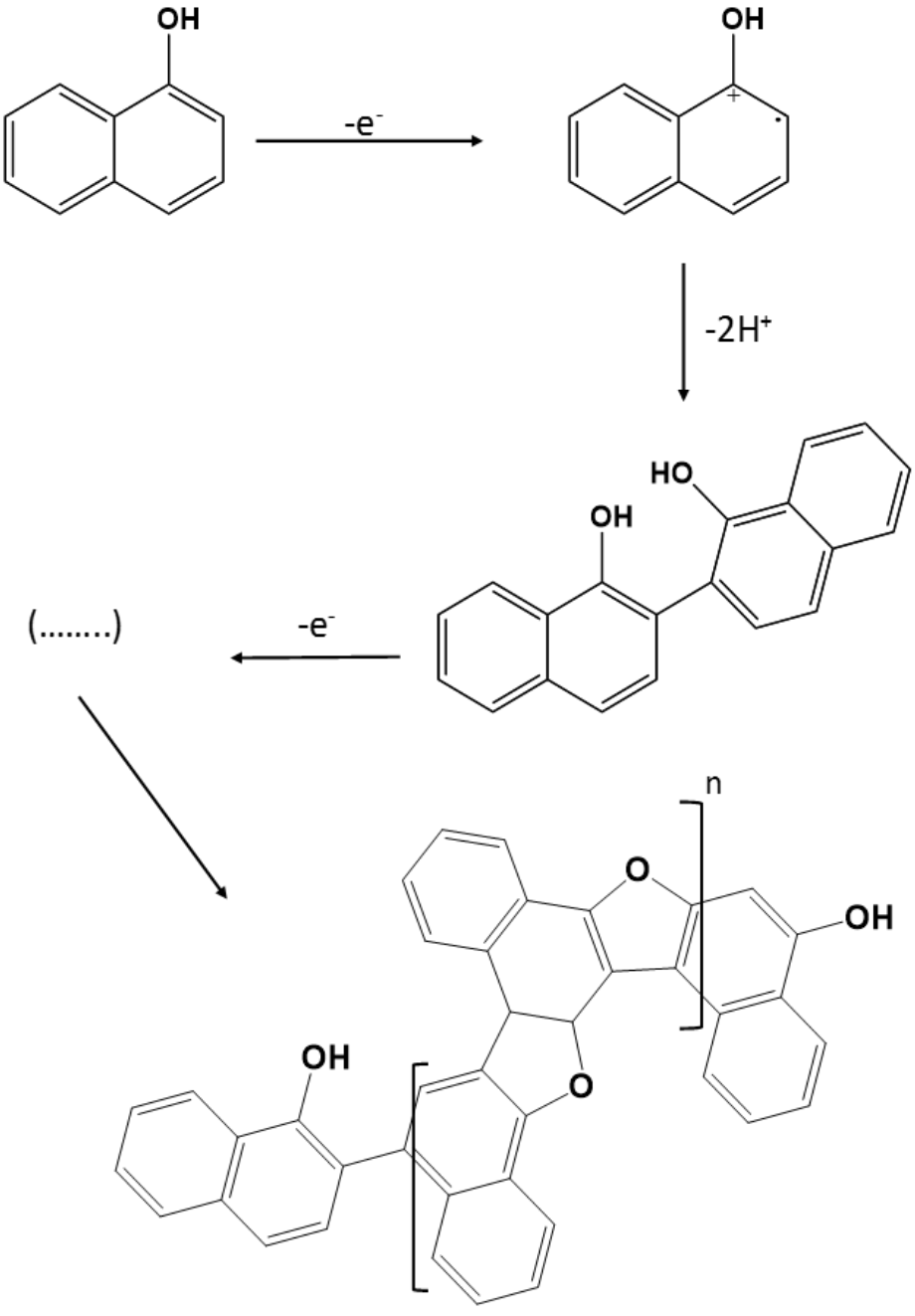


**Figure 3. 13. The polymerization mechanism for α-naphthol in aqueous medium.**

The p(α-NAP) have conducting nature due to presence of switching naphthalene and furan rings [131]. The polymerization mechanism for α-naphthol in aqueous medium is described in scheme 1. p(α-NAP) has ability to attach with the surface of electrode irreversibly, therefore disposable electrode is needed to detect p(α-NAP) with satisfactory results [132]. For this purpose, graphite pencil electrode (GPE) is best candidate. The electrochemical activity of GPE majorly depends on the electron transfer rate and surface functionality. To increase the electrochemical properties of GPE, various strategies can be adopted including electrochemical treatment of the electrode [133]. This process involves oxidation or reduction of bare GPE under certain conditions. As a result the whole chemistry of the GPE surface change as compare to bare electrode [134]. Properties of the treated GPE majorly depends on electrochemical treatment conditions like treatment solution, treatment potential and treatment scan rate. Characteristics of treated GPE basically depends on the treatment solution used during electrode preparation. Therefore, the supporting electrolyte used in electrochemical treatment solution has the ability to predict the electrochemical properties of the GPE for specific analyte [134][135].

In present work, GPE was treated by using KOH to have the single-use electrode surface with greater sensitivity and selectivity towards p(α-NAP) detection in real samples. After careful overview of published literature, we can claim that it is first time that p(α-NAP) is targeted for detection of α-NAP.

### 3.2.2 Experimental

#### 3.2.2.1 Reagents

All chemicals were analytical reagent grade and used without further purification. α-naphthol, sulfuric acid, potassium hydroxide, buffer solution (3.0 M, pH 5.2) were received from Sigma Aldrich® (USA). potassium ferricyanide and potassium ferrocyanide were obtained from Fisher Scientific (USA). All remaining chemicals are same as stated in 2.1.1.

#### 3.2.2.2 Apparatus

Same kind of apparatus is utilized in this study as pronounced in 2.1.2.

#### 3.2.2.3 Preparation of phosphate buffer saline of different pH

1 liter of 0.1 M phosphate buffer saline was prepared by adding calculated amount of monosodium phosphate, sodium chloride, potassium chloride and disodium phosphate which give PBS of pH 6.8. To vary the pH of PBS 0.1 M NaOH and 0.1 M HCl was used.

#### 3.2.2.4 Pretreatment of GPE

10 mm pencil graphite of lead was squeezed out of pencil holder, a reference and counter electrodes were plunged in a cell comprises diverse supporting electrolytes. For electrochemical treatment of GPE surface, 1.6 V potential was applied for 200 sec. Following, double mild sousing into double distilled water to clean the prepared pretreated electrodes. The whole electrochemical detections were executed just after the formulation of the pretreated electrodes. The electrolytes utilized for this purpose included 0.1 M KOH, HCl, $H_2SO_4$, NaOH, $CH_3COONa$, $Na_2HPO_4$, $NaH_2PO_4$, KOH +

$Na_2HPO_4$ mixture, KOH + $NaH_2PO_4$ mixture and KOH + $CH_3COONa$. The PGPEs were denoted as PGPE-PH, PGPE-HA, PGPE-SA, PGPE-NH, PGPE-NA, PGPE-$N_2P$, PGPE-NP, PGPE-PH$N_2P$, PGPE-PHNP and PGPE-PHNA according to supporting electrolytes used; KOH, HCl, $H_2SO_4$, NaOH, $CH_3COONa$, $Na_2HPO_4$, $NaH_2PO_4$, KOH + $Na_2HPO_4$ mixture, KOH + $NaH_2PO_4$ mixture and KOH + $CH_3COONa$, respectively.

### 3.2.2.5 Electrochemical detection

To deposit polymer film of α-naphthol -0.8 V potential was applied for 200 sec in 0.1 M PBS pH 7.0 solution. Afterwards, electrode was washed by dipping gently in double distilled water. Square wave voltammetric (SWV) detections of various concentrations of α-NAP were executed under optimal conditions in PBS (0.1 M, pH 7.0). Afterward, 10 s respite period under quiescent circumstances the deposited polymer of α-NAP on the surface of PGPE was detected.

### 3.2.2.6 Sample preparation

Water samples were gathered from tap in the lab, commercially available drinking water and sewage water in local area. Water samples were initially filtered by utilizing a filter paper of pore size 0.45 µm to eliminate any insoluble material and then for electrochemical detection 1.0 ml of each water sample was diluted up to 5 ml by utilizing 0.1 M PBS, pH 7.0.

### 3.2.2.7 Urine sample

Urine samples were gathered in vials and retain in refrigerator. Before analysis 0.5 µL of urine was dilute to 5 ml by using 0.1 M PBS pH 7.0.

### 3.2.3 Results and discussion

#### 3.2.3.1 Preliminary investigation

To activate surface of carbon electrodes electrochemical pretreatment is obligatory. The effect of electrochemical pretreatment at oxidation potential (e.g., +1.6 V vs. Ag/AgCl) on the graphite pencil electrode (GPE) surface was studied. The multiple CV scan of pretreated graphite pencil electrode (PGPE) in 50 µM solution of α-naphthol (α-NAP) show that in first scan a prominent reversible oxidation peak (P1) appeared at 0.310 V and two small peaks (P2 and P3) came along at +1.20 V and -1.60 V respectively. However, after the second scan, P2 and P3 continuously increase by increasing the number of CV scans. The appearance of P2 and P3 can be ascribed as the formation of conducting poly(α-naphthol) (p α-NAP) on the surface of PGPE. If we focus on reduction peaks for P1, P2, and P3, there is wide separation between P1 and P3. Though, the reduction peaks for P1 and P2 are overlapping and showing poor separation from each other as shown in Figure 3.14 A.

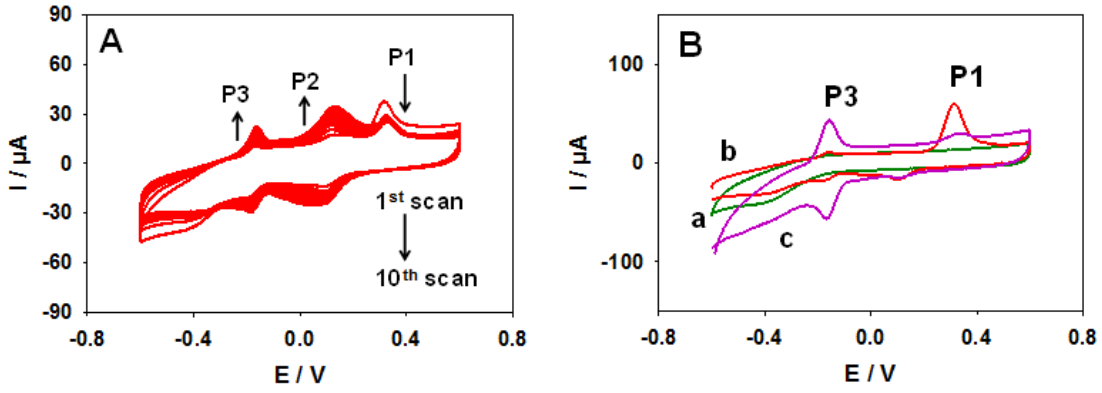


**Figure 3. 14. (A) CV scans of 50.0 µM α-naphthol in 0.1 M phosphate buffer saline, pH 7.0 (B) CVs in 0.1 M phosphate buffer saline, pH 7.0 in the absence (a) and presence (b and c) of 50.0 µM α-naphthol, scan rate 100 mV/s.**

In order to target the p(α-NAP) peak deposition potential was applied. Figure 3.13 B depicts that when no deposition potential was applied on PGPE there is prominent P1

peak for α-naphthol but very small P3 peak for p(α-NAP). Nevertheless, when -0.8 V deposition potential was applied to the PGPE the P3 at -1.6 V appeared confirming the formation of p(α-NAP) on PGPE during the deposition process. This peak P3 for p(α-NAP) is targeted, and conditions are optimized in the remaining study.

### 3.2.3.2 Effect of pretreatment conditions for the preparation of PGPE for the α-NAP determination

Potential for pretreatment of GPE plays very important role in sensitive and selective detection of target analyte. That is why consequence of treatment potential was studied on voltammetric signal of PGPE treated in 0.1 M NaOH at different potentials.

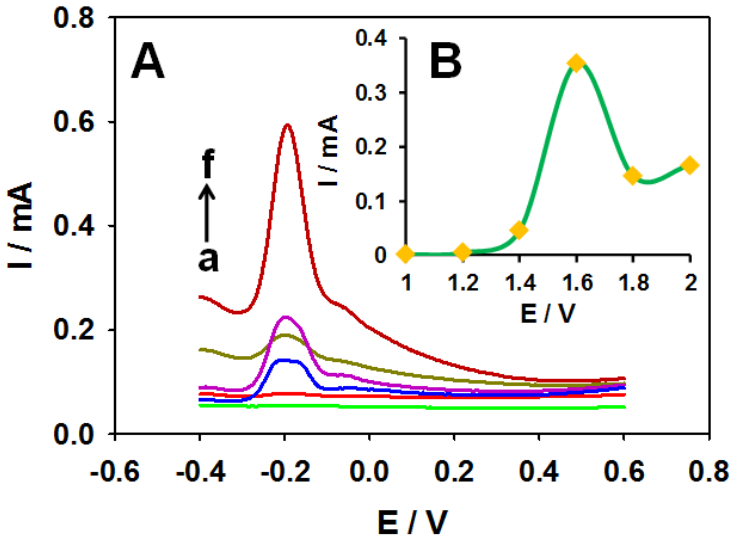


**Figure 3. 15. (A) SWVs of 1.0 µM poly α-naphthol in 0.1 M phosphate buffer saline, pH 7.0 at various pretreatment potentials: a) +1.0, b) +1.2, c) +2.0, d) +1.4, e) +1.8 and f) +1.6 V. Working conditions: Pretreatment is done in 0.1 M NaOH, pretreatment time 150 sec, frequency 50 Hz, amplitude 0.06 V, deposition potential -0.8 V and deposition time 200 sec (B) The corresponding plot of peak currents ip (mA) vs deposition potential (V).**

The electrochemical activities of the disposable electrodes were assessed by square wave adsorptive stripping voltammetry (SWASV) measurements of 1.0 µM α-NAP in PBS (pH 7.0). It was observed that there is no or very minute response of PGPE

when treated at +1.0 V, +1.2 V, +1.4 V, +1.8 and +2.0 (Figure 3. 15). However, the abrupt gain in peak current of 1.0 µM α-NAP was observed when +1.6 V potential was employed for treatment of electrode. So, +1.6 V was chose as optimal potential for pretreatment of GPE.

In order to optimize the treatment time, PGPE was pretreated for different intervals in 0.1 M NaOH potentiostatically. The outcomes proved that by increasing the treatment time upto 200 sec also increase the peak current for α-NAP. However, further, increase in treatment time prominently decrease (Figure 3 16). Therefore, 200 secs were considered to be optimum for the treatment of PGPE.

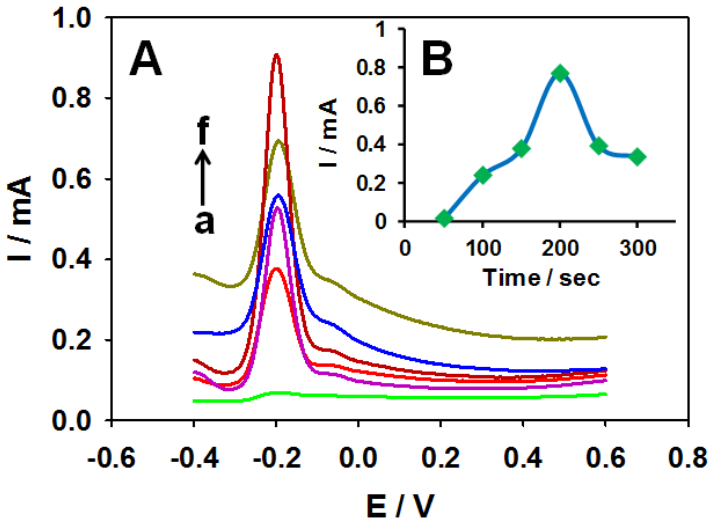


**Figure 3. 16. (A) SWVs of 1.0 µM poly α-naphthol in 0.1 M phosphate buffer saline, pH 7.0 at different treatment time: a) 50, b) 100, c) 250, d) 300, e) 150 and f) 200 sec. Other working conditions are same as in Figure 3. 14. (B) The corresponding plot of peak currents ip (mA) vs. pretreatment time (sec).**

For the electrochemical treatment of GPE different supporting electrolytes were employed under identical circumstances. Figure 3.17 shows the oxidation signal values of α-NAP in the presence of various supporting electrolytes. There was no or very small voltammetric response of GPE treated with 0.1 M HCl, 0.1 M $CH_3COONa$, 0.1 M $H_2SO_4$,

0.1 M $NaH_2PO_4$, 0.1 M $Na_2HPO_4$, 0.05 M KOH + 0.05 M $CH_3COONa$, 0.05 M KOH + 0.05 M $NaH_2PO_4$ and 0.1 M PBS. However, 0.1 M KOH, 0.1 M NaOH, and mixture of 0.05 M KOH + 0.05 M $Na_2HPO_4$ show sharp peaks with high signal strength. PGPE treated with 0.1 M KOH displayed highest peak current for 1.0 µM 1- NP. According to the outcomes, the aqueous solution of 0.1 M KOH was selected as the medium for pretreatment of GPE to get PGPE, and further optimization was done by utilizing the same mixture.

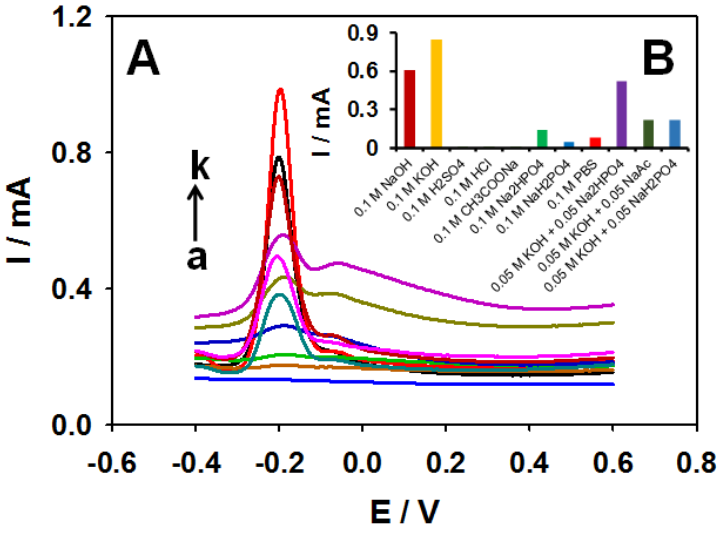


**Figure 3. 17. (A) SWVs of 1.0 µM α-naphthol in 0.1 M phosphate buffer saline, pH 7.0 at treated GPEs in various media: a) 0.1 M HCl, b) 0.1 M $CH_3COONa$, c) 0.1 M $H_2SO_4$, d) 0.1 M $NaH_2PO_4$, e) 0.05 M KOH + 0.05 M $CH_3COONa$, f) 0.1 M PBS, g) 0.05 M KOH + 0.05 M $NaH_2PO_4$, h) 0.1 M $Na_2HPO_4$, i) 0.05 M KOH + 0.05 M $Na_2HPO_4$, j) 0.1 M NaOH and k) 0.1 M KOH solutions. Pretreatment is done in 0.1 M NaOH, pretreatment potential +1.6, pretreatment time 200 sec, frequency 50 Hz, amplitude 0.06 V, deposition potential -0.8 V and deposition time 200 sec (B) corresponding histogram.**

Finally, impact of amount of KOH on the electrocatalytic activity of PGPE was studied. Concentration of KOH was varied between 0.05 to 1.4 M. The results showed (Figure 3. 18) that maximum oxidation current of α-NAP was obtained when 1.0 M KOH was utilized and this concentration was considered to be optimal for treatment of GPE.

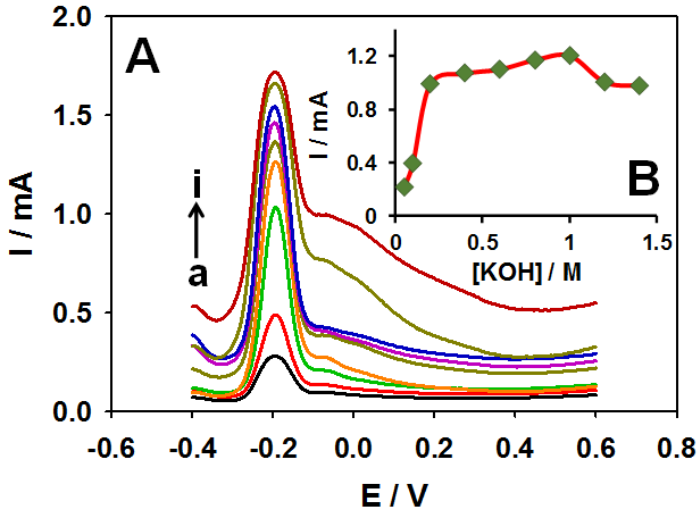


**Figure 3. 18. (A) SWVs of 0.5 µM poly α-naphthol in 0.1 M phosphate buffer saline, pH 7.0 pretreated GPEs in various concentrations of KOH: a) 0.05 M KOH, b) 0.1 M KOH, c) 0.2 M KOH, d) 0.4 M KOH, e) 0.6 M KOH, f) 0.8 M KOH, g) 1.0 M KOH, h) 1.2 M KOH and i) 1.4 M KOH solutions. Other working conditions are same as in Figure 15 (B) The corresponding plot of peak currents ip (mA) vs concentration of KOH (M).**

### 3.2.3.3 Characterization of PGPE

When GPE was pretreated in KOH, high electroactivity of subsequent electrode was observed. Therefore. all the characterizations of PGPE were focused on the PGPE prepared in 1.0 M KOH. The characterization of PGPE was done by utilizing different techniques like cyclic voltammetry (CV), electrochemical impedance spectroscopy (EIS) and square wave voltammetry (SWV).

The $Fe(CN)_6^{3-/4-}$ redox couple is commonly used to measure the electrochemical activity of modified surfaces of electrode. firstly, the CV measuring were executed in 0.1 M KCl solution of 5 mM $Fe(CN)_6^{3-/4-}$ and results are mentioned in Figure 3. 19 A, the results showed that use of bare-GPE showed very broad peak for $Fe(CN)_6^{3-/4-}$. On the other hand, utilization of 1 M KOH had a noticeable effect on the electrochemical behavior of electrode, where not only the peak current amplified but also there is a big

change in shape of redox peaks. The prominent increase in peak current for $Fe(CN)_6^{3-/4-}$ can be ascribed to the large surface area of PGPE and large number of functional groups attached during the pretreatment process. It can be concluded that PGPE showed different characteristics from bare-GPE.

In order to relate the cyclic voltammetric behavior of untreated and treated GPE in 6 M solution of NaOH at scan rate of 2 $mVs^{-1}$ (Figure 3. 19 B). Calculation of capacitance for both electrodes was done by using equation 3.1. [133]

$$C = Q / \Delta E \, . \, m \qquad 3.1$$

Where voltammetric charge is denoted by Q, mass of electrode material is ‘m‘ and potential window ‘ΔE‘ for the CV scan. The capacitance of PGPE was 79 times higher as compared to bare-GPE. The outstanding enhancement of specific capacitance of treated GPE surface can be ascribed to the accumulation and formation of charge carrier species on electrode during pretreatment of electrode.

Furthermore, Figure 19 C the Nyquist plots of untreated GPE and PGPE in 0.1 M KCl solution of 5 mM each of $K_4[Fe(CN)_6]$ and $K_3[Fe(CN)_6]$ by using a frequency range of 0.01 Hz to 100 kHz. The Z and –Z axes designate to the real and imaginary values of the imagined impedance variables, correspondingly. The Nyquist diagram attained from GPE consist of a semicircle and a straight line, whereas only a straight line was obtained for PGPE. The semicircular part at higher frequencies showed a limiting charge transfer process at the electrode/electrolyte interface, although straight line of the graph at low frequency area is attributed to the diffusion process in solid. Consequently, the ohmic resistance for electrochemical reaction is comparatively much smaller at PGPE. The

PGPE show high slop at low frequency region suggesting that PGPE is more capacitive as compared to untreated GPE.

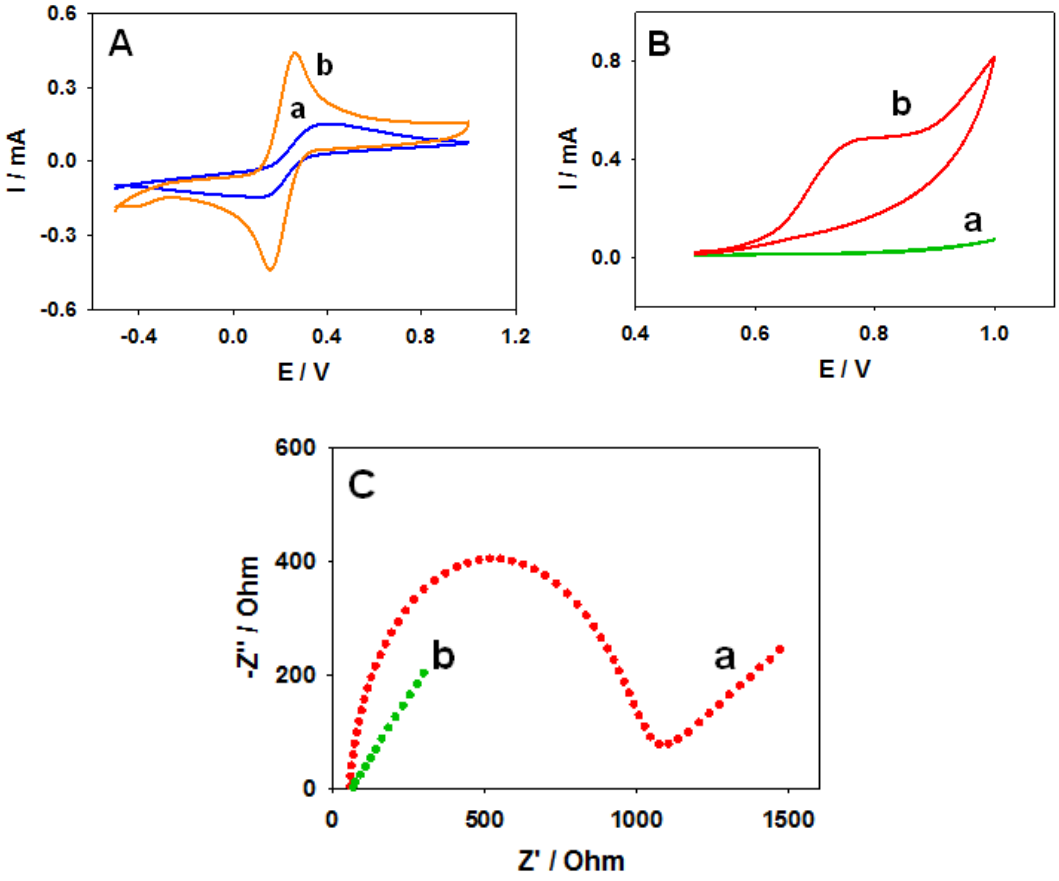


**Figure 3. 19. A) CVs of 5.0 mM $Fe(CN)_6^{3-/4-}$ obtained in 0.1 M KCl by the untreated a) GPE and b) GPE treated in 1.0 M KOH, B) CVs in 6 M NaOH electrolyte at 2 mV/sec scan rate a) untreated GPE and b) treated in 1.0 M KOH. C) Nyquist plots in 0.1 M KCl solution containing a mixture of 5 mM $K_4[Fe(CN)_6]$ and 5 mM $K_3[Fe(CN)_6]$ of untreated (a), and treated (b) GPE.**

The electroactive surface are of untreated and pretreated GPE was calculated by utilizing Randles–Sevcik equation 3.2. [136]

$$I_p = 2.69 \times 10^5 C n^{3/2} A D^{1/2} \gamma^{1/2} \qquad 3.2.$$

Where $I_p$ refers to anodic peak current, concentration of the analyte (mol $L^{-1}$) is denoted by C, number of electrons transferred during the redox reaction on the electrode surface are signified as n, electroactive surface area of the electrode ($cm^2$) is symbolized as A, diffusion coefficient ($cm^2s^{-1}$) is indicated as D and γ is the scan rate (V $s^{-1}$). For the electroactive area calculation, CV scans were recorded between 5 to 500 mV in 5 mM solution of $K_4[Fe(CN)_6]$, $K_3[Fe(CN)_6]$ and 0.1 M KCl by utilizing untreated GPE and PGPE Figure 3. 20. By using above mentioned equation, electroactive areas obtained 0.504 $mm^2$ and 1.07 $mm^2$ for untreated and pretreated GPEs respectively. Subsequently, it can be stated as the electroactive surface area of PGPE is higher as compare to untreated GPE.

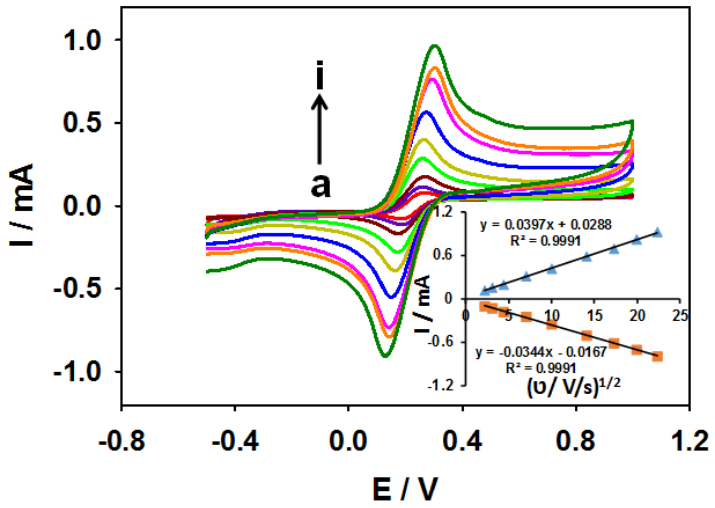


**Figure 3. 20. Cyclic voltammograms of the PGPE obtained in 5.0 mM $Fe(CN)_6^{3-/4-}$ at various scan rates: (a) 5, (b) 10, (c) 20, (d) 50, (e) 100, (f) 200, g) 300, (h) 400 and i) 500 mV/s. Inset is plot of peak currents vs. square root of scan rates.**

The electrochemical performances of the untreated and treated GPEs were analyzed by utilizing adsorptive stripping square wave voltammetric measurements in the presence and absence of 0.5 µM α-NAP in PBS, pH 7.0 (Figure 3. 21). When square voltammetric scan was run in PBS without adding α-NAP, no peak current was obtained

for both untreated and treated GPEs. However, the background peak current was significantly higher for PGPE as compared to untreated GPE. This was due to increase in surface area of GPE after treatment in KOH solution mixture. After that, addition of 0.5 µM α-NAP showed an oxidation peak for both treated and untreated GPEs. The oxidation of α-NAP occurred at -0.208 V for the untreated GPE, while oxidation peak for α-NAP appears at potential of -0.204 V for treated GPE. The number of functional groups on electrode surface depends on the treatment strategy and material used as electrode. Increase in hydrophilic character corresponds to the entrance of oxygen on GPE surface in the form of hydroxy, carbonylic and carboxyl groups. The comparative quantity of these functional groups conspicuously effects the selectivity of PGPE. Presence of hydroxyl and carbonyl group on the surface of electrode not affect the charge but change the adsorption properties of electrode, however high value of carboxylic group introduce a negative charge that resulted in more attraction for the cationic molecules [137]. The GPE treated with KOH produce noticeable impact on the electrochemical attributes of PGPE.

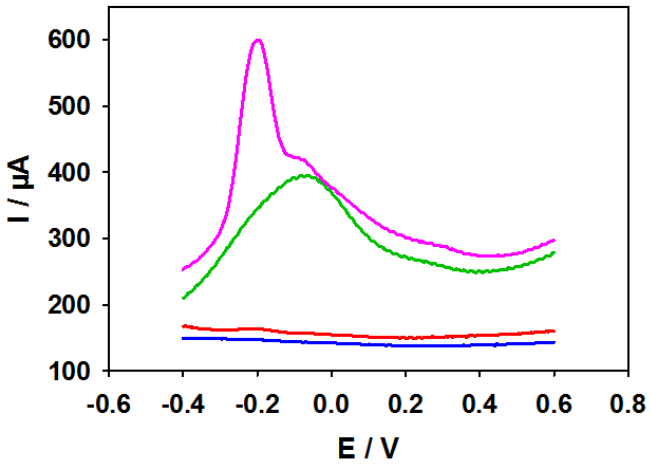


**Figure 3. 21. Square wave voltammograms of the untreated GPE (a and b) and PGPE (c and d) in the absence (a and c) and presence (b and d) of 0.5 µM 1-NP in PBS (pH 7.0). Amplitude 0.06 V, frequency 50 Hz, accumulation time 60 sec and deposition potential -0.8 V.**

### 3.2.3.4 Effect of detection medium and pH on the electrochemical behavior of α-NAP

In order to study the consequence of polymerization medium on voltammetric current of PGPE, assorted buffers such as PB, AB and PBS pH 7.0 were used. Results revealed that highest signal was found in case of PBS as detection medium. For selection of best detection medium PB, AB and PBS pH 7.0 solutions were utilized, and PBS presented maximum signal for α-NAP polymer (Data not shown).

Afterwards, effect of pH of detection medium on peak current of 0.5 µM α-NAP was investigated. For this purpose, PBS solutions of various pH were prepared, it was observed that change in pH prominently effect peak current. The peak current was plotted against the pH (Figure 3.22) that show increase in oxidation peak by increasing the pH from 5.0 to 6.5, subsequently signal become almost constant upto 7.5 and then suddenly decrease at pH value of 8.0. The outcomes demonstrate that the highest voltammetric current was found at pH 7.0, which was selected and maintained as the optimal pH for rest of study of α-NAP.

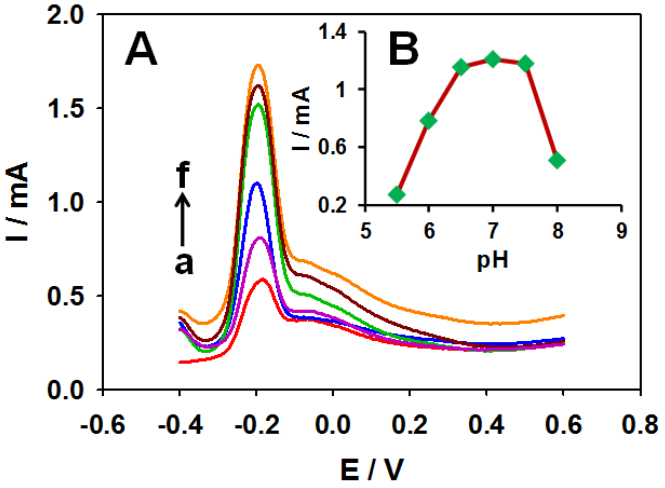


**Figure 3. 22. (A) SWVs of 0.5 µM α-naphthol in 0.1 M phosphate buffer saline of various pH: a) 5.0, b) 8.0, c) 6.0, d) 6.5, e) 7.5 and f) 7.0. Other working conditions are same as in Figure 3. 16 (B) The corresponding plot of peak currents ip (mA) vs pH of supporting electrolyte.**

### 3.2.3.5 Optimization of SWASV parameters

In order to get best oxidation current of α-NAP frequency and amplitude was optimized. The experiments proved that at 0.06 V amplitude and 50 Hz frequency highest signal for α-NAP polymer was obtained (Data not shown). Deposition potential plays very important role in getting best oxidation current but also determine peak shape and peak position. That is why optimization of deposition potential became very crucial. For this purpose, deposition potential was altered between -0.2 V to -1.4 V. Plot of peak current vs. deposition potential express that by increasing the potential from -0.2 to -0.8peak current of 0.5 µM α-NAP also increase, after -0.8 V the current signal started to decrease sharply (Figure 3. 23). Consequently -0.8 V was chose as the optimum deposition potential.

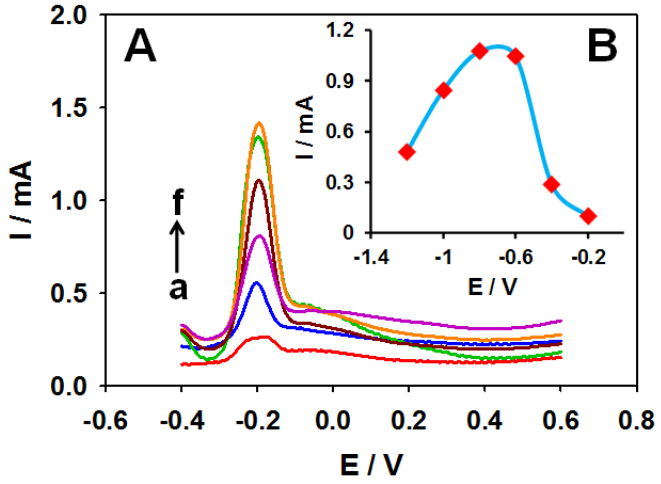


**Figure 3. 23. (A) SWVs of 0.5 µM α-naphthol in 0.1 M phosphate buffer saline pH 7.0 at various deposition potentials: a) -0.2, b) -0.4, c) -1.2, d) -1.0, e) -0.6 and f) -0.8 V. Pretreatment is done at +1.6 V for 200 sec in 1.0 M KOH and other working conditions are same as in Figure 3.16 (B) The corresponding plot of peak currents ip (mA) vs deposition potential (V).**

Finally, the upshot of deposition time on the oxidation current of α-NAP was studied. The magnitude of peak current of 0.5 µM α-NAP increased by increasing the contact time of PGPE at optimized potential (Figure 3.24). The surface concentration of α-NAP on the PGPE is mainly dependent on the contact time of electrode with analyte solution. As the deposition time prolonged the current also increase upto 320 sec, beyond 320 sec the peak current remains almost constant. Thus, the 320 sec was selected as optimum contact time.

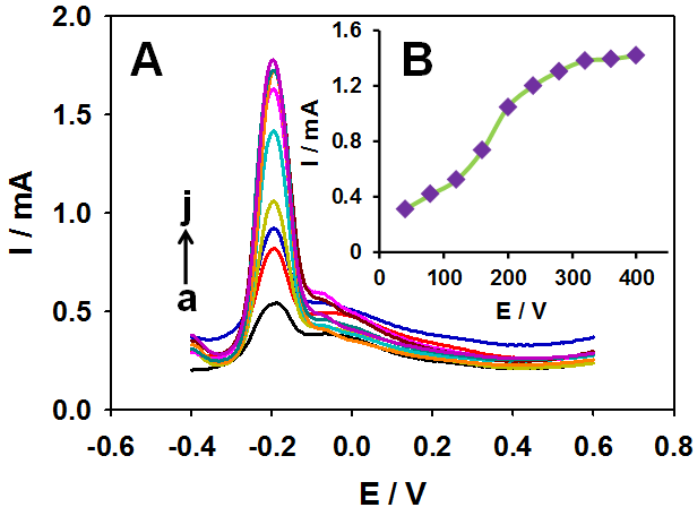


**Figure 3. 24. (A) SWVs of 0.5 µM α-naphthol in 0.1 M phosphate buffer saline pH 7.0 at different deposition time: a) 40, b) 80, c) 120, d) 160, e) 200, f) 240, g) 280, h) 320, i) 360 and j) 400 sec. Pretreatment is done at +1.6 V for 200 sec in 1.0 M KOH and other working conditions are same as in Figure 15 (B) The corresponding plot of peak currents ip (mA) vs deposition time (sec).**

### 3.2.3.6 Analytical parameters

The relation between concentration of α-NAP and oxidation peak current was investigated by utilizing SWASV measurements in the presence of different amounts of α-NAP in PBS pH 7.0 (Figure 3. 25). A linear relation was obtained between 0.02 µM (20 nM) and 0.3 µM (300 nM) (n=3) of α-NAP in the calibration plot of peak current vs. concentration. A linear regression of the calibration curve produced an equation I(µA) = 1252.3 $C_{\alpha\text{-NAP}(\mu M)}$ - 7.7939, with $R^2$ of 0.9986. The detection limit of proposed method was calculated as 0.0089 µM or 8.9 nM of α-NAP (S/N=3).

Reproducibility of fabricated PGPE was evaluated by SWASV measurements of 0.2 µM α-NAP in 0.1 M PBS pH 7.0. Relative standard deviation (RSD) of 4.27 was obtained for six different PGPE treated in same manner.

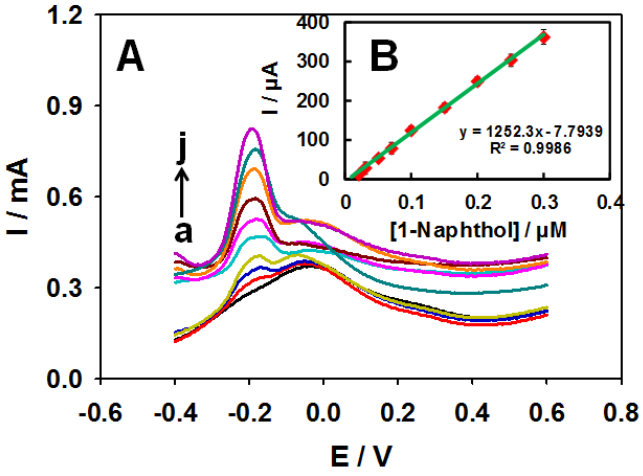


**Figure 3. 25. (A) SWVs of α-naphthol in 0.1 M phosphate buffer saline, pH 7.0 at different concentrations: a) blank, b) 0.02, c) 0.03, d) 0.05, e) 0.07, f) 0.1, g) 0.15, h) 0.2, i) 0.25 and j) 0.3. B) inset is corresponding plot of peak current vs concentration. Other working conditions are mentioned in above table 3.7 and 3.8.**

### 3.2.3.7 Interference Studies

In order to study the effect of possible interfering molecules, SWASV measurements of 0.2 µM α-NAP were done in the presence and absence of interferents; 4-aminophenol, 4-nitrophenol, 2-chlorophenol, 2,4-dichlorophenol, and 3,4-dichlorophenol. 0.2 µM phenol mono derivatives not affect the oxidation peak current conspicuously and introduced minute variation of 1 to 5 %. Di-chloro derivatives of phenol added to 0.2 µM solution of α-NAP increase the oxidation current by 3% or 5 %. In the light of present results, it can be concluded that PGPE is highly selective for the α-NAP and had affinity for the interferents.

**Table 3. 6. Optimized conditions for pretreatment of GPE.**

| Conditions | Transducer | Treatment solution | Treatment potential range | Treatment time |
|---|---|---|---|---|
| **Optimization** | Graphite pencil electrode | 1M KOH | +1.6 V | 200 sec |

**Table 3. 7. Optimized conditions for detection of α-naphthol polymer.**

| Conditions | Technique | Amplitude | Frequency | Deposition time | Deposition potential | Polymerization medium | Detection medium |
|---|---|---|---|---|---|---|---|
| **Optimization** | Square wave voltammetry | 0.06 V | 50 Hz | 320 sec | -0.8 V | PBS, pH 7.0 | PBS, pH 7.0 |

## 3.2.3.8 Analytical Application

The fabricated PGPE was tested in real life water and urine samples. The concentration of α-NAP in water and urine is lower than the detection limit of this method, that is why it in undetectable. In order to determine α-NAP, 0.2 µM α-NAP was added to the samples and equation straight line obtained from calibration curve was utilized to calculate recovery of added analyte. The outcomes reveled the recovery of 104.8 %, 103.9 % and 103.7 % in tap water, commercially available drinking water and sewage water. The recovery of the added α-NAP was 101.1% and 101.8 % for urine samples (table 3. 8). These satisfactory recoveries suggest that PGPE could be valuable for α-NAP detection in real samples which inclines to contain contaminations and interferents.

**Table 3. 8. Application of PGPE to real samples of water and urine.**

| Sr. # | Sample | Added (µM) | Found (µM) | % Recovery |
|---|---|---|---|---|
| **1** | Tap water | 0.200 | 0.209 | 104.80 |
| **2** | Drinking water | 0.200 | 0.207 | 103.94 |
| **3** | Sewage water | 0.200 | 0.207 | 103.70 |
| **4** | Urine | 0.200 | 0.203 | 101.82 |

## 3.3 Summary

The pretreatment of the graphite pencil electrode surface improves its electrochemical catalytic activity towards the oxidation of α-naphthol. Comparison of results obtained with non-pretreated GPE and PGPE reveals that PGPE show high sensitivity and low limit of detection (S/N=3), i.e. 1.5 nM. The surface fouling came with the appearance of reversible peaks at +1.20 V and -1.60 V, that get larger with cyclic voltammetric scans and ascribed to the redox reactions of yielded polymer film through electropolymerization. The electroanalytical oversight of acquired polymer led to extremely sensitive and selective methodology for sensing of α-naphthol. The pretreatment of GPE surfaces was conducted in 1.0 M KOH by the potential +1.6 V for 200 sec. The calibration curve displayed a linear range of 0.02 µM (20 nM) and 0.3 µM (300 nM) with a detection limit of 8.9 nM (S/N=3). PGPE can be considered as a sensor with very low cost and easy in preparation. The proposed sensor can be used for low level detection of α-naphthol, in real water samples with satisfactory results.

# Chapter 4

## The synergetic effect of a mixture of sodium hydroxide and sodium acetate on the graphite pencil electrodes for the trace detection of 4-chloro-1-naphthol in real water samples

### 4.1 Introduction

Polyaromatic hydrocarbons (PAHs) are widely existent and one of most structurally variable class of organic compounds. Polyaromatic hydrocarbons, polyaromatic compounds, polynuclear aromatic hydrocarbons or polycyclic aromatic hydrocarbons are the different names of same class of compounds [138,139]. They are omnipresent to our surroundings and categories as pollutants [119,120]. Majorly, burning of fossil fuels is one of the major source of PAHs in environment, although plants and microorganisms also contribute to concentration of PAHs in our surroundings [121,122]. Due to the fact that these compounds have long residence time in environment and not easily degradable.[140] Increased concertation of PAHs considered to be a major environmental and occupational health problem.[141] PAH are volatile in nature and detection of these compounds helps to measure extent of exposure and the amount of PAHs in body. Laboratory studies on animals showed that PAHs can effect pulmonic, gastral, nephritic, and dermatological structures, although in severe cases effect hematogenic and immune systems and can yield procreative, neurological, and growth impressions, even they can cause cancer [142–146]. Though lots merely not wholly, PAHs are cancer-causing and mutagenic, and composite combinations typically comprise both categories [147–149], the only approach to evaluate the jeopardy postured by those with lavishly carcinogenic nature is to characterize them separately.

4-Chloro-1-naphthol (4-CNP) is chloro derivative of α-naphthol and used as peroxidase substrate for chromogenic detection of horseradish peroxidase (HRP) in immunoblotting and immunohistochemical applications [150,151]. Although there is no enough animal or human study evidence to classify 4-CNP as harmful chemical, but there are some reports showing its toxic and hazardous nature [152]. Exposure to 4-CNP can cause skin, eyes, respiratory irritation and corrosion. In severe cases gastrointestinal irritation with nausea, vomiting, and diarrhea can be observed, it can effect respiratory organs, kidney and liver [153,154]. So, it is very important to detect 4-CNP at very low concentration in real life samples.

It is well known reality that high selectivity, high sensitivity, quick response and low cost make electrochemical techniques highly promising for the recognition of hazardous substances in ecological models [155]. Notwithstanding, detection of 4-CNP is by using bare electrode is very problematic due to lower response and large over-potential. To overwhelm these issues, surface of electrode can be modified by means of various methodologies. However, analyte containing aromatic alcoholic group have the instinct to polymerize on the surface of electrode [73,156] and this property force to move towards disposable electrodes. Owing to being cheap and easy availability, graphite pencil electrode (GPE) is best contender for single-use electrode material. The electrochemical activity of GPE majorly depends on the electron transfer rate and surface functionality. To increase the electrochemical properties of GPE, various strategies can be adopted including electrochemical treatment of the electrode. This process involves oxidation or reduction of bare GPE under certain conditions. As a result the whole chemistry of the GPE surface change as compare to bare electrode [133]. Properties of

the treated GPE majorly depends on electrochemical treatment conditions like treatment solution, treatment potential, and treatment scan rate. Characteristics of treated GPE basically depends on the treatment solution used during electrode preparation. Therefore, the supporting electrolyte used in electrochemical treatment solution has the ability to predict the electrochemical properties of the GPE for specific analyte [134,135].

In this present work, GPE was treated with different supporting electrolytes to have the single-use electrode surface with greater sensitivity and selectivity towards 4-CNP detection in water samples. The study showed that pretreated graphite pencil electrode (PGPE) had an electrocatalytic consequence on the oxidation of 4-CNP while it is treated in a solution comprising supporting electrolytes acetate buffer and NaOH. The electrochemical treatment conditions were optimized, and effect of observational parameters such a pH of detection medium, deposition potential and effect of interferents on the voltammetric response of 4-CNP were methodically inspected. To best of our knowledge, it is first time that mixture of acetate buffer and NaOH is utilized to get PGPE and then used for detection of 4-CNP.

## 4.2 Experimental

### 4.2.1 Reagents

All chemicals were analytical lab reagent grade and utilized with no refinement. 4-CNP, NaF, NaBr, $NaNO_3$, $Na_2SO_4$ $LiClO_4$, and sodium acetate (NA) solution (3.0 M, pH 5.2) were acquired from Sigma Aldrich® (USA). other reagents are same as mentioned in 2.1.1.

### 4.2.2 Apparatus

For trace detection of 4-chloro-1-naphthol, the apparatus utilized was as mentioned in 2.1.2.

### 4.2.3 Preparation of phosphate buffer saline of different pH

The preparation of PBS is done same as in 3.2.2.3.

### 4.2.4 Pretreatment of GPE

10 mm pencil graphite of lead was squeezed out of pencil holder, an Ag/AgCl reference and Pt counter electrodes were plunged in a cell comprises diverse supporting electrolytes. For electrochemical treatment of GPE surface, potential was cycled between 1.3 V – 1.9 V with scan rate of 100 $mVs^{-1}$ for 50 segments. Following, mild sousing twice into deionized water to clean the prepared pretreated electrodes. The whole electrochemical detections were executed just after the formulation of the pretreated electrodes. The electrolytes utilized for this purpose included 0.1 M $LiClO_4$, PBS, NA, NaOH, NaOH + $LiClO_4$ mixture, NaOH + PBS mixture and NaOH + NA mixture. The PGPEs were denoted as PGPE-LP, PGPE-PBS, PGPE-NA, PGPE-NH, PGPE-NHLP, PGPE-NHPBS and PGPE-NHNA according to supporting electrolytes used; $LiClO_4$, PBS, NA, NaOH, NaOH + $LiClO_4$ mixture, NaOH + PBS mixture and NaOH + NA mixture, respectively.

### 4.2.5 Electrochemical detection

Square wave voltammetric (SWV) detections of various concentrations of 4-CNP were executed by utilizing improved electrochemical settings in PBS (0.1 M, pH 7.0). Afterwards, 10 s respite period under quiescent circumstances the deposited 4-CNP on the surface of PGPE was detected.

### 4.2.6 Water sample preparation

Water samples were gathered from tap water in the laboratory, sea water in local area and drinking water were initially filtered by utilizing a filter paper of pore size 0.45 μm to eliminate any insoluble material and then for electrochemical detection 3.0 ml of each water sample was thinned to 5 ml with 0.1 M PBS, pH 7.0.

## 4.3 Results and discussion

### 4.3.1 Choice of electrolyte for the formulation of PGPE for the 4-CNP detection

For electrochemical treatment of GPE different supporting electrolytes were employed under identical circumstances. The electrochemical activities of the disposed electrode were assessed by square wave adsorptive stripping voltammetry (SWASV) measurements of 5 μM 4-CNP in PBS solution (pH 7.0). Figure 4. 1 shows the electro-oxidation current of 4-CNP in the existence of various supporting medium. The voltammetric response of GPE treated with sodium acetate (NA), NaOH + $LiClO_4$ mixture and NaOH + PBS mixture were virtually equivalent as that of untreated GPE. A broad peak was distinguished with PGPE-NH, that cannot be employed for sensitive detection of 4-CNP. A sharp and well illustrious peak with noteworthy increase in peak current was observed when PGPE-NHNA was utilized. It is interesting to discover that the summation of peak currents of 4-CNP acquired by treatment with NaOH and NA separately were much smaller as compared to that of the obtained by GPE treated with their mixture. The peak current for 4-CNP was increase 25 times after treatment with NaOH + NA mixture as compared to untreated GPE. Form this observation it can be

concluded that while GPE was treated with mixture of NaOH and NA, they showed synergistic effect on the activity of PGPE for oxidation of 4-CNP. Interestingly, the oxidation peak potential of 4-CNP shifted to more cathodic value at PGPEs. According to the outcomes, the assortment of NaOH and NA was selected as the medium for treatment of GPE to get PGPE, and further optimization was done by utilizing the same mixture.

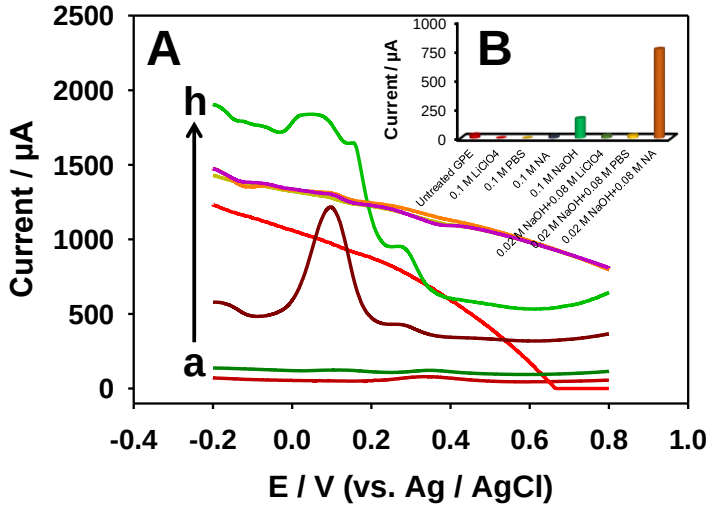


**Figure 4. 1. (A) SWVs of 5 µM 4-chloro-1-naphthol in 0.1 M phosphate buffer saline, pH 7.0 at a) untreated and treated GPEs in various 0.1 M media: b) 0.1 M NA, c) 0.02 M NaOH+0.08 M NA, d) 0.1 M $LiClO_4$, e) 0.1 M PBS, f) 0.02 M NaOH+0.08 M $LiClO_4$, g) 0.02 M NaOH+0.08 M PBS and h) 0.1 M NaOH solutions. Working conditions: Pretreatment potential 1.3 to 1.9 V, pretreatment segments 50, pretreatment scan rate 100 mV/s, frequency 50 Hz, amplitude 0.06 V, deposition potential 0.2 V and deposition time 60 sec (B) corresponding histogram.**

### 4.3.2 Characterization of PGPE-NHNA

When PGPE was made in the solution assortment of NaOH and NA, a synergetic influence was observed on the electro-oxidation peak current of 4-CNP. Therefore, all the characterizations of PGPE-NHNA were concentrated to PGPE prepared in individual solutions and mixture of electrolytes. The characterization of PGPE-NHNA was done by utilizing different techniques like cyclic voltammetry (CV), electrochemical impedance spectroscopy (EIS) and square wave voltammetry (SWV).

The $Fe(CN)_6^{3-/4-}$ redox couple is frequently utilized to measure the electrochemical activeness of modified surfaces of electrode. Initially, the CV was employed for measuring peak current of 5 mM $Fe(CN)_6^{3-/4-}$ in 0.1 M KCl and outcomes are mentioned in Figure 4. 2 A, the results showed that use of NA for treatment displayed no prominent influence on the electrochemical performance of GPE and showed very broad peak for $Fe(CN)_6^{3-/4-}$. On the other hand, utilization of NaOH had a noticeable impression on the activity of electrode, where not only the peak current amplified but also there is a big change in shape of redox peaks. However, use of mixture for the treatment resulted in synergistic influence on the oxidation peak current of $Fe(CN)_6^{3-/4-}$, that can be accredited to the huge surface area of PGPE-NHNA and large number of functional groups attached during the pretreatment process. It can be concluded that PGPE-NHNA showed different characteristics from individual solutions of these supporting electrolytes. In order to relate the cyclic voltammetric behavior of untreated and treated GPE in 6 M solution of NaOH at scan rate of 2 $mVs^{-1}$ (Figure 4. 2 B). Calculation of capacitance for both electrodes was done by using equation 4.1. [133]

$$C = Q / \Delta E \, . \, m \qquad 4.1.$$

whereas Q is denoting the voltammetric charge, mass of electrode stuff is indicated by m and ΔE is the potential window employed for the cyclic scan. The capacitance calculated on the founded on integrated area underneath voltammetric peak for untreated and treated GPE were 148.014 F/g and 8317.386 F/g respectively. The outstanding enhancement of specific capacitance of treated GPE surface can be ascribed to the accumulation and formation of charge carrier species on surface of electrode during the course of electrochemical treatment.

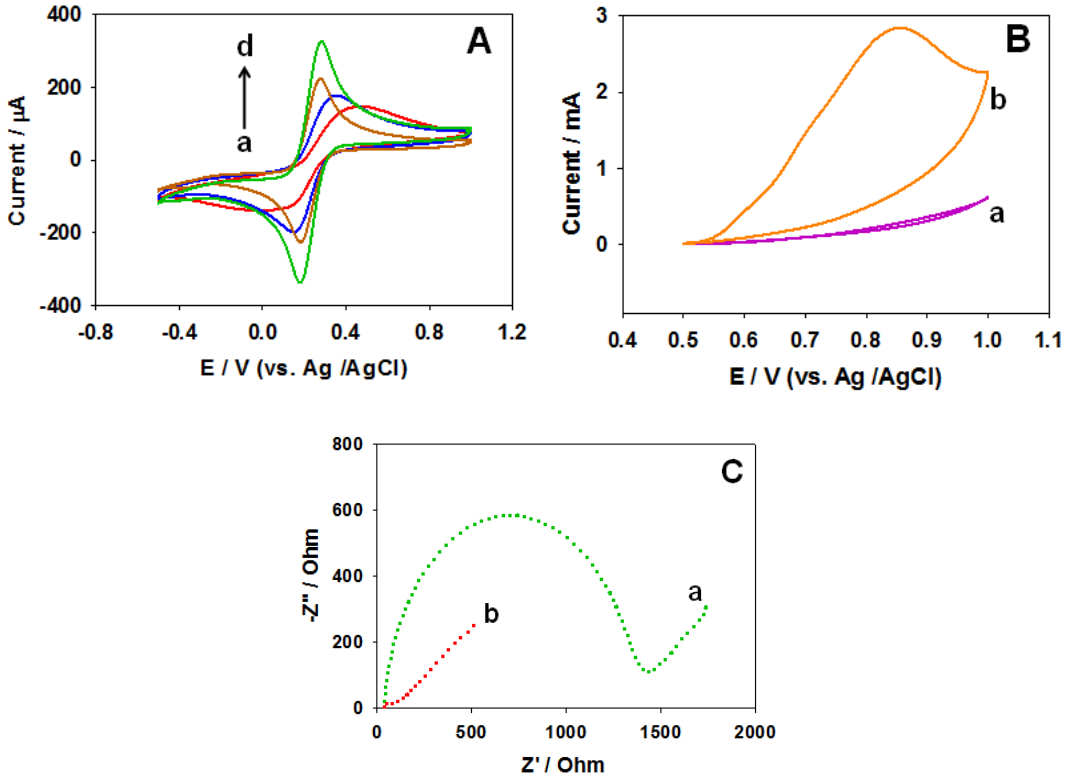


**Figure 4. 2. A) CVs of 5.0 mM $Fe(CN)_6^{3-/4-}$ obtained in 0.1 M KCl by the untreated a) GPE and GPE treated in b) acetate buffer, c) NaOH, d) NHNA mixture, B) CVs in 6 M NaOH electrolyte at 2 mV/sec scan rate a) untreated GPE and b) treated in NHNA mixture. C) Nyquist plots in 0.1 M KCl solution containing a mixture of 5 mM $K_4[Fe(CN)_6]$ and 5 mM $K_3[Fe(CN)_6]$ of untreated (a), and treated-NHNA (b) GPE.**

Furthermore, Figure 4. 2 C displayed Nyquist plots for untreated GPE and PGPE-NHNA in aqueous solution of 5 mM each of $K_4[Fe(CN)_6]$ and $K_3[Fe(CN)_6]$ containing 0.1 M KCl by using frequency array of 0.01 Hz to 100 kHz. The real and negative figures of the imagined impedance variables were designated by Z and –Z, correspondingly. Plot attained at GPE consist of a semicircle part with a straight line, whereas for PGPE-NHNA simply a line without any deviation was obtained. Semicircular part at higher frequencies showed a limiting charge transfer process on the electrode/electrolyte boundary, although straight line of the graph at low frequency area is attributed to the

diffusion process occurring in solid. Consequently, ohmic resistance for electrochemical process is comparatively much smaller at PGPE-NHNA. The PGPE-NHNA show high slop at low frequency region suggesting that PGPE is more capacitive as compared to untreated electrode.

The superficial electroactive area of untreated and pretreated GPE was calculated by utilizing Randles–Sevcik equation 4.2. [136]

$$I_p = 2.69 \times 10^5 C n^{3/2} A D^{1/2} \gamma^{1/2} \qquad 4.2.$$

Where $I_p$ refers to anodic peak current, amount of target analyte (mol $L^{-1}$) is denoted by C, electron numeral transferred during the oxidoreduction process are signified as n, electroactive surface area of the electrode ($cm^2$) is symbolized as A, diffusion constant ($cm^2 s^{-1}$) is indicated as D and $\gamma$ is the scan frequency (V $s^{-1}$).

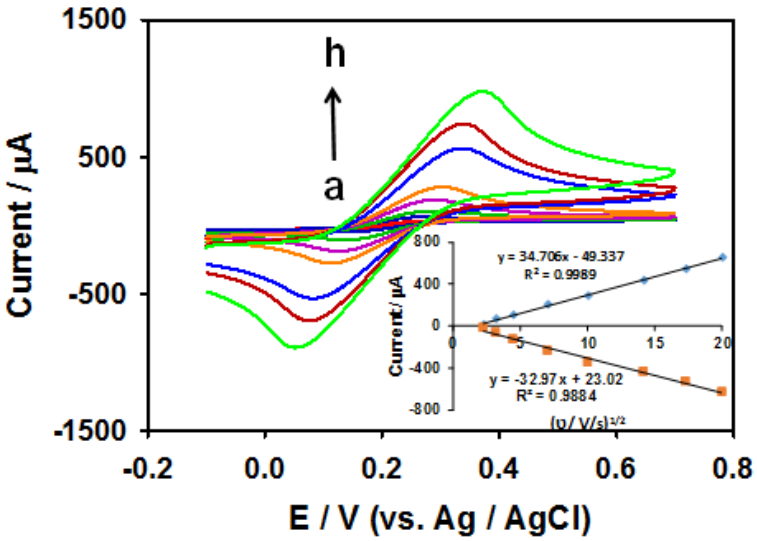


**Figure 4. 3. Cyclic voltammograms of the PGPE-NHNA in 0.1 M KCl at various scan rates: (a) 5, (b) 10, (c) 20, (d) 50, (e) 100, (f) 200, g) 300 and (h) 400 mV/s. Inset is plot of peak currents vs. square root of scan rates.**

For the electroactive area calculation CV scans were recorded between 5 to 400 mV in 5 mM solution of $K_4[Fe(CN)_6]$, $K_3[Fe(CN)_6]$ and 0.1 M KCl by utilizing untreated

GPE and PGPE Figure 4. 3. By using above mentioned equation, electroactive areas obtained 0.535 $mm^2$ and 0.94 $mm^2$ for untreated and pretreated GPEs respectively. Subsequently, it can be stated as the electroactive surface area of PGPE-NHNA is higher as compare to untreated GPE.

The effect of sweeping rate on the peak current was inspected by utilizing cyclic voltammograms of 10 µM 4-CNP at PGPE at different scan rate values. The Figure 4. 4 A shows that linear relation exists between oxidation peak current and square root of sweep rate, the equation (4.3.) could be shown as

$$I\ (\mu A) = 1.821\ (\nu)^{1/2} - 3.8814 \qquad r^2 = 0.9954 \qquad 4.3.$$

The Figure 4B shows that oxidation current vary in linear manner by rise in sweep rate. The equation (4.4.) of this linear relation can be expressed as

$$I\ (\mu A) = 0.1915\ (\nu) - 0.0477 \qquad r^2 = 0.9905 \qquad 4.4.$$

The relation of log of the oxidation current vs log of the scan rate provided a straight line with a slope of 1.3068 for PGPE-NHNA as shown in 4C the equation (4.5.) could be stated as

$$\log I\ (\mu A) = 1.3068 \log\ (\nu)\ -1.1609 \quad r^2 = 0.9364 \qquad 4.5.$$

As the slope obtained is near to 1.0 so the adsorption controlled process on the surface of electrode. The plot of log of oxidation current vs. log ν showed upsurge in current by increasing the sweep rate, approving that the PGPE-NHNA electrode surface has some adsorption dependence.

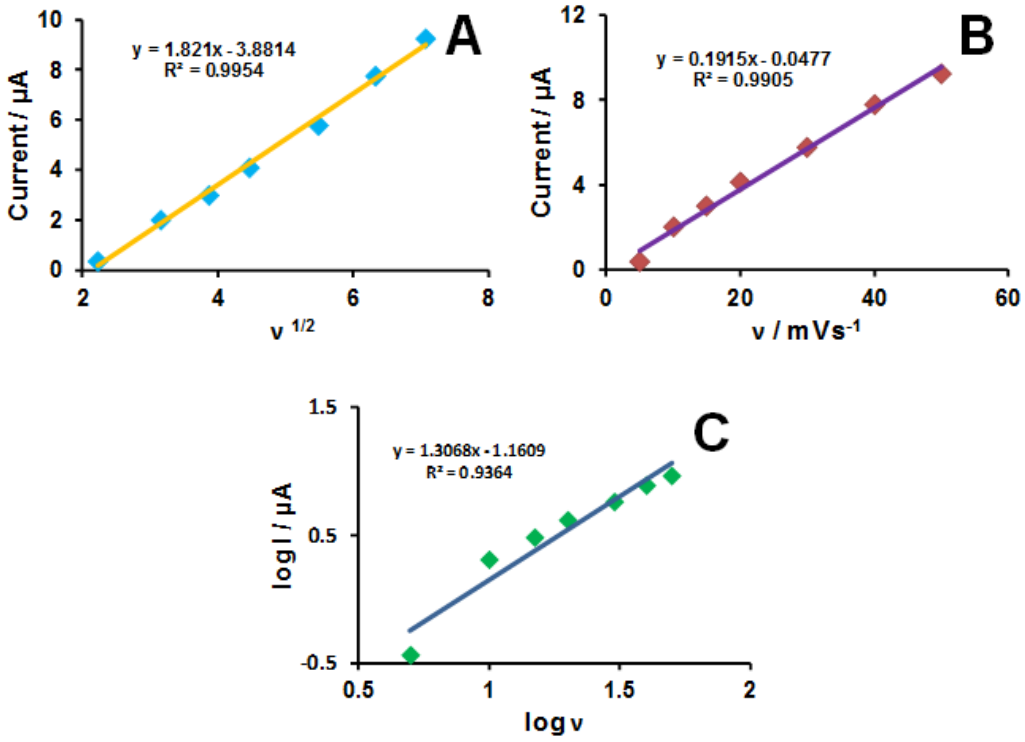


**Figure 4. 4. (A) Plot of the oxidation peak current vs. square root of scan rate of 10 µM 4-CNP. (B) Plot of the oxidation peak current vs. scan rate of 10 µM 4-CNP. (C) The plot of the logarithm of peak current vs. logarithm of scan rate of 10 µM 4-CNP.**

The electrochemical performances of the untreated and treated GPEs were analyzed by utilizing cyclic voltammetric measurements in the presence and absence of 5 µM 4-CNP in PBS, pH 7.0 Figure 4.5. When cyclic voltammetric scan was run in PBS without adding 4-CNP, no peak current was obtained for both untreated and treated GPEs. However, the background peak current was significantly higher for PGPE-NHNA as compared to untreated GPE. This was due to increase in surface area of GPE after treatment in NHNA solution mixture. After that, addition of 5 µM 4-CNP showed an oxidation peak for both treated and untreated GPEs. The oxidation of 4-CNP took place at 0.316 V for the untreated GPE, while oxidation peak for 4-CNP appears at potential of 0.096 V for treated GPE.

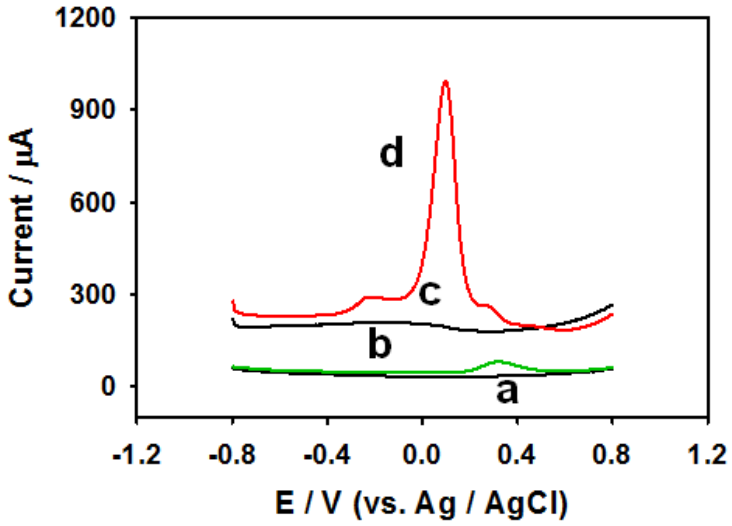


**Figure 4. 5. Square wave voltammograms of the untreated GPE (a and b) and PGPE (c and d) in the absence (a and c) and presence (b and d) of 5 µM 4-CNP in PBS (pH 7.0). Amplitude 0.06 V, frequency 50 Hz, accumulation time 60 sec and deposition potential 0.2 V.**

The quantity of functional groups on electrode surface depends on the treatment strategy and material used as electrode. Increase in hydrophilic character and synergetic consequence of combination of supporting electrolytes corresponds to the entrance of oxygen on the surface of GPE in the variety functional groups like hydroxyl, carbonylic and carboxylic groups. The comparative quantity of these functional groups prominently effects the selectivity of electrode. presence of hydroxyl and carbonyl group on the surface of electrode not affect the charge but change the adsorption properties of electrode, however high value of carboxylic group introduce a negative charge that resulted in more attraction for the cationic molecules [137]. The GPE treated with NA showed almost same character as bare-GPE, proving that NA treatment did not change the surface charge so much. On the other hand, GPE treated with mixture of supporting analytes produce noticeable impact on electrocatalytic performance of PGPE.

### 4.3.3 Optimization of electrochemical treatment conditions for the preparation of PGPE-NHNA

To get the optimum concentration of NaOH and NA the effect of variation in concentration of supporting electrolytes on the voltammetric response of PGPE-NHNA was studied. For this purpose, PGPE-NHNA were treated in different concentrations of NaOH and NA, and then their voltammetric responses were measured in 5 µM 4-CNP solution (Figure 4. 6 A). Concentration of both electrolytes were varied by keeping the final concentration of electrolyte constant, i.e. 0.1 M. It was observed that when 0.1 M NA was used for the treatment of GPE the peak current for the 5 µM 4-CNP was very low, interestingly when the we started to decrease the concentration of NA and gradually increase the concentration of NaOH, peak current for 4-CNP also increased and showed slow increase in peak current when concentration was 0.005 M NaOH + 0.095 M NA and 0.01 M NaOH + 0.09 M NA in mixture. A sudden increase in peak current was observed when concertation was 0.015 M NaOH + 0.085 M NA, and maximum current was obtained at 0.02 M NaOH + 0.08 M NA concertation of mixture. Although, beyond that concentration, the peak current was almost same, but the peak shape become distorted that is not suitable for sensitive and selective detection of 4-CNP. These observations helped to select the optimal concentration of supporting electrolyte, i.e. 0.02 M NaOH + 0.08 M NA (Figure 4. 6 B).

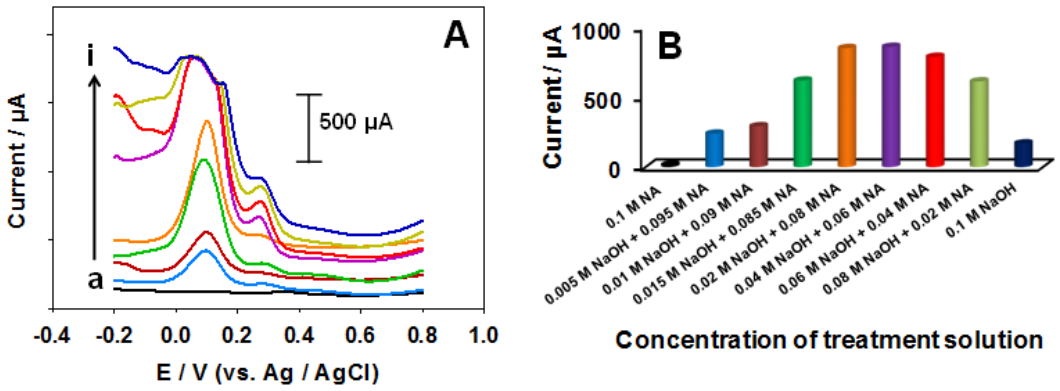


**Figure 4. 6. (A) SWVs of 5 µM 4-chloro-1-naphthol in 0.1 M phosphate buffer saline, pH 7.0 pretreated GPEs in various concentrations of NaOH+NA: a) 0.1 M NA, b) 0.005 M NaOH + 0.095 M NA, c) 0.01 M NaOH + 0.09 M NA, d) 0.015 M NaOH + 0.085 M NA, e) 0.02 M NaOH + 0.08 M NA, f) 0.04 M NaOH + 0.06 M NA , g) 0.06 M NaOH + 0.04 M NA, h) 0.08 M NaOH + 0.02 M NA and i) 0.1 M NaOH solutions. other working conditions were same as in Figure 4. 1 (B) corresponding histogram.**

The main constituent of graphite pencil electrode is graphite (65%), clay (30%) and only 5% is electro-inactive polymer as a binder. Thus, pencil lead is mainly consisting of graphite, in which every single carbon atom is linked together by very weak bonds. Clay is an aluminosillicate presenting ion exchange characteristics. Nevertheless, the graphitic part of pencil in connection with the pretreatment solution (i.e., NA and NaOH mixture) is cleaned, and various oxygen containing functional groups are attached [157]. Thus, interestingly enhancement in signal of PGPE-NHNA after pretreatment can be accredited to increased oxygen containing groups on the electrode surface or to graphite oxide film formation [76]. The active film or radicals generated on the surface of PGPE-NHNA and act as catalyst for the oxidation of 4-CNP.

Potential range for pretreatment of GPE plays very important role in sensitive and selective detection of target analyte. That is why influence of electrochemical treatment potential was studied on voltammetric reaction of PGPE-NHNA treated in 0.02 M NaOH and 0.08 M NA at diverse potential ranges. It was observed that there is no or very minute response of PGPE-NHNA when treated at 1.9 to 2.5 V, 0.1 to 0.7 V and 0.7 to 1.3

V (Figure 4. 7). However, the sudden gain in peak current was observed when 1.3 to 1.9 V potential was employed for treatment of electrode. So 1.3 to 1.9 V was selected as the optimum potential range.

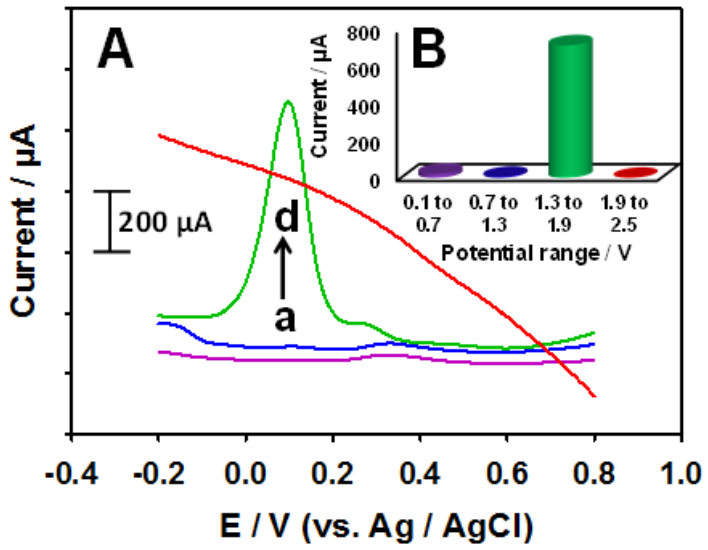


**Figure 4. 7. (A) SWVs of 5 µM 4-chloro-1-naphthol in 0.1 M phosphate buffer saline, pH 7.0 at GPEs in various pretreatment potential ranges: a) 0.1-0.7, b) 0.7-1.3, c) 1.3-1.9 and d) 1.9-2.5 V. Pretreatment is done in 0.02 M NaOH + 0.08 M NA mixture, other working conditions were same as in Figure 4. 1 (B) corresponding histogram.**

To prepare PGPE-NHNA either constant potential or cyclic scanning of potential between selected ranges was applied. To evaluate the efficiency of these two approaches, the PGPE-NHNA prepared by applying constant potential of 1.3 V and 1.9 V under different treatment times (Figure 8 A) compared with that of produced sweeping the potential between 1.3 to 1.9 V and in the combination of 0.02 M NaOH + 0.08 M NA solution (Figure 4. 7).

The performance of prepared electrodes was evaluated in 5 µM 4-CNP solution. The peak current was 5 times lower than cyclic sweeping for same concentration of 4-CNP when treatment of GPE was done at +1.9 V (Figure 4. 8 B). However, the PGPE treated at +1.3 V showed comparable peak current when treated for 400 sec (Figure 4. 8 A), but the treatment time is very high when compared with the cyclic sweeping between

1.3 to 1.9V. Consequently, the cycling sweeping for selected range of potential was selected as the treatment strategy for remaining analysis.

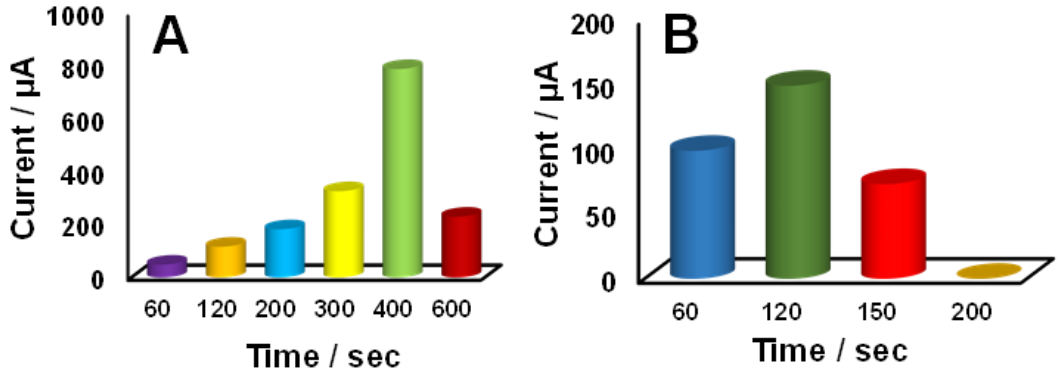


**Figure 4. 8. Corresponding histogram of 5 µM 4-chloro-1-naphthol in 0.1 M phosphate buffer saline, pH 7.0 under fix potential treatment A) +1.3 V and B) + 1.9 V with variable treatment times. Pretreatment is done in 0.02 M NaOH + 0.08 M NA mixture; other working conditions were same as in Figure 4. 1.**

In order to optimize the other treatment conditions, number of cyclic potential sweep segments and their scan rate was evaluated. The potentiodynamic treatment of PGPE-NHNA was carried out by scanning with varying number of CV segments. The outcomes proved that by increasing the number of treatment segments up to 50, the peak current for 4-CNP also increase but further increase in number of treatment segments minutely decrease the current and then made it constant up to 100 segments (Figure 4. 9). So, the maximum current obtained when 50 treatment segments of CV potential scanning were applied. Therefor 50 segments were considered to be optimum for the treatment of PGPE-NHNA.

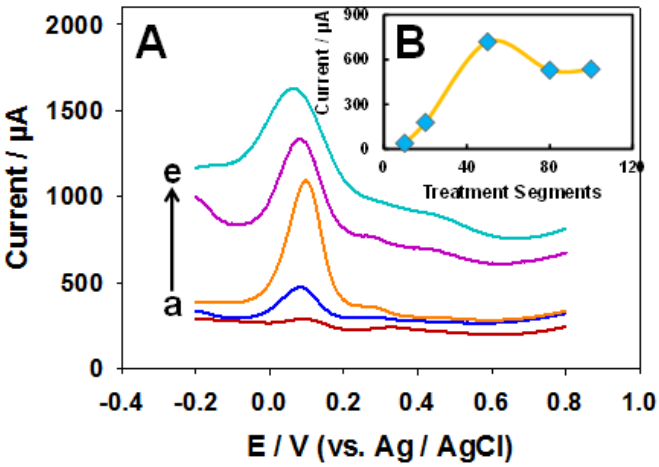


**Figure 4. 9. (A) SWVs of 5 µM 4-chloro-1-naphthol in 0.1 M phosphate buffer saline, pH 7.0 at various pretreatment segments: a) 10, b) 20, c) 50, d) 80 and e) 100. Pretreatment is done in 0.02 M NaOH + 0.08 M NA mixture; other working conditions were same as in Figure 4. 1 (B) corresponding plot of peak current vs number of treatment segments.**

Finally, influence of treatment scan rate on the activity of PGPE-NHNA was analyzed. Sweep rate was varied between 20 to 100 $mVs^{-1}$ (Figure 4. 10), the results showed that maximum oxidation current of 4-CNP was obtained when 100 $mVs^{-1}$ was applied and this scan rate was considered to be optimal for treatment of GPE.

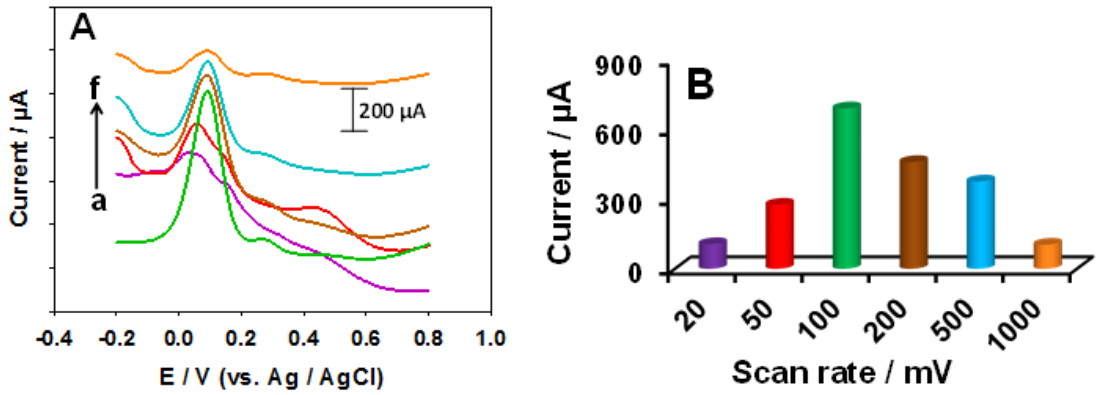


**Figure 4. 10. (A) SWVs of 5 µM 4-chloro-1-naphthol in 0.1 M phosphate buffer saline, pH 7.0 at various pretreatment scan rates: a) 100, b) 20, c) 50, d) 200, e) 500 and e) 1000. Pretreatment is done in 0.02 M NaOH + 0.08 M NA minxture, other working conditions were same as in Figure 4. 1 (B) corresponding histogram.**

### 4.3.4 Impact of detection medium and pH on the electrochemical behavior of 4-CNP

To study the detection medium on voltammetric current of PGPE-NHNA different buffers like PB, AB and PBS pH 7.0 were used. Results revealed that highest peak current was obtained when PBS was used as detection medium (Figure 4. 11).

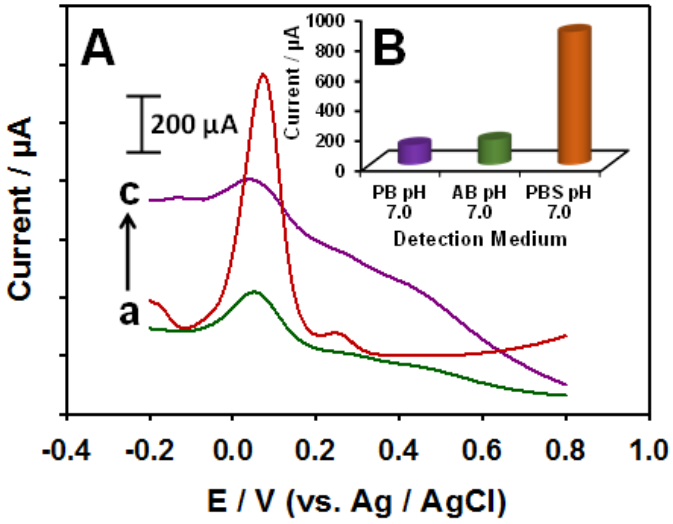


**Figure 4. 11. (A) SWVs of 5 µM 4-chloro-1-naphthol in various 0.1 M, pH 7.0 detection mediums: a) AB, b) PBS and c) PB. Pretreatment is done in 0.02 M NaOH + 0.08 M NA mixture; other working conditions were same as in Figure 4. 1 (B) corresponding histogram.**

As PBS consist of phosphate buffer, NaCl, and KCl, that is why effect of type of salt on peak current of 4-CNP was studied. Firstly, for this purpose, 1.37 M NaCl, NaF, NaBr, $NaNO_3$, and $Na_2SO_4$ were utilized for detection of 4-CNP in the absence and presence of KCl (data not shown). Interestingly, the oxidation peak current for 5 µM 4-CNP in the buffer solutions containing NaCl, NaF, NaBr, $NaNO_3$, and $Na_2SO_4$ in the presence of KCl was higher as compared to the buffer solutions in the absence of KCl. Overall results depicted that PBS containing NaCl and KCl proved to be supporting electrolyte for recognition of 4-CNP. The concentration ratio of NaCl to KCl is 50.74, by keeping this ratio constant the amount of both salts was varied. Fascinatingly, increase in

concentration ratio of NaCl and KCl also positively affect the oxidation current of 4-CNP. The highest current was obtained at 1.37 M NaCl, and 0.027 M KCl, further increase in concentration of both salts showed little decrease in peak current (data not shown). Consequently, 1.37 M NaCl and 0.027 M KCl was chosen as the optimal concentration of salts in PBS and utilized for the further study.

After that relation between pH of PBS and oxidation peak current of 5 µM 4-CNP was investigated. For this purpose, PBS solutions of various pH were prepared, it was observed that change in pH prominently effect not only peak current but also the peak position of 4-CNP. The peak current and peak potential values were plotted against the pH (Figure 4. 12). Increase in pH move the peak towards the cathodic potential and plot of peak potential vs. pH yield a slope of – 40.0 mV $pH^{-1}$. On the other hand, the peak current increase by increasing the pH from 5.0 to 7.0, then started to decrease progressively up to pH value of 9.0. the outcomes show that the maximum voltammetric current was obtained at pH 7.0, which was preferred and continued as the optimum pH for the remaining analysis of 4-CNP.

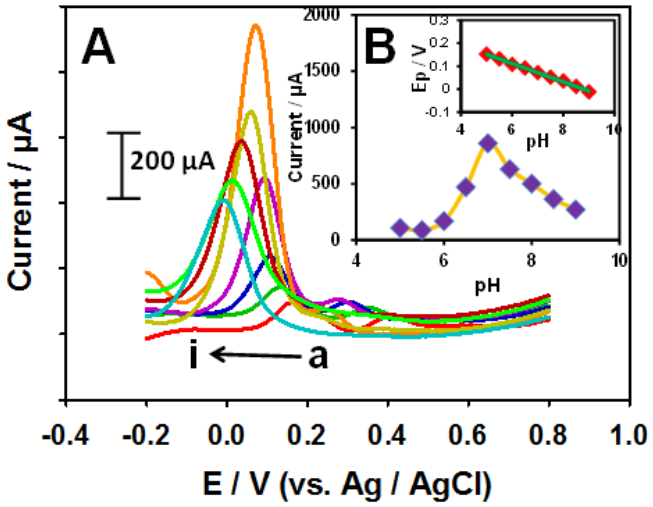


**Figure 4. 12. (A) SWVs of 5 µM 4-chloro-1-naphthol in 0.1 M phosphate buffer saline of various pH: a) 5.0, b) 5.5, c) 6.0, d) 6.5, e) 7.0, f) 7.5, g) 8.0, h) 8.5 and i) 9.0. Pretreatment is done in 0.02 M NaOH + 0.08 M NA mixture; other working conditions were same as in Figure 4. 1. (B) The corresponding plot of peak currents ip (µA) vs. pH and inset is the plot of peak potential (V) vs. pH.**

### 4.3.5 Optimization of SWASV parameters

In order to get the best oxidation current of 4-CNP frequency and amplitude was optimized. The results showed that as we increase the amplitude from 0.02 V to 0.06 V the oxidation response also increase, afterwards further increase in amplitude reduce the current upto 0.1 V. Consequently, 0.06 V was selected as the optimal amplitude (Figure 4. 13 A). in the same way, change in frequency also effect the oxidation current of 4-CNP. Frequency was varied from 10 to 100 Hz, and maximum current was obtained at 50 Hz (Figure 4. 13 B) that was selected as optimum frequency for detection of 4-CNP by using PGPE-NHNA.

Deposition potential plays very important role in getting best oxidation current but also determine peak shape and peak position. In case of bare-GPE and PGPE-NHNA when no deposition potential was applied the oxidation potential was 0.4 V and 0.18 V correspondingly. However, application of 0.2 V accumulation potential for 60 sec shift the peak towards cathodic potential, i.e. 0.3 V and 0.1 V for bare-GPE and PGPE-NHNA respectively. Due to deposition potential peak current also increase. That is why optimization of deposition potential became very crucial. For this purpose, deposition potential was changed amongst -0.4 V to 0.8 V. plot of peak current vs. deposition potential shows that by increasing the potential peak current of 5 µM 4-CNP also increase gradually, after 0.4 V the peak response started to decrease due to increase in accumulation potential (Figure 4. 13 C). Consequently, 0.4 V was designated as the finest deposition potential.

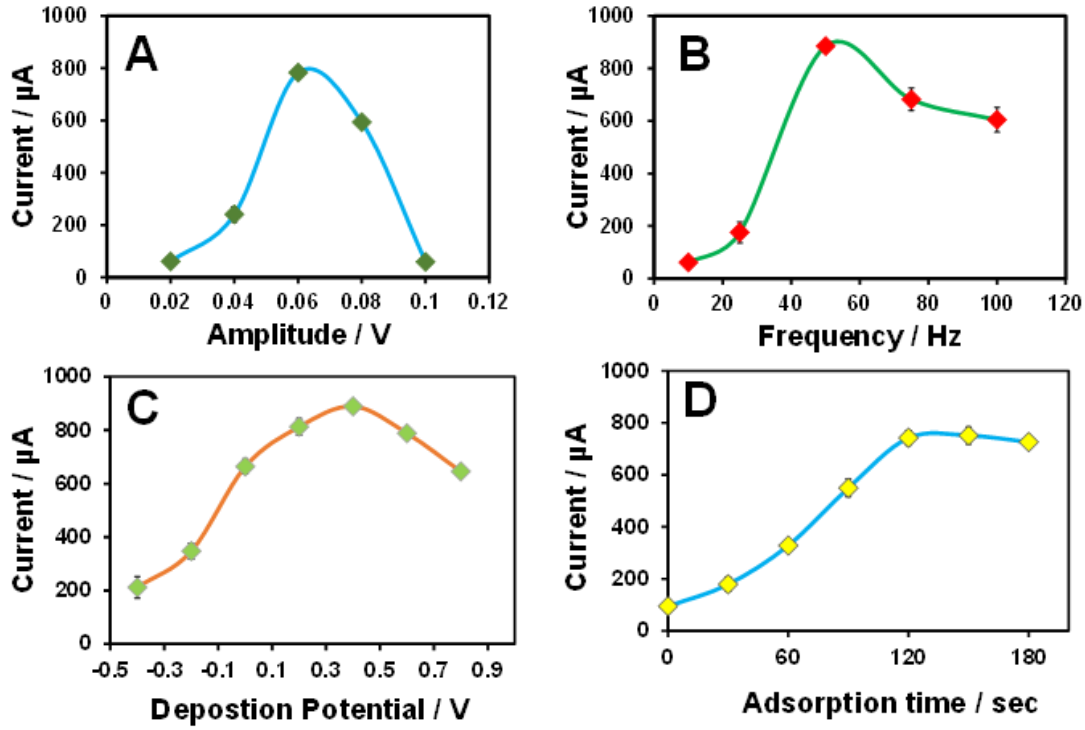


**Figure 4. 13. (A) Corresponding plots of SWVs peak current of 5 µM 4-chloro-1-naphthol in 0.1 M phosphate buffer saline, pH 7.0 vs.: A) Amplitude, B) Frequency, C) deposition potential and SWV peak current of 2 µM 4-chloro-1-naphthol in 0.1 M phosphate buffer saline, pH 7.0 vs D) deposition time. Pretreatment was done in 0.02 M NaOH + 0.08 M NA minxture; other working conditions were same as in Figure 4. 1.**

Finally, influence of deposition time on the oxidation current of 4-CNP was premeditated. The magnitude of peak current of 2 µM 4-CNP increased by increasing the contact time of PGPE-NHNA at optimized potential (Figure 4. 13 D). The surface concentration of 4-CNP on the PGPE-NHNA is chiefly relied on the interaction time of electrode with analyte solution. As the deposition time prolonged the peak current also increase up to 120 sec, Beyond 120 sec the peak current remain almost constant. Thus, the 120 sec was selected as optimum contact time.

**Table 4. 1. Optimized conditions for pretreatment of GPE-NHNA.**

| Conditions | Transducer | Treatment solution | Treatment potential range | Treatment scan rate | Number of treatment segments |
|---|---|---|---|---|---|
| **Optimization** | Graphite pencil electrode | 0.02 M NaOH + 0.08 M NA minxture | 1.3-1.9 V | 100 mV/s | 50 |

## 4.3.6 Analytical parameters

The relation between concentration of 4-CNP and oxidation peak current was investigated by utilizing optimized conditions (Table 4. 1 and 4. 2), in the existence of diverse amounts of 4-CNP in PBS pH 7.0 (Figure 4. 14). A linear relation was obtained between 0.01 µM and 1.0 µM (n=3) of 4-CNP in the calibration plot of peak current vs. concentration. A linear regression of the calibration curve produced an equation I(µA) = 540.07 $C_{4\text{-CNP}(\mu M)}$ + 33.028, with $R^2$ of 0.9986. The detection limit of suggested strategy was computed as 0.00157 µM or 1.57 nM of 4-CNP (S/N=3).

**Table 4. 2. Optimized conditions for detection of 4-CNP.**

| Conditions | Technique | Amplitude | Frequency | Deposition time | Deposition potential | Detection medium |
|---|---|---|---|---|---|---|
| **Optimization** | Square wave voltammetry | 0.06 V | 50 Hz | 120 sec | 0.4 V | PBS, pH 7.0 |

Reproducibility of fabricated PGPE-NHNA was evaluated by SWASV measurements of 5.0 µM 4-CNP in 0.1 M PBS solution (pH 7.0). Relative standard deviation (RSD) of 3.43 was obtained for six different PGPE-NHNA treated in same manner.

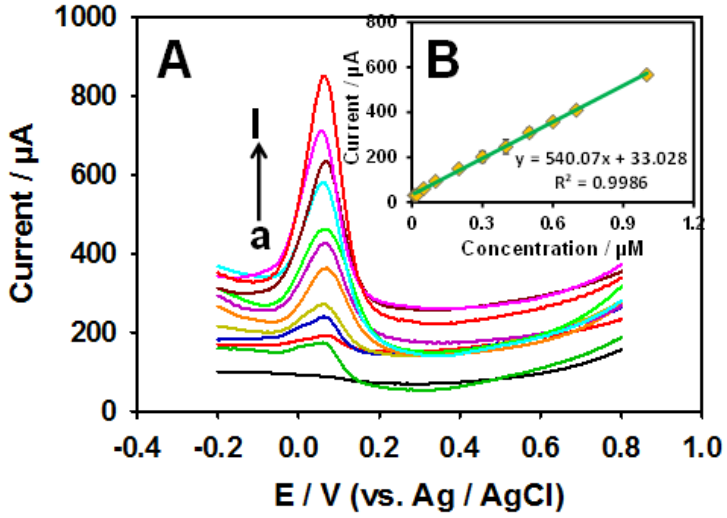


**Figure 4. 14. (A) SWVs of 5 µM 4-chloro-1-naphthol in 0.1 M phosphate buffer saline, pH 7.0 at different concentrations: a) blank, b) 0.01 c) 0.02, d) 0.05, e) 0.1, f) 0.2, g) 0.3, h) 0.4, i) 0.5, j) 0.6, k) 0.7 and l) 1.0 µM. B) inset is corresponding plot of peak current vs concentration. Other working conditions are mentioned in above table 4. 1 and 4. 2.**

### 4.3.7 Interference Studies

In order to study the effect of possible interfering molecules, SWASV measurements of 0.5 µM 4-CNP were done in the presence and absence of interferents; phenol, 4-bromophenol, 4-nitrophenol, 4-aminophenol, 2,3-dichlorophenol, 2,4-dichlorophenol and some common metal ions $Co^{+2}$, $Ca^{+2}$, $K^{+}$ and $Na^{+}$ (Figure 4. 15). 0.5 µM phenol and its derivatives not affect the oxidation peak current conspicuously and introduced minute variation of 5 to 10 %. 0.5 µM or 5 µM $Co^{+2}$, $Ca^{+2}$, $K^{+}$ and $Na^{+}$ added metal ions to 0.5 µM solution of 4-CNP effect the oxidation current by 11% or 7 % respectively (Table 4. 3). In the illumination of current fallouts, it can be established that PGPE-NHNA is highly selective for the 4-CNP.

**Table 4. 3. Effect of versatile contaminants (0.5 µM) on peak current of 0.5 µM 4-CNP at PGPE-NHAB under optimal conditions.**

| Potential interferences | Signal changes |
|---|---|
| Phenol | 7.72% |
| 4-Bromophenol | -9.46% |
| 4 Nitrophenol | -7.78% |
| 4-Aminophenol | 4.84% |
| 2,3-Dichlorophenol | 8.23% |
| 2,4-Dichlorophenol | 6.88% |
| $Co^{+2}$, $Ca^{+2}$, $K^{+}$, $Na^{+}$ | -10.75% |
| $Co^{+2}$, $Ca^{+2}$, $K^{+}$, $Na^{+}$ 10 times | -6.97% |

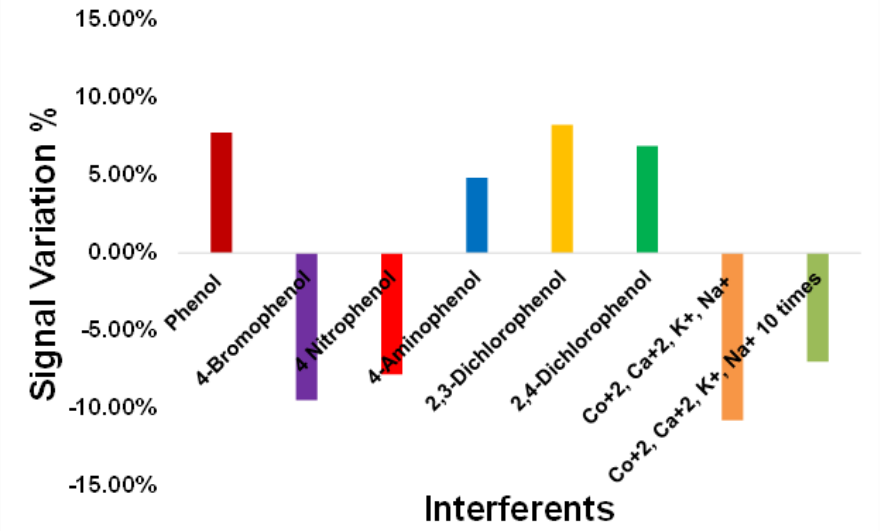


**Figure 4. 15. (A) corresponding histograms showing effect on oxidation current of 0.5 µM 4-CNP in the presence of 0.5 µM of different interferents.**

### 4.3.8 Analytical Application

The fabricated PGPE-NHNA was tested in real life water samples. The amount of 4-CNP in water is lesser than the detection limit of this method, that is why it in undetectable. In order to determine 4-CNP, 0.5 µM 4-CNP was added to water samples,

and equation straight line obtained from calibration curve was utilized to calculate recovery of added analyte. The outcomes reveled the recovery of 100.5 %, 100.1 %, 102.0 % and 101.2 % in sea water, tap water, commercially available drinking water and drinking water from filtration plant in town respectively. These satisfactory recoveries suggest that PGPE-NHNA could be valuable for 4-CNP detection in real water samples which inclines to contain contaminations and interferents.

## 4.4 Summary

Sensitivity and selectivity of PGPE-NHNA predominantly rely on the method of preparation and the features of the target analyte. First time solution mixture of NaOH and sodium acetate was utilized for pretreatment of GPE to get PGPE-NHNA. The PGPE-NHNA allowed convenient and low-cost determination of 4-CNP in real water samples. Cyclic potential and concentration of treatment mixture showed prominent effect on voltammetric response of treated surface of electrode. To get the best results, pretreatment and SWV parameters effecting oxidation peak current of 4-CNP were optimized. The proposed method showed very low detection limit and can be effectively employed for detection and quantification of 4-CNP in real water samples.

# Chapter 5

# Simple and sensitive detection of 4-nitrophenol in real water samples by utilizing gold nanoparticles modified pretreated graphite pencil electrode

## 5.1 Introduction

Nitrophenols are categorized as lethal, repressive and biorefractory composites, widely present in natural and industrial wastes [158]. Naturally, nitrophenols are produced due to the reaction of nitrite ions with phenol in water, on the other pesticides, pharmaceuticals and dyes are the man-made sources. Particularly 4-nitrophenol is degradation product of folidol insecticides [159]. It has long residence time in environment and show bioaccumulation, due to these reasons 4-nitrophenol is categorize as priority contaminant by United States environmental protection agency (USEPA) [160]. It is root cause of various problems like respiratory, cardiac, digestive, hematological, musculoskeletal, hepatic, renal, dermal/ocular in living organisms [161]. Consequently, detection of 4-nitrophenol at trace level is very important.

There are various methods employed to detect 4-nitrophenol in different samples, that include chromatography [162,163], spectrophotometry [164], fluorescence [165,166] and electrophoresis [167,168]. High performance liquid chromatography and electrophoresis required expensive columns and large amount of organic solvents [169]. In gas chromatography, aqueous samples cannot be used directly, so pretreatment and derivatization of sample is required, consequently the time of analysis and cost increase. Spectrophotometric and fluorometric methods are effected by interferences of related compounds. Therefore, a simple, inexpensive and fast procedure for detection of 4-nitrophenol is required. Electrochemical methods attract attention of scientists for

detection of 4-nitrophenol due to the fact that nitro group can be easily reduce by electrochemical method [170]. Thus, characteristic of nitro group reduction make voltammetric detection of toxic 4-NP at trace level very famous. Electrochemical methods are very attractive due to high sensitivity, selectivity, cost-efficiency, and rapidity.

The inadequate electrocatalytic characteristics of conservative electrodes, nevertheless, restrain their role in determining 4-NP trace concentrations. To improve the electrocatalytic attributes of electrodes various sort of modifications can be applied such as nanoporous gold [171], graphene oxide [170,172], hybrid inorganic coating [173] bismuth film [174], porous copper [75], molecularly imprinted polymer [175] and multi-walled carbon nanotubes [176] has been reported for sensitive detection of 4-NP. Nevertheless, a simple, novel and sensitive electrocatalyst is still required for detection of 4-NP in existent models. Electrochemical treatment of graphite pencil electrode seems to be a unproblematic, quick and enormously appropriate approach as compared to other strategies [27,133]. Interestingly, nanomaterials are widely utilized in different electrocatalytic detections because of high surface area and quick electron transferal rates. Various electrodes modified by AuNP were employed to identify 4-NP e.g. AuNP-GCE [177], NiDMG /AuNP- GCE, [178] RGO / AuNP- GCE [179] and AuNP-ITO [180]. For the electroanalysis of other important analytes such as hydrazine, hydroxylamine, homocysteine, diethylstilbestrol, catechol and hydroquinone, the highly electroactive AuNP based electrodes are used [181–184].

In present study, the advantages of AuNPs and PGPE were combined to get low cost, disposable, sensitive and selective AuNP-PGPE. As continuation of our efforts

[75,133] to overcome the fouling of electrode surface by phenols and its derivatives, a simple electrochemical detection procedure established on the base of gold nanoparticles modified electrochemically activated graphite pencil electrode (AuNP-PGPE) is explored to quantify trace amount of 4-nitrophenol. Correspondingly, the PGPE and AuNP-PGPE were applied to real water samples and all determinations are described in the subsequent divisions.

## 5.2 Experimental

### 5.2.1 Reagents

Analytical laboratory grade chemicals were utilized in this study and consumed without further refinement. 4-nitrophenol, Hydrogen tetrachloroaurate (III) hydrate, phenol, 4-aminobenzoic acid, 4-acetamindophenol, 2,3-dichlorophenol, 3,4-dichlorophenol. L-ascorbic acid (AA), sodium acetate buffer (AB) solution (3.0 M), ICP standards of Na, K, Ca, Cu and Co were acquired from Sigma Aldrich (USA). Double distilled water was employed for formulation of all the solutions. The remaining chemicals utilized in this study were same as listed in 2.1.1.

### 5.2.2 Apparatus

Auto Lab, Netherlands electrochemical work station was utilized to perform electrochemical impedance spectroscopy (EIS) trials. The cell for electrochemical measurements comprised a bare GPE or PGPE, or AuNP-PGPE were applied as per working electrode, auxiliary electrode was a Pt wire and Ag/AgCl (Sat. KCl) as reference electrode. other apparatus was same as written in 2.1.2.

### 5.2.3 Preparation of phosphate buffer saline of different pH

Preparation of PBS was done as described in 3.2.2.3.

### 5.2.4 Pretreatment of GPE and AuNP modification

For treatment of pencil graphite 10 mm of lead was squeezed out of pencil holder, counter and reference electrodes plunged in a cell comprises diverse amount of sodium hydroxide. Diverse potentials were used to electrochemically activate the surface of GPE. Following, two times mild sousing into double distilled water to clean the surface of prepared pretreated electrodes. These pretreated graphite pencil electrodes (PGPE) were used for electrochemical detection or further modification by AuNPs to get AuNP-PGPE.

Gold nanoparticles (AuNPs) were produced by the method describe in [185] to modify the surface of bare GPE or PGPE. Gold nanoparticles (AuNP) were formed at room temperature by mixing equal volumes of 1.0 mM gold (III) chloride and 1.65 mM of ascorbic acid (1.5 ml of each aqueous solution) in 3.0 ml test tube. In order to get gold nanoparticle loaded graphite pencil electrode (AuNP-GPE) or pretreated graphite pencil electrode (AuNP-PGPE), a bare GPE or pretreated GPE is immersed in 3.0 ml test tube containing AuNPs placed inside a water bath at 75$^{o}$C. After 15 min the AuNP modified electrode was removed and washed by sousing twice into double distilled water. Before consuming the electrode for 4-NP detection, it was dried at room temperature for 60 min. This methodology reported here was utilized for preparation of AuNP-GPE or AuNP-PGPE throughout the optimizations and detection of 4-NP, except differently declared.

### 5.2.5 Water sample preparation

Aquatic models were gathered from water tap in laboratory, sewage water, sea water from local area, swimming pool water from a facility in the university, and

drinking water were initially sieved by utilizing a filter paper of pore size 0.45 µm to eliminate any insoluble material and then 1.0 ml of each water sample was thinned up to 5 ml by using 0.1 M PBS for electrochemical detection.

## 5.3 Results and discussion

### 5.3.1 Electrode materials and pretreatment medium evaluation

For quantification of 4-nitrophenol (4-NP) the current intensity on the surface of electrode was observed. For this purpose, electrocatalytic attributes of diverse transducers for the 4-NP reduction were assessed by employing CVs. Glassy carbon (GC), Pt disc, carbon paste (CP), bare graphite pencil (GP), Au disc and pretreated graphite pencil (PGPE) electrodes were experienced. The outcomes exposed that apart from untreated GPE remaining four probes (GC, CP, Pt, and Au) did not respond fine to 1 mM concentration of 4-NP, GPE presented a distinct 4-NP peak response (Figure 5. 1 A). Then effect of pretreatment medium was assessed by utilizing NaOH and phosphate buffer (PB) solution. Very broad peak was obtained from graphite pencil treated with PB. On the other hand, NaOH pretreated GPE (PGPE) showed well defined peak with highest peak current Figure 5.1 B. The coupling among PGPE and the 4-NP outputs exceedingly sensitive and selective electrochemical detection.

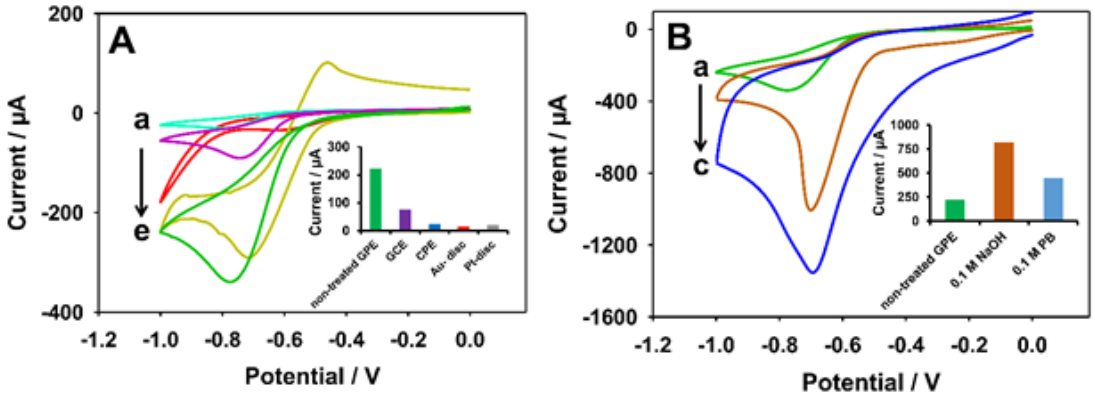


**Figure 5. 1. (A) CVs of 1 mM 4-nitrophenol in 0.1 M acetate buffer, pH 4.8 at untreated (a) CPE, (b) GCE, (c) Au, (d) Pt and (e) GPE, inset is corresponding histogram, (B) CVs of 1 mM 4-nitrophenol in 0.1 M acetate buffer, pH 4.8 at a) non-treated GPE, (b) 0.1 M NaOH treated GPE and (c) 0.1 M PB treated GPE. Working conditions: Pretreatment potential 1.3 to 1.9 V, pretreatment segments 50, pretreatment and detection scan rates 100 mV/s.**

Graphite pencil electrode mainly consist of 65% graphite, 30% clay and only 5% is electro-inactive polymer as a binding agent. Hence, graphite lead is chiefly consisting of a carbon allotropic form graphite which has atoms interconnected by weak bonds. Clay occurs in nature as aluminosillicate that display ion exchange features. Nevertheless, the graphitic portion of lead pencil become clean, and numerous oxygen carrying functional groups are bonded when electrochemically pretreated in electrolyte solution. The prominent improvement in electrocatalytic activity of GPE after pretreatment can be accredited to the magnified concentration of functional groups on the surface of electrode or development of graphite oxide layer [27].

Concentration of pretreatment solution display a major effect on the GPE response, diverse concentrations of NaOH extending between 0.1 M to 1.0 M. CVs exposed that electrode pretreated in 0.8 M NaOH support the reduction of 4-NP and presented highest peak current (Data not shown).

### 5.3.2 Characterization of PGPE

The PGPE obtained from pretreatment of bare GPE in 0.8 M NaOH displayed highest reduction current for 4-NP. Consequently, all of characterizations for PGPE were mostly focused on the PGPE prepared in NaOH solution. The characterization of PGPE was done by utilizing different techniques such as CV and EIS.

On the way to measure the electrocatalytic activity of pretreated GPE surfaces $Fe(CN)_6^{3-/4-}$ redox pair was employed. Firstly, CV measurements were accomplished in 0.1 M KCl aqueous solution comprising 5 mM $Fe(CN)_6^{3-/4-}$ and results are mentioned in Figure 5. 2 A. The outcomes depicted that very broad peak for $Fe(CN)_6^{3-/4-}$ was obtained on untreated GPE. Conversely, utilization of NaOH had a noticeable effect on the electrochemical behavior of electrode, where not only the peak current amplified by 4 times but also there is a big change in shape of redox peaks. The dramatic upsurge in reduction signal of PGPE could be accredited to huge surface area of and large number of functional groups attached during the pretreatment process. It can be concluded that PGPE showed different characteristics from untreated GPE. In order to relate the cyclic voltammetric behavior of untreated and treated GPE in 6 M solution of NaOH at sweeping frequency of 2 mV/s (information not shown). Calculation of capacitance for both electrodes was done by using equation 5.1. [133]

$$C = Q / \Delta E \, . \, m \qquad 5.1.$$

The voltammetric charge is denoted by Q, weight of electrode is mentioned by m and potential window employed for the cyclic scan is indicated by ΔE. The capacitance calculated on the established on integrated region underneath the cyclic voltammogram for untreated and treated GPE were 147.76 F/g and 4767.46 F/g respectively. The

spectacular enhancement of specific capacitance of treated GPE surface might be credited to accumulation and establishment of charge carrier entities on exterior of electrode because of treatment in NaOH aqueous solution.

Furthermore, Figure 5. 2 B showed Nyquist diagrams of untreated GPE and PGPE in 0.1 M KCl comprising 5 mM each of $K_4[Fe(CN)_6]$ and $K_3[Fe(CN)_6]$ by using frequency array between 0.01 Hz to 100 kHz. The actual and negative values of the imagined impedance variables were designated by Z and –Z correspondingly. The graph of untreated GPE comprise a semicircle and also a straight line, whereas PGPE showed just a straight line. At higher frequencies appearance of semicircular part is due to a limiting charge transfer process at boundary of electrode and electrolyte, although straight part of the graph at low frequency area could be due to diffusion process in solid. Consequently, ohmic resistance for reaction at electrode surface is comparatively much smaller at PGPE. The PGPE show high slop at low frequency region suggesting that PGPE is more capacitive as compared to untreated GPE. These results also support the conclusion drawn from Figure 5. 2A.

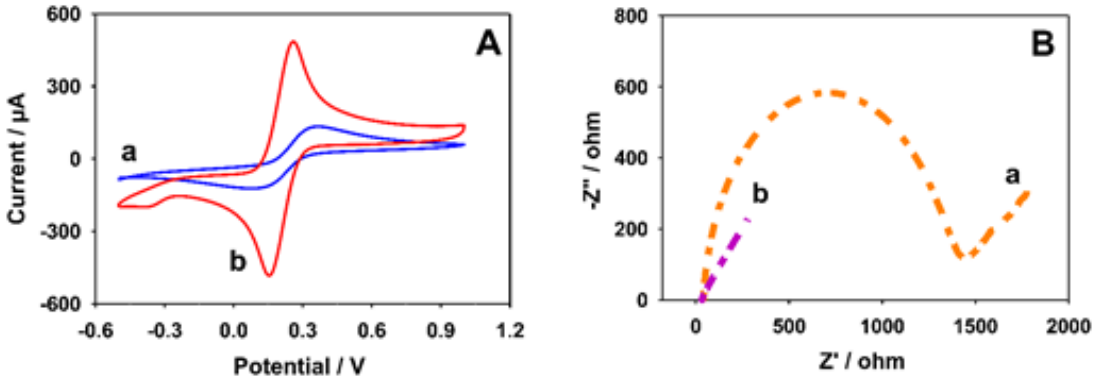


**Figure 5. 2. (A) CVs of 5.0 mM Fe(CN)63-/4- obtained in 0.1 M KCl by the untreated (a) GPE and (b) GPE treated in 0.8 M NaOH, (B) Nyquist plots in 0.1 M KCl solution containing a mixture of 5 mM K4[Fe(CN)6] and 5 mM K3[Fe(CN)6] of untreated (a), and treated (b) GPE.**

The electroactive surface are of untreated and pretreated GPE was calculated by utilizing Randles–Sevcik equation 5.2. [136]

$$I_p = 2.69 \times 10^5 C n^{3/2} A D^{1/2} \gamma^{1/2} \qquad 5.2.$$

Where $I_p$ refers to anodic peak current, analyte concentration (mol/L) is denoted by C, count of electrons transferred during the redox process on the conductor exterior are signified as n, electroactive surface area of detection probe ($cm^2$) is symbolized as A, diffusion constant ($cm^2 s^{-1}$) is indicated as D and γ denotes sweep rate (V/s). For the calculation of electroactive area CV scans were recorded between 10 to 400 mV in aqueous solution of $K_4[Fe(CN)_6]$, $K_3[Fe(CN)_6]$ and 0.1 M KCl by means of untreated GPE and PGPE Figure 5. 3. By using above mentioned equation electroactive areas obtained 0.0536 $cm^2$ and 0.11 $cm^2$ for untreated and pretreated GPEs respectively. Consequently, it can be stated as, the electroactive surface area of PGPE is higher as compare to untreated GPE.

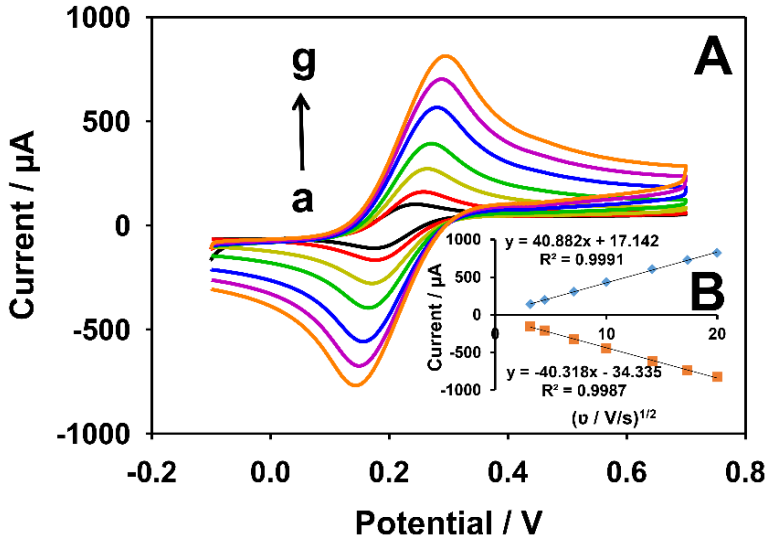


**Figure 5. 3. (A) Cyclic voltammograms of the pretreated graphite pencil electrode in 0.1 M KCl at various scan rates: (a) 10, (b) 20, (c) 50, (d) 100, (e) 200, (f) 300 and (g) 400 mV/s. (B) Plots of peak currents vs. square root of scan rates.**

The electrochemical performances of the untreated and treated GPEs were analyzed by utilizing cyclic voltammetric measurements in the incidence and absence of 20 µM 4-NP in PBS as shown in Figure 5. 4. Without 4-NP no cyclic voltammetric current was detected for both untreated and treated GPEs. However, the background peak current was significantly higher for PGPE as compared to untreated GPE because of improvement in surface area of GPE after treatment in basic solution. Afterward, addition of 20 µM 4-NP showed a reduction peak for reverse scan for both treated and bare GPEs. The reduction process of 4-NP took place at -0.786 V and -0.62 for untreated GPE and treated GPE respectively. Nevertheless, in the forward scan, there was no electroactivity for both electrodes. The outcomes indicate that reduction of 4-NP was irreversible on both surfaces of electrodes. The PGPE displayed an electrocatalytic effect on reduction of 4-NP and change in reduction potential was also observed as compared to bare GPE. Moreover, the reduction peak current increased dramatically when PGPE was used, which refers to high surface area and functionality of PGPE which are either lower or absent in the untreated GPE. The electrochemical characterizations of PGPE agreed with one another, treatment of GPE enhance the electroactive area and increase the amount of charge on the surface of electrode that results in higher electroactivity and sensitivity.

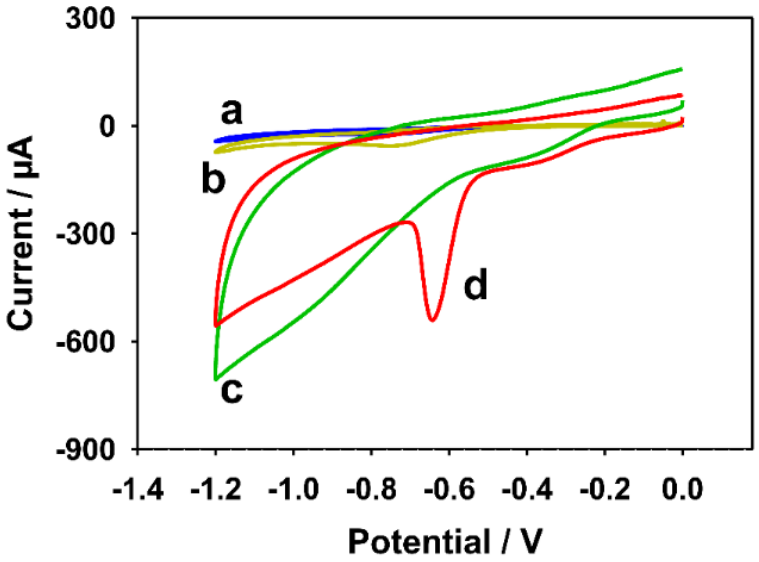


**Figure 5. 4. Cyclic voltammograms of the untreated GPE (a and b) and PGPE (c and d) in the absence (a and c) and presence (b and d) of 20 µM 4-NP in PBS (pH 5.6). Scan rate 50 mV/s, sample interval 0.001 V, accumulation time 60 sec and deposition potential -0.5 V.**

### 5.3.3 Optimizing the electrochemical treatment parameters

Pretreatment of electrode is very decisive in determining the sensitivity and selectivity of transducer for specific analyte. That is why it is enormously vital to optimize the pretreatment conditions for GPE. Primarily, to assess the upshot of number of peak segments, the activation of GPE was performed by applying diverse number of CV cycles between 1.3 – 1.9 V at 100 mV/s. Based on obtained fallouts (Figure 5. 5) highest current signal was obtained when activation of GPE was done at 50 pretreatment scan numbers.

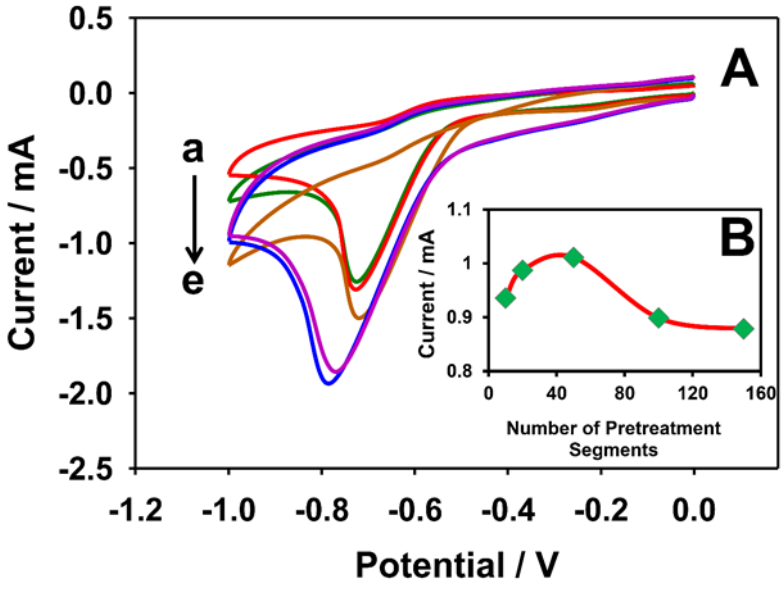


**Figure 5. 5. (A) CVs of 1 mM 4-nitrophenol in 0.1 M Acetate buffer, pH 4.8 at different number of pretreatment segments: a) 10, b) 20, c) 50, d) 100 and e) 150. Pretreatment is done in 0.8 M NaOH; other working conditions were same as in Figure 5. 1 (B) corresponding plot of current vs. number of treatment segments.**

Afterwards, to observe the upshot of pretreatment scan rate on reduction current of 1mM 4-NP, scan rate was altered between 20 – 1000 $mVs^{-1}$ and consequences (Figure 5. 6) disclosed that peak current for 20 and 1000 $mVs^{-1}$ were almost equivalent. At 100 $mVs^{-1}$ highest reduction was observed, that is why it was conceived as optimal scan rate for activation.

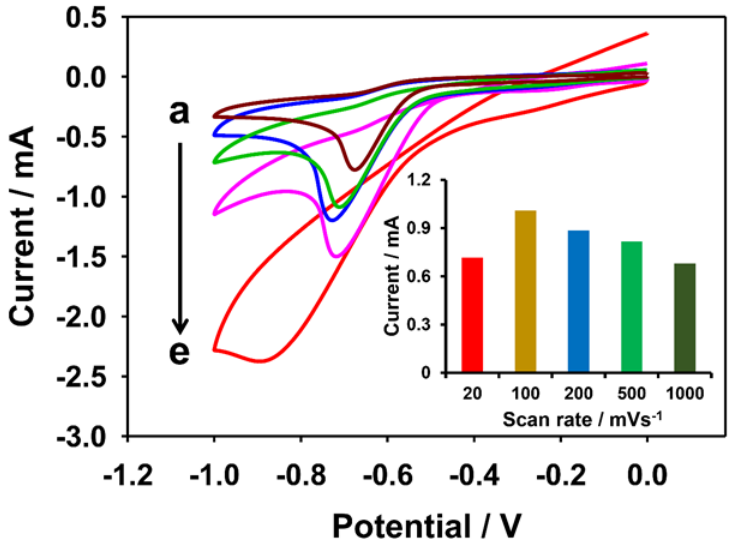


**Figure 5. 6. CVs of 1 mM 4-nitrophenol in 0.1 M Acetate buffer, pH 4.8 at various scan rates: a) 20, b) 100, c) 200, d) 500 and e) 1000 mV/s. Pretreatment is done in 0.8 M NaOH; other working conditions were same as in Figure 5. 1, inset is corresponding histogram.**

Ultimately, the influence of scan potential on GPE was analyzed. It was observed that potential range of 1.3 – 1.9 V display maximum voltammetric current (Figure 5. 7). The optimal pretreatment parameters are summed up in Table 5. 1.

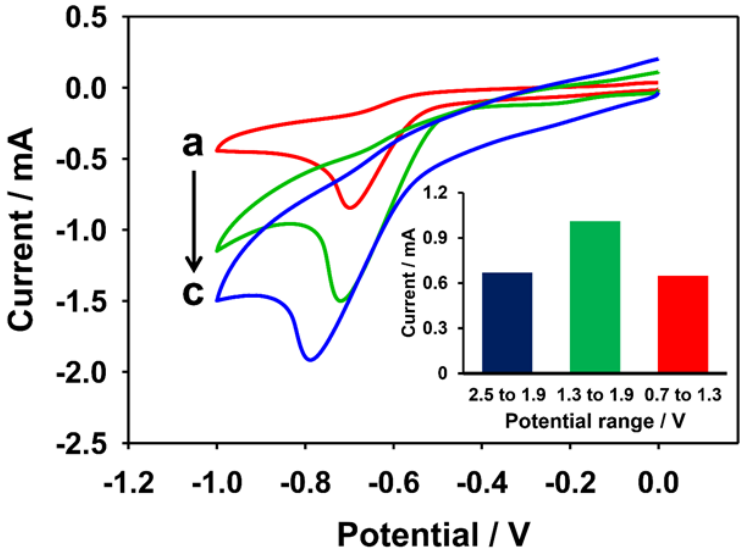


**Figure 5. 7. CVs of 1 mM 4-nitrophenol in 0.1 M Acetate buffer, pH 4.8 at GPEs in various pretreatment potential ranges: a) 0.7-1.3, b) 1.3-1.9 and c) 1.9-2.5 V. Pretreatment is done in 0.8 M NaOH, other working conditions were same as in Figure 5. 1, inset is corresponding histogram.**

**Table 5. 1. Optimized conditions for pretreatment of GPE**

| Conditions | Transducer | Treatment solution | Treatment potential range | Treatment scan rate | Number of treatment segments |
|---|---|---|---|---|---|
| **Optimization** | Graphite pencil electrode | 0.8 M NaOH | 1.3-1.9 V | 100 mV/s | 50 |

### 5.3.4 Detection technique, medium, and pH

In order to get most effective detection medium for 4-NP, numerous electrolyte solutions were employed such as AB, PB, and PBS (0.1 M, pH 4.8). It was discovered that 0.1M phosphate buffer saline yield maximum voltammetric signal for 4-NP (Data not shown), thus for all other optimization phosphate buffer saline was utilized. Figure 5. 8 displays that altering the pH of supporting electrolyte (PBS) between 3.2 to 6.4 displays obtrusive consequence on peak current. The outcomes disclosed that reduction peak potential shifted by increasing the pH, reduction peak potential depends linearly on pH per following equation 5.3.

$$E_p = -0.013\ pH - 0.627 \qquad 5.3.$$

Figure 5. 8 revealed that pH of 5.6 in the supporting electrolyte was optimum for sensing 4-NP. Dependence of peak potential on pH confirms that reduction process of 4-NP is completed due to participation of proton. So, the possible reduction process of 4-NP is

$$HOC_6H_4NO_2 + 4H^+ + 4e^- \longrightarrow HOC_6H_4NHOH + H_2O$$

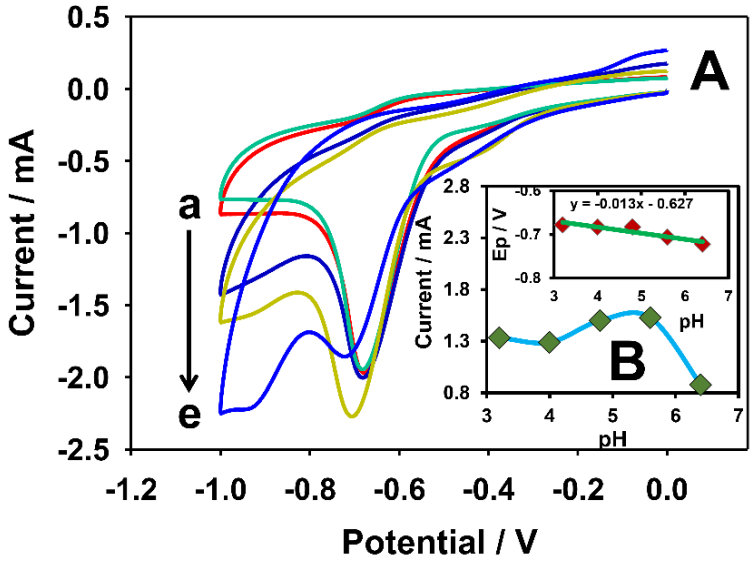


**Figure 5. 8. (A) CVs of 1 mM 4-nitrophenol in in 0.1 M phosphate buffer saline of various pH: (a) 4.8, (b) 3.2, (c) 4.0, (d) 5.6 and (e) 6.4. Pretreatment is done in 0.8 M NaOH; other working conditions were same as in Figure 5. 1. (B) The corresponding plot of peak current (µA) vs. pH and inset is the plot of peak potential (V) vs. pH.**

In pursuance of getting highest peak current for recognition of 4-NP diverse voltammetric techniques were employed such as; square wave, differential pulse, differential normal pulse, linear sweep and stair case voltammetry, the consequences (Figure 5. 9) led us to set linear sweep voltammetry as best technique for detection of 4-NP by utilizing PGPE.

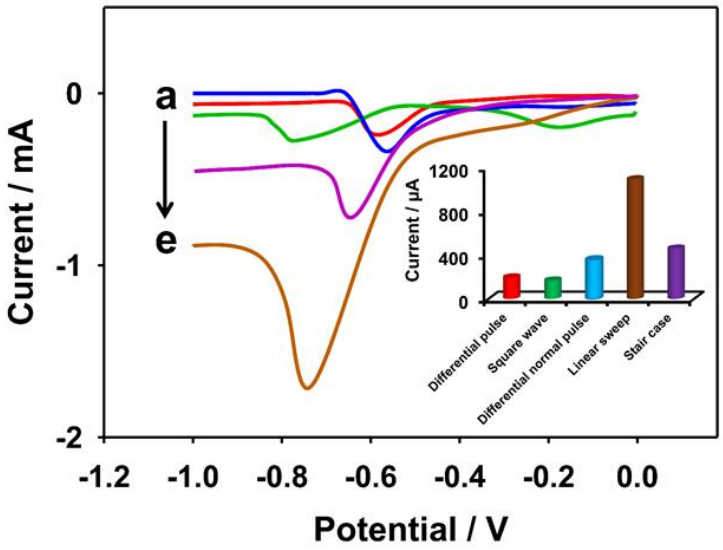


**Figure 5. 9. Voltammograms of 1 mM 4-nitrophenol in 0.1 M Acetate buffer, pH 5.6 under different techniques: a) differential normal pulse, b) differential pulse, c) square wave , d) stair case and e) linear sweep voltammetry. Inset is corresponding histogram. Pretreatment is done in 0.8 M NaOH; other working conditions were same as in Figure 5. 1.**

### 5.3.5 Optimization of LSASV parameters

To ascertain the effect of LSASV parameter on reduction current of 4-NP, scan rate and sample interval were optimized. Firstly, varying sample intervals were used for sensing 1 mM 4-NP by holding all the parameters fixed to study impression of square voltammetric sample interval on the electroactivity of PGPE, (Figure 5. 10 A).

Most prominent peak current was attained when 0.003V was employed. So, 0.003V was optimum sample interval for 4-NP detection. Results brought out that by changing scan rate activity of PGPE also change. LS curves display a large fluctuation in peak current and peak potential as well. From Figure 5. 10 B it can be observed that by increasing scan rate the peak current also heighten up to 4000 $mVs^{-1}$.

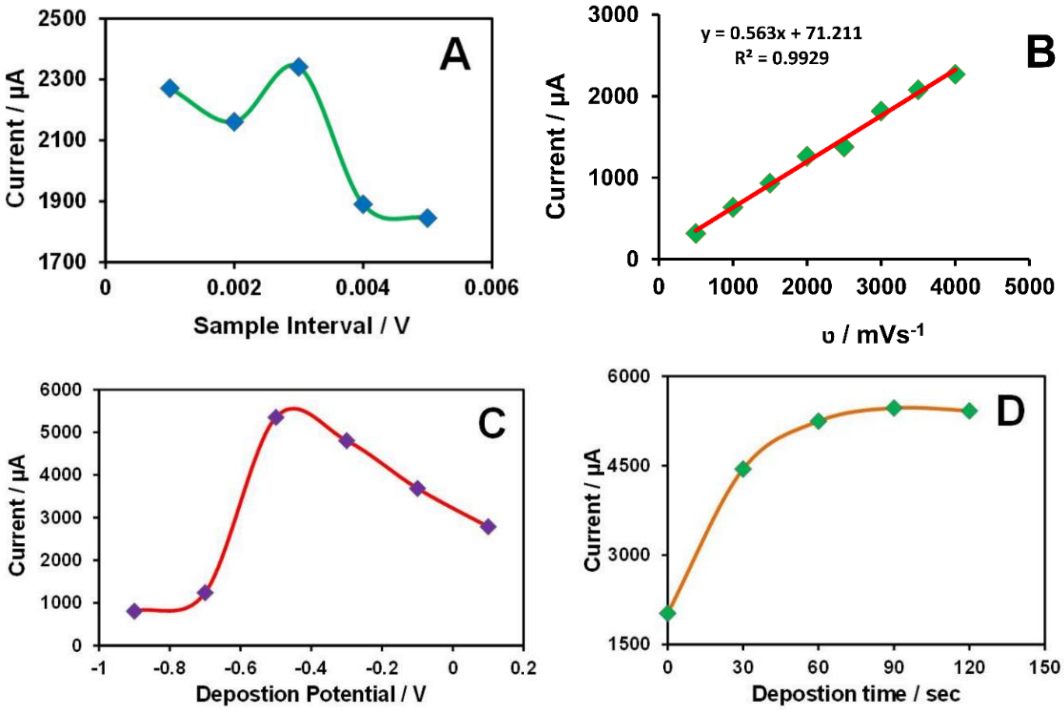


**Figure 5. 10. (A) Corresponding plots of LSVs peak current of 50 µM 4-nitrophenol in 0.1 M phosphate buffer saline, pH 5.6 vs: (B) Scan rate, (C) Deposition potential, (D) Deposition time, 1 mM 4-nitrophenol in 0.1 M phosphate buffer saline, pH 5.6 vs A) sample interval. Pretreatment was done in 0.8 M NaOH; other working conditions were same as in Figure 1.**

Correspondingly, Figure 5. 10 C shows that deposition potential deviations conspicuously effect the peak current of 50 µM 4-NP at PGPE. The potential was altered between -0.9 V to 0.1 V, outcomes disclosed that reduction signal was maximum for 4-NP at -0.5 V as mentioned in Figure 5. 10 C. Lastly, effect of deposition time was monitored using PGPE in PBS, pH 5.6, containing 4-NP. As the deposition time was raised the peak current also amplified up to 60 secs, subsequently, it flattened off to fixed number as publicized in Figure 5. 10 D. These reflections directed us to fix 60 secs as the optimal deposition time for 4-NP. The optimum LSASV parameters are summed up in Table 5. 2.

**Table 5. 2. Optimized conditions for detection of 4-NP.**

| Conditions | Technique | Scan rate | Sample interval | Deposition Time | Deposition Potential | Detection medium |
|---|---|---|---|---|---|---|
| **Optimization** | Linear sweep voltammetry | 4000 mV/s | 0.003 V | 60 sec | -0.5 V | PBS, pH 5.6 |

## 5.3.6 Calibration

### 5.3.6.1 Detection of 4-NP by PGPE

Dependence of 4-NP peak currents on its concentration was observed by plotting the peak maxima of the LSVs in Figure 5. 11. Under optimum conditions as mentioned in Table 5. 1 and 5. 2 voltammetric signal were linearly proportionate to increasing amount of 4-NP between 0.01 to 0.8 µM with a regression factor of $R^2$ = 0.998 (Figure 5. 11, inset). So, the limit of quantification is 0.01 µM or 10 nM, and limit of detection is 2 nM (S/N=3) for 4-NP by PGPE. When outcomes for detection of 4-NP were compared with other sensors, PGPE showed lower detection limit (Table 5. 3). Interestingly, the simplicity in preparation of PGPE make it striking for laboratory and field application as compared to other transducers mentioned in table 5. 3.

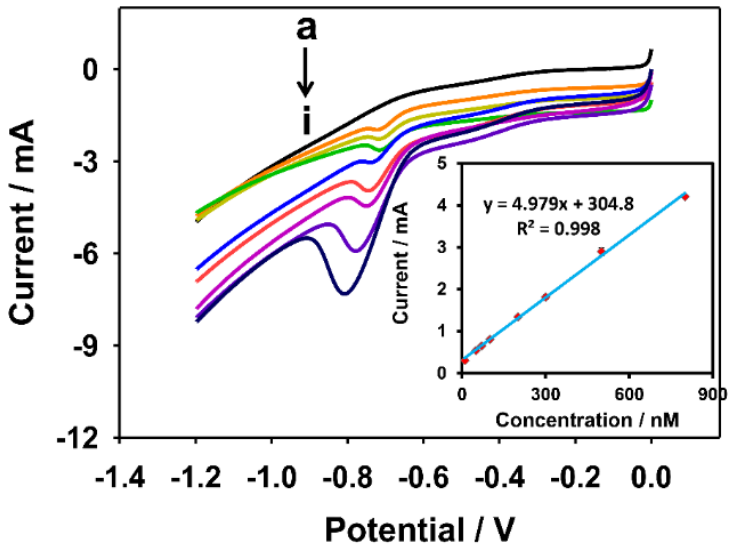


**Figure 5. 11. LSVs of 4-nitrophenol in 0.1 M phosphate buffer saline, pH 5.6 at different concentrations: (a) blank, (b) 10, (c) 30, (d) 50, (e) 70, (f) 100, (g) 200, (h) 300, (i) 400, (j) 500 and (k) 800 nM. Inset is corresponding plot of peak current vs concentration. Other working conditions are mentioned in above table 5. 1 and 5. 2.**

### 5.3.6.2 Detection of 4-NP by AuNP-PGPE

4-NP can be present in real samples at concentration higher than the linear range of PGPE for 4-NP, i.e. 0.01 – 0.8 µM. That is why AuNPs were introduced on the surface of PGPE to increase the linear range of already developed electrode. The AuNP-PGPE under optimized conditions displayed linear dependence of square wave voltammetric signal against concentration of 4-NP between 0.5 to 100 µM with regression equation y = 3.597x - 2.3772 ($R^2$ = 0.9994) as mentioned in Figure 5. 12. The AuNP-PGPE can be applied to the samples having very high concentration of 4-NP.

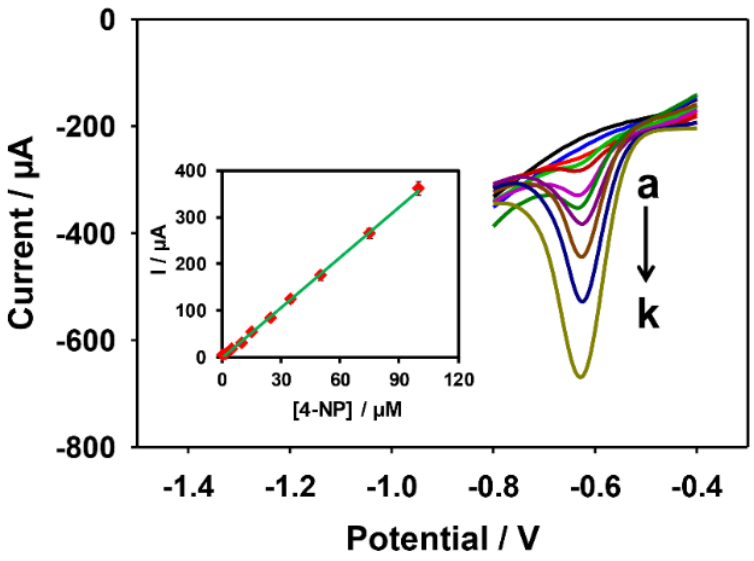


**Figure 5. 12. CVs in 0.1 M PBS in the absence (a) or presence (b) of 0.5 mM 4-NP at bare GPE (A), at AuNP-GPE (B) and AuNP-PGPE (C). Scan rate: 100 mV/s.**

### 5.3.7 Reproducibility of PGPE and AuNP-PGPE

The duplicability of the 4-NP detection procedure was established by electrochemically reducing 4-NP using 5 freshly fabricated PGPE electrodes. The outcomes displayed a good reproducibility with standard deviation of 2.93 %. On the other hand, 5 newly formed AuNP modified PGPE exhibited satisfactory RSD value of 2.80 %. These results revealed that the PGPE or AuNP-PGPE can be applied to wide range of concentration with higher reproducibility rate.

**Table 5. 3. Comparison of present work with some other electrochemical sensors for 4-NP.**

| Technique | Sensing materials | Sensing media (pH) | Linear range (µM) | Limit of detection (µM) | Limit of quantification (µM) | Ref. |
|---|---|---|---|---|---|---|
| Linear sweep voltammetry | Pretreated GPE | 0.1 M PBS (pH 5.6) | 0.01 – 0.8 | 0.002 | 0.01 | This work |
| Square wave voltammetry | AuNP-PGPE | | 0.5 – 100 | 0.30 | 0.50 | |
| Linear sweep voltammetry | Graphene oxide / GCE | 0.1 M acetate buffer (pH 4.8) | 0.1 – 120 | 0.02 | 0.1 | [170] |
| Square wave voltammetry | Prussian blue / platinum electrode | 0.1 M PB (pH 6.0) + 0.1 M KCl | 0.01 – 0.09 | 0.01 | 0.01 | [173] |
| Square wave voltammetry | AuNP / RGO /GCE | 0.067 M phosphate buffer (pH 6.0) | 0.05 – 2.0 | 0.02 | 0.05 | [180] |
| Differential pulse voltammetry | Multi-wall carbon nanotubes Nafion / GCE | 0.1 M PB (pH 4.0) | 0.1 – 10 | 0.04 | 0.1 | [177] |
| Amperometry | Porous copper / GPE | 0.1 M acetate buffer (pH 4.8) | - | 1.9 | - | [175] |
| Square wave voltammetry | Bismuth film / GCE | 0.04 M BR buffer (pH 4.0) | 0.007 – 0.07 | 0.004 | 0.007 | [174] |
| Square wave voltammetry | AgNP / RGO /GCE | 0.1 M phosphate buffer (pH 7.2) | 0.01 – 0.1 | 0.0012 | 0.01 | [172] |
| Differential pulse voltammetry | RGO / MIP | 0.1 M phosphate buffer (pH 5.5) | 0.01 - 100 | 0.005 | 0.01 | [176] |

### 5.3.8 Electrochemical behavior and characterization of AuNP-PGPE

The impression of AuNP on the reduction of 4-NP was evaluated by cyclic voltammograms of untreated GPE (A), AuNP-GPE (B) and AuNP-PGPE (C) in the absence (a) and existence (b) of 0.5 mM 4-NP. The AuNP on the surface of bare GPE did not show any prominent effect on the electrochemical reduction current of 4-NP (Figure 5. 13 B). However, AuNP on the surface of PGPE increase the reduction signal by more than 2 times as compared to bare GPE (Figure 5. 13 C). Correspondingly there is reduction peak shift from -0.786 to -0.668 for bare GPE and AuNP-PGPE respectively. The AuNP-PGPE also displayed a characteristics reduction peak for gold at -0.453 V in 0.1 M PBS (pH 7.0)[186, 187]. Thus, CV experiment established the existence of Au on AuNP-PGPE.

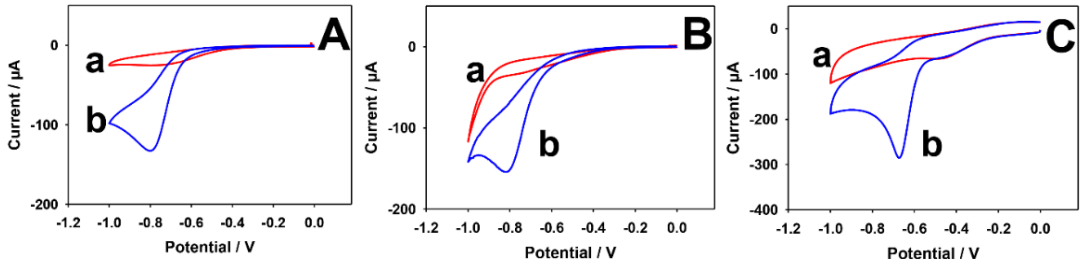


**Figure 5. 13. Square wave voltammograms in PBS (0.1 M, pH 6.5) containing different µmol L−1 concentrations of 4-NP at a AuNP-PGPE: (a) 0.0, (b)0.5, (c) 2.0, (d) 5.0, (e) 10.0, (f) 15.0, (g) 25.0, (h) 35.0, (i) 50.0, (j) 75.0, and (k) 100.0 µM 4-NP. Inset is corresponding calibration curve.**

The electroactive surface are of untreated and pretreated GPE was calculated by utilizing Randles–Sevcik equation 5.4. [136]

$$I_p = 2.69 \times 10^5 C n^{3/2} A D^{1/2} \gamma^{1/2} \qquad 5.4.$$

For the calculation of electroactive area CV scans were recorded between 2 to 200 mV in 5 mM solution of $K_4[Fe(CN)_6]$, $K_3[Fe(CN)_6]$ and 0.1 M KCl by utilizing untreated GPE and AuNP-PGPE Figure 5. 14. By using above mentioned equation, electroactive areas obtained 0.0536 $cm^2$ and 0.099 $cm^2$ for untreated GPE and AuNP-PGPE

respectively. Consequently, it can be stated as the electroactive surface area of AuNP-PGPE is higher as compare to untreated GPE.

The well-known method for synthesis of AuNP is applied, where Au in solution form is reduced to metal nanoparticles by ascorbic acid [187]. At 75$^{o}$C the AuNP not only bind to the surface of electrode but AA sorbed on the surface of AuNP can be detached by using this temperature.

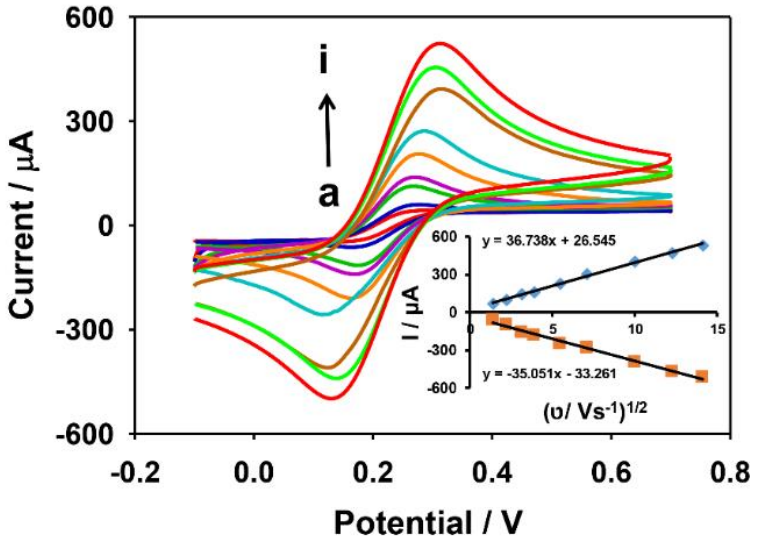


**Figure 5. 14. (A) Cyclic voltammograms of the AuNP-PGPE obtained from 5.0 mM Fe(CN)63-/4- in 0.1 M KCl at various scan rates: (a) 2, (b) 5, (c) 10, (d) 15, (e) 30, (f) 50, g) 100, (h) 150 and (i) 200 mV/s. Inset is plot of peak currents vs. square root of scan rates.**

### 5.3.9 Quantification of 4-NP in water samples and effect of interferences

Recognition of 4-NP in aqueous samples utilizing untreated GPE is out of the question due to its low electrocatalytic activity. The capability of the PGPE was inspected to sense low quantities of 4-NP in real samples. The 4-NP content in actual water usually does not exceed the detection limit of the described technique, that is why it cannot be detected directly. Due to this reason 0.2 µM 4-NP was supplied to the water samples. Outcomes showed promising recovery of 97 %, 98% and 103 % in swimming pool water,

tap water from laboratory and sea water respectively. On the other hand, the AuNP-PGPE was employed to aqueous samples containing relatively higher amount of 4-NP, i.e. 25 µM. AuNP-PGPE also displayed an acceptable recovery ranging between 96 – 100 %. The outcomes displayed a wide range of concentration that can be measure by using PGPE or AuNP-PGPE.

In order to estimate outcome of diverse interfering compounds on the reduction signal of 4-NP, a study has been done Figure 5. 15. It was observed that 0.2 µM added amount of 3,4-dichlorophenol, 2,3-dichlorophenol, phenol, 4-acetamidophenol, 4-aminobenzoic acid and combination of metallic ion solution ($Co^{+2}$, $Cu^{+2}$, $Ca^{+2}$, $K^{+}$, $Na^{+}$) variate the 4-NP reduction current by -8.04 %, +10.87%, +5.66%, -11.69%, -6.85% and +2.53% respectively. Instead, AuNP-PGPE show variation of signals in between -1.5 – +5.1 % for the 25 µM phenol, 4-bromophenol, 4-aminophenol, 4-actamidophenol, 2,4-dichlorophenol and 3,4-dichlorophenol as shown in Table 4. These experiments showed the decent sensing selectivity and sensitivity of the PGPE and AuNP-PGPE.

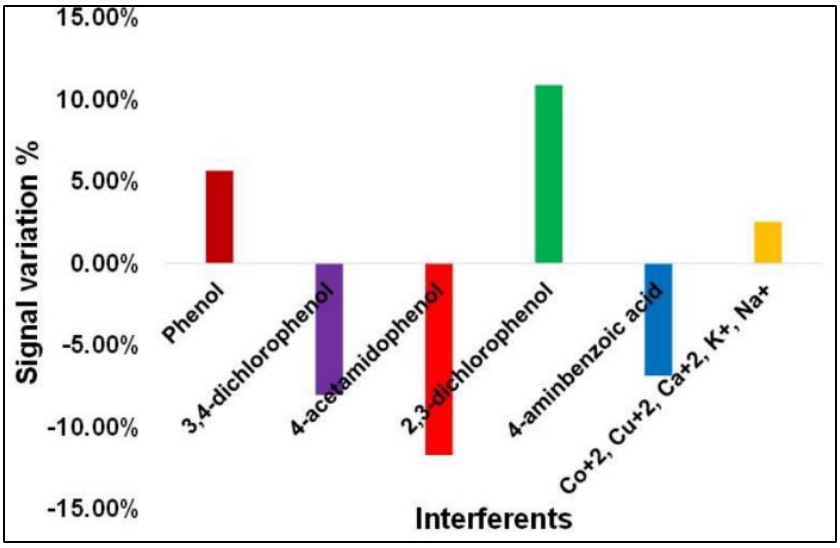


**Figure 5. 15. Corresponding histograms in 0.1 M phosphate buffer saline, pH 5.6 showing effect of 200 nM interferents on reduction peak current of 4-NP.**

**Table 5. 4. Effect of different contaminants (25.0 µM) on peak current of 25.0 µM 4-NP at AuNP-PGPE under optimal conditions.**

| Potential interferences | % Signal changes |
|---|---|
| Phenol | +4.57 |
| 4-aminophenol | -0.59 |
| 4-bromophenol | +2.24 |
| 3,4-dichlorophenol | +5.15 |
| 4-acetamidophenol | -1.56 |
| 2,4-dichlorophenol | -1.44 |

## 5.4 Summary

Activation of graphite pencil electrode in basic media increases its electrocatalytic activity for reducing 4-NP. Appraisal of outcomes achieved with untreated GPE and PGPE discloses that PGPE show better selectivity, sensitivity and low limit of detection (S/N=3), i.e. 2 nM. PGPE can be believed as a detector exhibiting remarkable electrocatalytic characteristics, inexpensive and easy to produce. AuNP modification was applied to enhance the working linear range of PGPE. Thus, the AuNP-PGPE displayed a dependence on concentration ranging from 0.5 – 100 µM of 4-NP with satisfactory RSD and high resistivity for higher concentration of interference added. The proposed sensors can be satisfactorily employed for wide range of quantity of 4-NP in actual aqueous models.

# Chapter 6

## Conclusion

In the present scenario, trace level detection of environmental pollutants is very crucial. The origin of such circumstances resulted in high demand of novel electrocatalyst. Among various carbon electrodes, GPE attracted the attention of scientific community due to its simplicity, viability and low cost. Present work described the fabrication, characterization, and investigation of the electrochemically activated GPE. This work tested various type of pretreatment solution, and it was inferred that the selectivity and sensitivity of the carbon electrodes majorly depends on the nature of electrolyte utilized for the activation of electrode surface. The electrochemical pretreatment introduce oxygen-containing functional groups on the surface of electrode and presence of these functional groups on the surface of pretreated carbon electrodes also helps in enhancing the selectivity of electrode towards the target analytes. The developed working electrodes displayed specific structural, electronic and chemical characteristics. The electrochemical pretreatment of carbon electrodes produces such transducers that display undistorted, distinct and consistent signals. The pretreated carbon electrodes also resolve the signal of close peaks with good signal-to-background characteristics as compared to untreated and modified electrodes.

The starting material utilized in all experimental work is commercially available graphite pencil electrode. The GPE was modified through facile activation by electrochemical pretreatment in aqueous media for the detection of target analytes. A new strategy has been described in chapter 2 to detect phenols at trace level. A charge is stored on the surface of GPE when it was activated in the basic aqueous solution. Open-

circuit polymerization was done by immersing the charged electrode in a solution containing phenol. The pCGPE was never used before for this purpose, and it displayed very low detection limit for phenol, i.e. 4.17 nM. Chapter 3 describes that by varying the pretreatment electrolyte and deposition potential, the PGPE shows distinct behavior towards same analyte. When aqueous solution of NaOH was employed for treatment of GPE surface, it shows affinity towards the α-naphthol. While on the other hand, replacement of NaOH with KOH and application of certain deposition potential resulted in formation of poly-α-naphthol with very low detection limit, i.e. 9.0 nM. Chapter 4 describes that selectivity of the treated surface majorly depends on nature of electrolyte solutions. For trace level detection of 4-chloro-1-naphthol, a mixture of NaOH and sodium acetate aqueous solution was utilized to treat the surface. The PGPE-NHNA was applicable to wide range of concentration of 4-CNP, i.e. 0.01 – 1.0 µM with detection limit of 1.57 nM. Another significant contribution this dissertation has made is that in chapter 5, which describes pretreated GPE can be utilized as the platform for the nanoparticle modification. The workable range of PGPE increases dramatically from 0.01 – 0.8 µM to 0.5 – 100 µM when AuNPs are deposited on the pretreated surface of graphite pencil electrode. This chapter has opened a new dimension, which was not considered before. The performance of the novel PGPEs demonstrated to be outstanding and was found to be appropriate for the analytical determination of various concentrations of target species in the incidence of many interfering agents. Evaluation of outcomes attained with non-pretreated GPE and PGPE discloses that PGPE shows high sensitivity and low limit of detection. The electrochemical pretreatment eliminates the use of hazardous material that are needed for the complex modification of electrode

surface. So, it can be inferred that pretreatment of the carbon electrode is easy, safe and environment-friendly.

The area of electrochemical transducers is uninterruptedly budding, contributing more and more materials for identifying the environmental pollutants. Development of highly specific electrochemical detector and multiplex determination in the presence of complex matrix is the demand of today application-oriented scientific world. The collection, treatment, and analysis of the sample to measure the quantities of hazardous chemicals is a tedious job. So, there is a great need to commercialize the electrochemically treated GPE for the individual or simultaneous detection of environmental pollutants. In short, there is a considerable room for the development of more sensitive, selective, quick response and sophisticated sensors for detection of phenol, α-naphthol and their derivatives.

# References


[1] A.J.S. Ahammad, J.J. Lee, M.A. Rahman, Electrochemical sensors based on carbon nanotubes, Sensors. 9 (2009) 2289–2319.

[2] J.X. Qiao, H.Q. Luo, N.B. Li, Electrochemical behavior of uric acid and epinephrine at an electrochemically activated glassy carbon electrode, Colloids Surfaces B Biointerfaces. 62 (2008) 31–35.

[3] J.M. Nugent, K.S. V. Santhanam, A. Rubio, P.M. Ajayan, Fast electron transfer kinetics on multiwalled carbon nanotube microbundle electrodes, Nano Lett. 1 (2001) 87–91.

[4] R.S. Nicholson, Theory and application of cyclic voltammetry for measurement of electrode reaction kinetics, Anal. Chem. 37 (1965) 1351–1355.

[5] D.B. Sepa, M.V. Vojnovic, A. Damjanovic, Reaction intermediates as a controlling factor in the kinetics and mechanism of oxygen reduction at platinum electrodes, Electrochim. Acta. 26 (1981) 781–793.

[6] M. Mogensen, K.V. Jensen, M.J. Jorgensen, S. Primdahl, Progress in understanding SOFC electrodes, Solid State Ionics. 150 (2002) 123–129.

[7] R.L. McCreery, Advanced carbon electrode materials for molecular electrochemistry, Chem. Rev. 108 (2008) 2646–2687.

[8] J. Lee, D.W.M. Arrigan, D.S. Silvester, Mechanical polishing as an improved surface treatment for platinum screen-printed electrodes, Sens. Bio-Sensing Res. 9 (2016) 38–44.

[9] A. Dekanski, J. Stevanović, R. Stevanović, B.Ž. Nikolić, V.M. Jovanović, Glassy carbon electrodes: I. Characterization and electrochemical activation, Carbon N. Y. 39 (2001) 1195–1205.

[10] S. Ranganathan, T.-C. Kuo, R.L. McCreery, Facile preparation of active glassy carbon electrodes with activated carbon and organic solvents, Anal. Chem. 71 (1999) 3574–3580.

[11] D.T. Fagan, I.F. Hu, T. Kuwana, Vacuum heat-treatment for activation of glassy carbon electrodes, Anal. Chem. 57 (1985) 2759–2763.

[12] K.J. Stutts, P.M. Kovach, W.G. Kuhr, R.M. Wightman, Enhanced electrochemical reversibility at heat-treated glassy carbon electrodes, Anal. Chem. 55 (1983) 1632–1634.

[13] M. Poon, R.L. McCreery, In situ laser activation of glassy carbon electrodes, Anal. Chem. 58 (1986) 2745–2750.

[14] R. DeClements, G.M. Swain, T. Dallas, M.W. Holtz, R.D. Herrick, J.L. Stickney, Electrochemical and surface structural characterization of hydrogen plasma treated glassy carbon electrodes, Langmuir. 12 (1996) 6578–6586.

[15] J. Schreurs, J. van den Berg, A. Wonders, E. Barendrecht, Characterization of a glassy-carbon-electrode surface pretreated with rf-plasma, Recl. Des Trav. Chim. Des Pays-Bas. 103 (2010) 251–259.

[16] J. Wang, L.D. Hutchins, Activation of glassy carbon electrodes by alternating current electrochemical treatment, Anal. Chim. Acta. 167 (1985) 325–334.

[17] M.A. Miller, A. Bourke, N. Quill, J.S. Wainright, R.P. Lynch, D.N. Buckley, R. F. Savinell, Kinetic study of electrochemical treatment of carbon fiber microelectrodes leading to in situ enhancement of vanadium flow battery efficiency, J. Electrochem. Soc. 163 (2016) 2095–2102.

[18] A. Bourke, M.A. Miller, R.P. Lynch, J.S. Wainright, R.F. Savinell, D.N. Buckley, Effect of cathodic and anodic treatments of carbon on the electrode kinetics of V IV /V V oxidation-reduction, J. Electrochem. Soc. 162 (2015) 1547–1555.

[19] H. Notsu, I. Yagi, T. Tatsuma, D.A. Tryk, A. Fujishima, Introduction of oxygen-containing functional groups onto diamond electrode surfaces by oxygen plasma and anodic polarization, Electrochem. Solid-State Lett. 2 (1999) 522–524.

[20] T. Tojo, K. Sakurai, H. Muramatsu, T. Hayashi, K.-S. Yang, Y.C. Jung, C. M. Yang,
M. Endo, Y. A. Kim, Electrochemical role of oxygen containing functional groups on activated carbon electrode, RSC Adv. 4 (2014) 62678–62683.

[21] Z.R. Yue, W. Jiang, L. Wang, S.D. Gardner, C.U. Pittman, Surface characterization of electrochemically oxidized carbon fibers, Carbon N. Y. 37 (1999) 1785–1796.

[22] R. Bowling, R.T. Packard, R.L. McCreery, Mechanism of electrochemical activation of carbon electrodes: role of graphite lattice defects, Langmuir. 5 (1989) 683–688.

[23] R.J. Bowling, R.T. Packard, R.L. McCreery, Activation of highly ordered pyrolytic graphite for heterogeneous electron transfer: relationship between electrochemical performance and carbon microstructure, J. Am. Chem. Soc. 111 (1989) 1217–1223.

[24] L.J. Bjelica, L.S. Jovanović, Activation of glassy carbon electrode in aqueous and non-aqueous media, Electrochim. Acta. 37 (1992) 371–372.

[25] K. Ravichandran, R.P. Baldwin, Enhanced voltammetric response by electrochemical pretreatment of carbon paste electrodes, Anal. Chem. 56 (1984) 1744–1747.

[26] A. Rana, A.N. Kawde, Novel electrochemically treated graphite pencil electrode surfaces for the determination of trace α-naphthol in water samples, J. Chinese Chem. Soc. 63 (2016) 668–676.

[27] E. Alipour, M.R. Majidi, A. Saadatirad, S. mahdi Golabi, A.M. Alizadeh, Simultaneous determination of dopamine and uric acid in biological samples on the pretreated pencil graphite electrode, Electrochim. Acta. 91 (2013) 36–42.

[28] K. Farhadi, A. Karimpour, Electrochemical behavior and determination of clozapine on a glassy carbon electrode modified by electrochemical oxidation., Anal. Sci. 23 (2007) 479–83.

[29] Q. Chi, W. Göpel, T. Ruzgas, L. Gorton, P. Heiduschka, Effects of pretreatments and modifiers on electrochemical properties of carbon paste electrodes, Electroanalysis. 9 (1997) 357–365.

[30] R.C. Engstrom, V.A. Strasser, Characterization of Electrochemically Pretreated Glassy Carbon Electrodes, Anal. Chem. 56 (1984) 136–141.

[31] J.C. Hoogvliet, M. Dijksma, B. Kamp, W.P. van Bennekom, Electrochemical pretreatment of polycrystalline gold electrodes to produce a reproducible surface roughness for self-assembly: A study in phosphate buffer pH 7.4, Anal. Chem. 72 (2000) 2016–2021.

[32] J. Wang, T. Peng, Enhanced stability of glassy carbon detectors following a simple electrochemical pretreatment, Anal. Chem. 58 (1986) 1787–1790.

[33] Q.L. Zhao, L. Bao, Q.Y. Luo, M. Zhang, Y. Lin, D.W. Pang, Z. L. Zhang, Surface manipulation for improving the sensitivity and selectivity of glassy carbon electrodes by electrochemical treatment, Biosens. Bioelectron. 24 (2009) 3003–3007.

[34] P.S. Feng, S.M. Wang, W.Y. Su, S.H. Cheng, Electrochemical oxidation and sensitive determination of pyrogallol at preanodized screen-printed carbon electrodes, J. Chinese Chem. Soc. 59 (2012) 231–238.

[35] S.M. Wang, W.Y. Su, S.H. Cheng, A simultaneous and sensitive determination of hydroquinone and catechol at anodically pretreated screen-printed carbon electrodes, Int. J. Electrochem. Sci. 5 (2010) 1649–1664.

[36] W.Y. Su, S.M. Wang, S.H. Cheng, Electrochemically pretreated screen-printed carbon electrodes for the simultaneous determination of aminophenol isomers, J. Electroanal. Chem. 651 (2011) 166–172.

[37] A.D. Arulraj, M. Vijayan, V.S. Vasantha, Highly selective and sensitive simple sensor based on electrochemically treated nano polypyrrole-sodium dodecyl sulphate film for the detection of para-nitrophenol, Anal. Chim. Acta. 899 (2015) 66–74.

[38] J. Zhao, G.Z. Hu, Z.S. Yang,, Y.Y. Zhou, Determination of 1- Naphthol with denatured DNA–modified pretreated glassy carbon electrode, Anal. Lett. 40 (2007) 459–470.

[39] R.F. Brocenschi, R.C. Rocha-Filho, S.R. Biaggio, N. Bocchi, DPV and SWV determination of estrone using a cathodically pretreated boron-doped diamond electrode, Electroanalysis. 26 (2014) 1588–1597.

[40] J. Zavázalová, H. Dejmková, J. Barek, K. Pecková, Voltammetric and amperometric determination of mixtures of aminobiphenyls and aminonaphthalenes using boron doped diamond electrode, Electroanalysis. 25 (2012) 253–262.

[41] E. Nurhayati, Y. Juang, M. Rajkumar, C. Huang, C.C. Hu, Effects of dynamic polarization on boron-doped NCD properties and on its performance for electrochemical-analysis of Pb (II), Cu (II) and Hg (II) in aqueous solution via direct LSV, Sep. Purif. Technol. 156 (2015) 1047–1056.

[42] P. Patnaik, Phenols, John Wiley & Sons, Inc, 2007.

[43] O. Gimeno, M. Carbajo, F.J. Beltrán, F.J. Rivas, Phenol and substituted phenols AOPs remediation, J. Hazard. Mater. 119 (2005) 99–108.

[44] W.E. Luttrell, Toxic tips: Phenol, Chem. Heal. Saf. 10 (2003) 20–21.

[45] C.D. Selassie, T. V. DeSoyza, M. Rosario, H. Gao, C. Hansch, Phenol toxicity in leukemia cells: a radical process, Chem. Biol. Interact. 113 (1998) 175–190.

[46] C.E. Paisio, P.S. González, A. Gerbaudo, M.L. Bertuzzi, E. Agostini, Toxicity of phenol solutions treated with rapeseed and tomato hairy roots, Desalination. 263 (2010) 23–28.

[47] United States Environmental Protection Agency, Phenol | Technology transfer network air toxics web site | US EPA, (n.d.).

[48] ATSDR, Toxicological Profile: Phenol, 2003.

[49] M. Chand Meena, R. Band, G. Sharma, Phenol and its toxicity: A case report, Iran. J. Toxicol. 8 (2015) 1222–1224.

[50] S. Gupta, G. Ashrith, D. Chandra, A.K. Gupta, K.W. Finkel, J.S. Guntupalli, Acute phenol poisoning: a life-threatening hazard of chronic pain relief., Clin. Toxicol. (Phila). 46 (2008) 250–253.

[51] S. Amlathe, V.K. Gupta, Spectrophotometric determination of phenol in air, Fresenius. J. Anal. Chem. 339 (1991) 199–200.

[52] W. Medjor, C. Wepuaka, S. Godwill, Spectrophotometric determination of phenol

in natural waters by trichloromethane extraction method after steam distillation, Int. Res. J. Pure Appl. Chem. 7 (2015) 150–156.

[53] S. Chakravarty, M.K. Deb, R.K. Mishra, Simple spectrophotometric determination of phenol in industrial waste water, Asian J. Chem. 6 (1994) 766–770.

[54] J.-J. Ye, W. Feng, M.-M. Tian, J.-L. Zhang, W.-H. Zhou, Q. Jia, Spectrophotometric determination of phenol by flow injection on-line preconcentration with a micro-column containing magnetic microspheres functionalized with cyanex, Anal. Methods. 5 (2013) 1046.

[55] O. Agrawal, V.K. Gupta, Sub-parts-per-million spectrophotometric determination of phenol and related pesticides using diazotizedp-aminoacetophenone, Microchem. J. 62 (1999) 147–153.

[56] J.P. Rawat, K.P.S. Muktawat, Sensitive, selective spectrophotometric determination of phenols with periodic acid, Microchem. J. 30 (1984) 289–296.

[57] Y.C. Fiamegos, C.D. Stalikas, G.A. Pilidis, M.I. Karayannis, Synthesis and analytical applications of 4-aminopyrazolone derivatives as chromogenic agents for the spectrophotometric determination of phenols, Anal. Chim. Acta. 403 (2000) 315–323.

[58] M. Nassiri, M.M. Zahedi, S.M. Pourmortazavi, M. Yousefzade, Optimization of dispersive liquid-liquid microextraction for preconcentration and spectrophotometric determination of phenols in Chabahar Bay seawater after derivatization with 4-aminoantipyrine., Mar. Pollut. Bull. 86 (2014) 512–7.

[59] R. Sun, Y. Wang, Y. Ni, S. Kokot, Spectrophotometric analysis of phenols, which involves a hemin-graphene hybrid nanoparticles with peroxidase-like activity., J. Hazard. Mater. 266 (2014) 60–7.

[60] N. Venugopal, A.V.B. Reddy, G. Madhavi, Development and validation of a systematic UPLC-MS/MS method for simultaneous determination of three phenol impurities in ritonavir., J. Pharm. Biomed. Anal. 90 (2014) 127–33.

[61] I. V. Gruzdev, I.M. Kuzivanov, I.G. Zenkevich, B.M. Kondratenok, Gas-chromatographic identification of products formed in iodination of methyl phenols by retention indices, Russ. J. Appl. Chem. 85 (2012) 1355–1365.

[62] M.T. Oliva-Teles, C. Delerue-Matos, H.P.A. Nouws, M.C.M. Alvim-Ferraz, Chromatographic techniques for the determination of free phenol in foundry resins, Anal. Lett. 44 (2011) 1536–1543.

[63] H. Gao, W. Cao, Y. Liang, N. Cheng, B. Wang, J. Zheng, Determination of thymol and phenol in honey by LC with electrochemical detection, Chromatographia. 72 (2010) 361–363.

[64] R. Sadeghi, H. Karimi-Maleh, M.A. Khalilzadeh, H. Beitollahi, Z. Ranjbarha, M.B.P. Zanousi, A new strategy for determination of hydroxylamine and phenol in water and waste water samples using modified nanosensor., Environ. Sci. Pollut. Res. Int. 20 (2013) 6584–93.

[65] H. Guan, X. Liu, W. Wang, Encapsulation of tyrosinase within liposome bioreactors for developing an amperometric phenolic compounds biosensor, J. Solid State Electrochem. 17 (2013) 2887–2893.

[66] J. Ren, T.F. Kang, R. Xue, C.N. Ge, S.Y. Cheng, Biosensor based on a glassy carbon electrode modified with tyrosinase immmobilized on multiwalled carbon nanotubes, Microchim. Acta. 174 (2011) 303–309.

[67] N. Negash, H. Alemu, M. Tessema, Determination of phenol and chlorophenols at single-wall carbon nanotubes / poly ( 3 , 4-ethylenedioxythiophene ) modified glassy carbon electrode using flow injection amperometry, Am. J. Anal. Chem. 5 (2014) 188–198.

[68] Z. Zhong, G. Li, R. Wu, B. Zhu, Z. Luo, Determination of aminophenols and phenol in hair colorants by ultrasound-assisted solid-phase dispersion extraction coupled with ion chromatography, J. Sep. Sci. 37 (2014) 2208–2214.

[69] N.N.M. Zain, N.K. Abu Bakar, S. Mohamad, N.M. Saleh, Optimization of a greener method for removal phenol species by cloud point extraction and spectrophotometry, Spectrochim. Acta - Part A Mol. Biomol. Spectrosc. 118 (2014) 1121–1128.

[70] X. Yang, J. Kirsch, J. Fergus, A. Simonian, Modeling analysis of electrode fouling during electrolysis of phenolic compounds, Electrochim. Acta. 94 (2013) 259–268.

[71] J. Wang, T. Martinez, D.R. Yaniv, L.D. McCormick, Scanning tunneling microscopic investigation of surface fouling of glassy carbon surfaces due to phenol oxidation, J. Electroanal. Chem. Interfacial Electrochem. 313 (1991) 129–140.

[72] T.A. Enache, A.M. Oliveira-Brett, Phenol and para-substituted phenols electrochemical oxidation pathways, J. Electroanal. Chem. 655 (2011) 9–16.

[73] A.N. Kawde, M. a. Morsy, N. Odewunmi, W. Mahfouz, From electrode surface fouling to sensitive electroanalytical determination of phenols, Electroanalysis. 25 (2013) 1547–1555.

[74] J. Iniesta, Electrochemical oxidation of phenol at boron-doped diamond electrode, Electrochim. Acta. 46 (2001) 3573–3578.

[75] A.-N. Kawde, M.A. Aziz, Porous copper-modified graphite pencil electrode for the amperometric detection of 4-nitrophenol, Electroanalysis. 26 (2014) 2484–

2490.

[76] L.J. Kepley, A.J. Bard, Ellipsometric, electrochemical, and elemental characterization of the surface phase produced on glassy carbon electrodes by electrochemical activation, Anal. Chem. 60 (1988) 1459–1467.

[77] T. Brousse, P.L. Taberna, O. Crosnier, R. Dugas, P. Guillemet, Y. Scudeller, Y. Zhou, F. Favier, D. Bélanger, P. Simon, , Long-term cycling behavior of asymmetric activated carbon/$MnO_2$ aqueous electrochemical supercapacitor, J. Power Sources. 173 (2007) 633–641.

[78] A. Yuan, Q. Zhang, A novel hybrid manganese dioxide/activated carbon supercapacitor using lithium hydroxide electrolyte, Electrochem. Commun. 8 (2006) 1173–1178.

[79] C. a. Elmets, S.K. Katiyar, H. Xu, H. Mukhtar, Host defense mechanisms in polyaromatic hydrocarbon carcinogenesis, Skin Pharmacol. Appl. Skin Physiol. 14 (2001) 386–392.

[80] R.G. Mahurin, R.L. Bernstein, Fluorocarbon-enhanced mutagenesis of polyaromatic hydrocarbons, Environ. Res. 45 (1988) 101–107.

[81] B.L. Allen-Hoffmann, J.G. Rheinwald, Polycyclic aromatic hydrocarbon mutagenesis of human epidermal keratinocytes in culture, Proc. Natl. Acad. Sci. U. S. A. 81 (1984) 7802–7806.

[82] T. Nielsen, H.E. Jørgensen, J.C. Larsen, M. Poulsen, City air pollution of polycyclic aromatic hydrocarbons and other mutagens: occurrence, sources and health effects, Sci. Total Environ. 189–190 (1996) 41–49.

[83] C. Leyval, P. Binet, Effect of polyaromatic hydrocarbons in soil on arbuscular mycorrhizal plants, J. Environ. Qual. 27 (1998) 402–407.

[84] G. Mastrangelo, E. Fadda, V. Marzia, Polycyclic Aromatic Hydrocarbons and Cancer in Man, Environ. Health Perspect. 104 (1996) 1166–1170.

[85] A. Tiehm, L. Mikrobiologie, U. Karlsruhe, D. Karlsruhe, Degradation of polycyclic aromatic degradation of polycyclic aromatic hydrocarbons in the presence of synthetic surfactants, Appl. Environ. Microbiol. 60 (1994) 258–263.

[86] F.J. Jongeneelen, Benchmark guideline for urinary 1-hydroxypyrene as biomarker of occupational exposure to polycyclic aromatic hydrocarbons, Ann. Occup. Hyg. 45 (2001) 3–13.

[87] C. Croera, D. Ferrario, L. Gribaldo, In vitro toxicity of naphthalene, 1-naphthol, 2-naphthol and 1,4-naphthoquinone on human CFU-GM from female and male cord blood donors, Toxicol. Vitr. 22 (2008) 1555–1561.

[88] T.M. Cho, R.L. Rose, E. Hodgson, In vitro metabolism of naphthalene by human liver microsomal cytochrome P450 enzymes, Drug Metab. Dispos. 34 (2006) 176–183.

[89] G. Bieniek, The presence of 1-naphthol in the urine of industrial workers exposed to naphthalene., Occup. Environ. Med. 51 (1994) 357–359.

[90] A.R. Buckpittb, S. Wilson, C.D. Davis, D.P. Williams, M. Pirmohamedb, B.K. Parkb, Characterisation of the toxic metabolite (s) of naphthalene, Toxicology. 114 (1996) 233–242.

[91] M. Schwenk, M. Locher, 1-Naphthol conjugation in isolated cells from liver, jejunum, ileum, colon and kidney of the guinea pig, Biochem. Pharmacol. 34 (1985) 697–701.

[92] R. V. Heyningen, A. Pirie, The metabolism of naphthalene and its toxic effect on the eye, Biochem. J. 102 (1967) 842–852.

[93] D.M. Rao, A.S. Murty, P.A. Swarup, Relative toxicity of technical grade and formulated carbaryl and 1-naphthol to, and carbaryl-induced biochemical changes in, the fish Cirrhinus mrigala, Environ. Pollution. Ser. A, Ecol. Biol. 34 (1984) 47–54.

[94] M. Kapuci, Z. Ulker, S. Gurkan, L. Alpsoy, Determination of cytotoxic and genotoxic effects of naphthalene, 1-naphthol and 2-naphthol on human lymphocyte culture, Toxicol. Ind. Health. 30 (2014) 82–89.

[95] D.R. Laurence, Clinical Toxicology of Commercial Products. Acute Poisoning, 4th edition, J. Clin. Pathol. 30 (1977) 193.

[96] K.A.F. O'Brien, L.L. Smith, G.M. Cohen, Differences in naphthalene-induced toxicity in the mouse and rat, Chem. Biol. Interact. 55 (1985) 109–122.

[97] S. Zhong, S.N. Tan, L. Ge, W. Wang, J. Chen, Determination of bisphenol A and naphthols in river water samples by capillary zone electrophoresis after cloud point extraction, Talanta. 85 (2011) 488–492.

[98] Y. Jidong, Simultaneous determination of α-naphthol and β-naphthol with resonance rayleigh scattering spectrometry, Chemistry (Easton). 7 (2008) 12.

[99] D. Amin, B.W. A., Spectrophotometric determination of α-naphthol, β-naphthol, and oxine in aqueous solution., Microchem. J. 33 (1986) 78–80.

[100] R. Andreoli, P. Manini, E. Bergamaschi, A. Mutti, I. Franchini, W.M.A. Niessen, Determination of naphthalene metabolites in human urine by liquid chromatography-mass spectrometry with electrospray ionization, J. Chromatogr. A. 847 (1999) 9–17.

[101] J. Hu, J. Yang, G. Zhou, W. Ma, Synchronous scanning fluorescence dual wavelength standard addition method for simultaneous determination of α-naphthol and β-naphthol, Fenxi Huaxue. 24 (1996) 1061.

[102] R.W. Frei, J.F. Lawrence, P.E. Belliveau, An in situ fluorimetric method for the determination of Sevin and α-naphthol on thin-layer chromatograms, Fresenius' Zeitschrift Für Anal. Chemie. 254 (1971) 271–274.

[103] T. Yasukawa, Y. Yoshimoto, T. Goto, F. Mizutani, Highly-sensitive electrochemical immunosensing method based on dual amplification systems, Biosens. Bioelectron. 37 (2012) 19–23.

[104] S. Amidi, F. Mojab, A. Bayandori, A simple electrochemical method for the rapid estimation of antioxidant potentials of some selected medicinal plants, Iran. J. Pharm. Res. 11 (2012) 117–121.

[105] J. Zhao, G.Z. Hu, Z.S. Yang, Y.Y. Zhou, Determination of 1- naphthol with denatured DNA-modified pretreated glassy carbon electrode, Anal. Lett. 40 (2007) 459–470.

[106] X. Huang, G. Zhao, M. Liu, F. Li, J. Qiao, S. Zhao, Highly sensitive electrochemical determination of 1-naphthol based on high-index facet $SnO_2$ modified electrode, Electrochim. Acta. 83 (2012) 478–484.

[107] Y. Zhang, H. Zhuang, Poly (acridine orange) film modified electrode for the determination 1-naphthol in the presence of 2-naphthol, Electrochim. Acta. 54 (2009) 7364–7369.

[108] G. Liang, X. Liu, X. Li, Highly sensitive detection of α-naphthol based on G-DNA modified gold electrode by electrochemical impedance spectroscopy., Biosens. Bioelectron. 45 (2013) 46–51.

[109] G. Zhu, P. Gai, Y. Yang, X. Zhang, J. Chen, Electrochemical sensor for naphthols based on gold nanoparticles/hollow nitrogen-doped carbon microsphere hybrids functionalized with SH-β-cyclodextrin, Anal. Chim. Acta. 723 (2012) 33–38.

[110] X.G. Wang, Q.S. Wu, Y.P. Ding, Direct simultaneous determination of α- and β-naphthol isomers at GC-electrode modified with CNTs network joined by pt nanoparticles through derivative voltammetry, Electroanalysis. 18 (2006) 517–520.

[111] G. Zhu, P. Gai, L. Wu, J. Zhang, X. Zhang, J. Chen, β-Cyclodextrin-platinum nanoparticles/graphene nanohybrids: enhanced sensitivity for electrochemical detection of naphthol isomers, Chem. - An Asian J. 7 (2012) 732–737.

[112] Y.L. Wei, C. Shao, H.F. Han, L.P. Zhang, C. Li, B.J. Liu, Voltammetric determination of α-naphthol and β-naphthol by a Nano-$TiO_2$/MWNTs composite film modified glassy carbon electrode., Adm. Tech. Environ. Monit. 4 (2009) 11.

[113] X.R. Li, S. Zhang, Electrochemical determination of 1-naphthol at a glassy carbon electrode modified with multiwall carbon nanotubes, J. Xianyang Norm. Univ. 6 (2009) 14.

[114] H.S. Wang, H.X. Ju, H.Y. Chen, Simultaneous determination of guanine and adenine in DNA using an electrochemically pretreated glassy carbon electrode, Anal. Chim. Acta. 461 (2002) 243–250.

[115] F. Li, J. Song, D. Gao, Q. Zhang, D. Han, L. Niu, Simple and rapid voltammetric determination of morphine at electrochemically pretreated glassy carbon electrodes, Talanta. 79 (2009) 845–850.

[116] E.D.P. Troiani, R.C. Faria, Cathodically pretreated poly(1-aminoanthraquinone)-modified electrode for determination of ascorbic acid, dopamine, and uric acid, J. Appl. Electrochem. 43 (2013) 919–926.

[117] W. Geremedhin, M. Amare, S. Admassie, Electrochemically pretreated glassy carbon electrode for electrochemical detection of fenitrothion in tap water and human urine, Electrochim. Acta. 87 (2013) 749–755.

[118] B.C. Lourencao, M. Baccarin, R. a. Medeiros, R.C. Rocha-Filho, O. Fatibello-Filho, Differential pulse voltammetric determination of albendazole in pharmaceutical tablets using a cathodically pretreated boron-doped diamond electrode, J. Electroanal. Chem. 707 (2013) 15–19.

[119] S.K. Samanta, O. V Singh, R.K. Jain, Polycyclic aromatic hydrocarbons: environmental pollution and bioremediation., Trends Biotechnol. 20 (2002) 243–248.

[120] J. Weuve, J.D. Yanosky, Polycyclic aromatic hydrocarbons, particulate air pollution, and cognitive decline-reply., Arch. Intern. Med. 172 (2012) 1045–1046.

[121] T. Rengarajan, P. Rajendran, N. Nandakumar, B. Lokeshkumar, P. Rajendran, I. Nishigaki, Exposure to polycyclic aromatic hydrocarbons with special focus on cancer, Asian Pac. J. Trop. Biomed. 5 (2015) 182–189.

[122] National Research Council (US), Polycyclic aromatic hydrocarbons from natural and stationary anthropogenic sources and their atmospheric concentrations, in: Polycycl. Aromat. Hydrocarb. Eval. Sources Eff., 1983: pp. 1–32.

[123] E. Elovaara, J. Mikkola, M. Mäkelä, B. Paldanius, E. Priha, Assessment of soil remediation workers' exposure to polycyclic aromatic hydrocarbons (PAH): Biomonitoring of naphthols, phenanthrols, and 1-hydroxypyrene in urine, Toxicol. Lett. 162 (2006) 158–163.

[124] K.-H. Kim, S.A. Jahan, E. Kabir, R.J.C. Brown, A review of airborne polycyclic aromatic hydrocarbons (PAHs) and their human health effects, Environ. Int. 60 (2013) 71–80.

[125] N. Zaitseva, S. Alekseev, V. Zaitsev, V. Raks, Solid-phase spectrophotometric analysis of 1-naphthol using silica functionalized with m-diazophenylarsonic acid, Nanoscale Res. Lett. 11 (2016) 149.

[126] R. Preuss, J. Angerer, Simultaneous determination of 1- and 2-naphthol in human urine using on-line clean-up column-switching liquid chromatography-fluorescence detection, J. Chromatogr. B Anal. Technol. Biomed. Life Sci. 801 (2004) 307–316.

[127] G. Jia, L. Li, J. Qiu, X. Wang, W. Zhu, Y. Sun, Z. Zhou, , Determination of carbaryl and its metabolite 1-naphthol in water samples by fluorescence spectrophotometer after anionic surfactant micelle-mediated extraction with sodium dodecylsulfate, Spectrochim. Acta Part A Mol. Biomol. Spectrosc. 67 (2007) 460–464.

[128] Y. Zhang, H. Zhuang, Poly (acridine orange) film modified electrode for the determination 1-naphthol in the presence of 2-naphthol, Electrochim. Acta. 54 (2009) 7364–7369.

[129] X. Zheng, S. Duan, S. Liu, M. Wei, F. Xia, D. Tian, C. Zhou, , Sensitive and simultaneous method for the determination of naphthol isomers by an amino-functionalized, SBA-15-modified carbon paste electrode, Anal. Methods. 7 (2015) 3063–3071.

[130] M.Y. Abdelaal, Electrochemical polymerization of naphthols in aqueous medium, Int. J. Polym. Mater. 54 (2005) 151–159.

[131] M.H. Mashhadizadeh, T. Yousefi, A. Nozad Golikand, A nickel hexacyanoferrate and poly(1-naphthol) hybrid film modified electrode used in the selective electroanalysis of dopamine, Electrochim. Acta. 59 (2012) 321–328.

[132] M. Pharn, J. Moslih, P.-C. Lacaze, New conducting films by electrochemical oxidation of In-situ MIRFIYIRS study of the electropolymerization mechanism, J. Electroanal. Chem. Interfacial Electrochem. 278 (1990) 415–423.

[133] A. Rana, A.-N. Kawde, Open-circuit electrochemical polymerization for the sensitive detection of phenols, Electroanalysis. 28 (2016) 898–902.

[134] A. Özcan, Y. Şahin, Preparation of selective and sensitive electrochemically treated pencil graphite electrodes for the determination of uric acid in urine and blood serum, Biosens. Bioelectron. 25 (2010) 2497–2502.

[135] A. Özcan, Y. Şahin, Selective and sensitive voltammetric determination of dopamine in blood by electrochemically treated pencil graphite electrodes, Electroanalysis. 21 (2009) 2363–2370.

[136] N. Baig, A.-N. Kawde, A novel, fast and cost effective graphene-modified graphite pencil electrode for trace quantification of l -tyrosine, Anal. Methods. 7

(2015) 9535–9541.

[137] A. Özcan, Synergistic effect of lithium perchlorate and sodium hydroxide in the preparation of electrochemically treated pencil graphite electrodes for selective and sensitive Bisphenol A detection in water samples, Electroanalysis. 26 (2014) 1631–1639.

[138] K.T. Benlahcen, A. Chaoui, H. Budzinski, J. Bellocq, P. Garrigues, Distribution and sources of polycyclic aromatic hydrocarbons in some Mediterranean coastal sediments, Mar. Pollut. Bull. 34 (1997) 298–305.

[139] S.O. Baek, R.A. Field, M.E. Goldstone, P.W. Kirk, J.N. Lester, R. Perry, A review of atmospheric polycyclic aromatic hydrocarbons: Sources, fate and behavior, Water. Air. Soil Pollut. 60 (1991) 279–300.

[140] U. Förstner, G. Müller, Concentrations of heavy metals and polycyclic aromatic hydrocarbons in river sediments: geochemical background, man's influence and environmental impact, GeoJournal. 5 (1981) 417–432.

[141] K. Srogi, Monitoring of environmental exposure to polycyclic aromatic hydrocarbons: a review, Environ. Chem. Lett. 5 (2007) 169–195.

[142] J. Dejmek, I. Solanský, I. Benes, J. Lenícek, R.J. Srám, The impact of polycyclic aromatic hydrocarbons and fine particles on pregnancy outcome., Environ. Health Perspect. 108 (2000) 1159–1164.

[143] B.J. Finlayson-Pitts, Tropospheric air pollution: Ozone, airborne toxics, polycyclic aromatic hydrocarbons, and particles, Science 276 (1997) 1045–1051.

[144] I.C.T. Nisbet, P.K. LaGoy, Toxic equivalency factors (TEFs) for polycyclic aromatic hydrocarbons (PAHs), Regul. Toxicol. Pharmacol. 16 (1992) 290–300.

[145] P.J. Tsai, H.Y. Shieh, W.J. Lee, S.O. Lai, Health-risk assessment for workers exposed to polycyclic aromatic hydrocarbons (PAHs) in a carbon black manufacturing industry., Sci. Total Environ. 278 (2001) 137–150.

[146] S.C. Chen, C.M. Liao, Health risk assessment on human exposed to environmental polycyclic aromatic hydrocarbons pollution sources., Sci. Total Environ. 366 (2006) 112–123.

[147] Y. V Pashin, L.M. Bakhitova, Mutagenic and carcinogenic properties of polycyclic aromatic hydrocarbons., Environ. Health Perspect. 30 (1979) 185–189.

[148] L.K. Siddens, A. Larkin, S.K. Krueger, C.A. Bradfield, K.M. Waters, S.C. Tilton, C.B. Pereira, C.V. Löhr, V.M. Arlt, D.H. Phillips, D.E. Williams, W.M. Baird, , Polycyclic aromatic hydrocarbons as skin carcinogens: comparison of benzo[a]pyrene, dibenzo[def,p]chrysene and three environmental mixtures in the FVB/N mouse., Toxicol. Appl. Pharmacol. 264 (2012) 377–386.

[149] Y.B. Man, K.L. Chow, Y. Kang, M.H. Wong, Mutagenicity and genotoxicity of Hong Kong soils contaminated by polycyclic aromatic hydrocarbons and dioxins/furans, Mutat. Res. Toxicol. Environ. Mutagen. 752 (2013) 47–56.

[150] L. Hou, Y. Cui, M. Xu, Z. Gao, J. Huang, D. Tang, Graphene oxide-labeled sandwich-type impedimetric immunoassay with sensitive enhancement based on enzymatic 4-chloro-1-naphthol oxidation., Biosens. Bioelectron. 47 (2013) 149–156.

[151] T. Juřík, P. Skládal, Detection of hydrogen peroxide and glucose by enzyme product precipitation on sensor surface, Chem. Pap. 69 (2015) 167–175.

[152] OSHA, Safety Data Sheet, 4-Chloro-1-naphthol, 2008.

[153] S.C. Biotechnology, 4-Chloro-1-naphthol, 2006.

[154] F. Scientific, 4-chloro-1-naphthol, 2015.

[155] G. Hanrahan, D.G. Patil, J. Wang, Electrochemical sensors for environmental monitoring: design, development and applications., J. Environ. Monit. 6 (2004) 657–664.

[156] X. Yang, J. Kirsch, J. Fergus, A. Simonian, Modeling analysis of electrode fouling during electrolysis of phenolic compounds, Electrochim. Acta. 94 (2013) 259–268.

[157] T. Nagaoka, T. Yoshino, Surface properties of electrochemically pretreated glassy carbon, Anal. Chem. 58 (1986) 1037–1042.

[158] C. Yang, Electrochemical determination of 4-nitrophenol using a single-wall carbon nanotube film-coated glassy carbon electrode, Microchim. Acta. 148 (2004) 87–92.

[159] J. Michałowicz, W. Duda, Phenols - sources and toxicity, Polish J. Environ. Stud. 16 (2007) 347–362.

[160] Y. Tang, R. Huang, C. Liu, S. Yang, Z. Lu, S. Luo, Electrochemical detection of 4-nitrophenol based on a glassy carbon electrode modified with a reduced graphene oxide/Au nanoparticle composite, Anal. Methods. 5 (2013) 5508–5524.

[161] U.S.P. health Agency for toxic substances and disease service, ATSDR - Toxicological profile: nitrophenols, 1992.

[162] B. Schultz, Determination of 4-aminophenol in water by high-performance liquid chromatography with fluorescence detection., J. Chromatogr. 299 (1984) 484–6.

[163] D. Jahr, Determination of alkyl, chloro and mononitrophenols in water by sample-acetylation and automatic on-line solid phase extraction-gas chromatography-

mass spectrometry, Chromatographia. 47 (1998) 49–56.

[164] A. Niazi, A. Yazdanipour, Spectrophotometric simultaneous determination of nitrophenol isomers by orthogonal signal correction and partial least squares., J. Hazard. Mater. 146 (2007) 421–427.

[165] C. Nistor, A. Oubiña, M.-P. Marco, D. Barceló, J. Emnéus, Competitive flow immunoassay with fluorescence detection for determination of 4-nitrophenol, Anal. Chim. Acta. 426 (2001) 185–195.

[166] X. Yang, J. Wang, D. Su, Q. Xia, F. Chai, C. Wang, F. Qu, , Fluorescent detection of TNT and 4-nitrophenol by BSA Au nanoclusters., Dalton Trans. 43 (2014) 10057–63.

[167] J. Fischer, J. Barek, J. Wang, Separation and detection of nitrophenols at capillary electrophoresis microchips with amperometric detection, Electroanalysis. 18 (2006) 195–199.

[168] P. Kuban, M. Berg, C. García, B. Karlberg, On-line flow sample stacking in a flow injection analysis-capillary electrophoresis system: 2000-fold enhancement of detection sensitivity for priority phenol pollutants., J. Chromatogr. A. 912 (2001) 163–70.

[169] S.J. Gluck, M.H. Benkö, R.K. Hallberg, K.P. Steele, Indirect determination of octanol-water partition coefficients by microemulsion electrokinetic chromatography, J. Chromatogr. A. 744 (1996) 141–146.

[170] J. Li, D. Kuang, Y. Feng, F. Zhang, Z. Xu, M. Liu, A graphene oxide-based electrochemical sensor for sensitive determination of 4-nitrophenol., J. Hazard. Mater. 202 (2012) 250–259.

[171] Z. Liu, J. Du, C. Qiu, L. Huang, H. Ma, D. Shen, Y. Ding, Electrochemical sensor for detection of p-nitrophenol based on nanoporous gold, Electrochem. Commun. 11 (2009) 1365–1368.

[172] N.I. Ikhsan, P. Rameshkumar, N.M. Huang, Controlled synthesis of reduced graphene oxide supported silver nanoparticles for selective and sensitive electrochemical detection of 4-nitrophenol, Electrochim. Acta. 192 (2016) 392–399.

[173] S. Lupu, C. Lete, M. Marin, N. Totir, P.C. Balaure, Electrochemical sensors based on platinum electrodes modified with hybrid inorganic–organic coatings for determination of 4-nitrophenol and dopamine, Electrochim. Acta. 54 (2009) 1932–1938.

[174] E.A. Hutton, B. Ogorevc, M.R. Smyth, Cathodic electrochemical detection of nitrophenols at a bismuth film electrode for use in flow analysis, Electroanalysis. 16 (2004) 1616–1621.

[175] Y. Zeng, Y. Zhou, T. Zhou, G. Shi, A novel composite of reduced graphene oxide and molecularly imprinted polymer for electrochemical sensing 4-nitrophenol, Electrochim. Acta. 130 (2014) 504–511.

[176] W. Huang, C. Yang, S. Zhang, Simultaneous determination of 2-nitrophenol and 4-nitrophenol based on the multi-wall carbon nanotubes Nafion-modified electrode., Anal. Bioanal. Chem. 375 (2003) 703–7.

[177] L. Chu, L. Han, X. Zhang, Electrochemical simultaneous determination of nitrophenol isomers at nano-gold modified glassy carbon electrode, J. Appl. Electrochem. 41 (2011) 687–694.

[178] F.O.G. Olorundare, D. Nkosi, O.A. Arotiba, Voltammetric determination of nitrophenols at a nickel dimethylglyoxime complex - gold nanoparticle modified glassy carbon electrode, Int. J. Electrochem. Sci. 11 (2016) 7318–7332.

[179] Y. Tang, R. Huang, C. Liu, S. Yang, Z. Lu, S. Luo, Electrochemical detection of 4-nitrophenol based on a glassy carbon electrode modified with a reduced graphene oxide/Au nanoparticle composite, Anal. Methods. 5 (2013) 5508.

[180] Y.Y. Tang, P.Y. Chen, Gold nanoparticle-electrodeposited electrodes used for p-nitrophenol detection in acidic media: effect of electrodeposition parameters on particle density, size distribution, and electrode performance, J. Chinese Chem. Soc. 58 (2011) 723–731.

[181] J. Li, X. Lin, Electrocatalytic oxidation of hydrazine and hydroxylamine at gold nanoparticle-polypyrrole nanowire modified glassy carbon electrode, Sensors Actuators, B Chem. 126 (2007) 527–535.

[182] L. Agüí, C. Peña-Farfal, P. Yáñez-Sedeño, J.M. Pingarrón, Electrochemical determination of homocysteine at a gold nanoparticle-modified electrode, Talanta. 74 (2007) 412–420.

[183] X. Ma, M. Chen, Electrochemical sensor based on graphene doped gold nanoparticles modified electrode for detection of diethylstilboestrol, Sensors Actuators, B Chem. 215 (2015) 445–450.

[184] Y.H. Huang, J.H. Chen, L.J. Ling, Z.B. Su, X. Sun, S.R. Hu, W. Weng, Y. Huang, W.B. Wu, Y.S. He, , Simultaneous electrochemical detection of catechol and hydroquinone based on gold nanoparticles@carbon nanocages modified electrode, Analyst. 140 (2015) 7939–7947.

[185] M. Abdul Aziz, A.N. Kawde, Gold nanoparticle-modified graphite pencil electrode for the high-sensitivity detection of hydrazine., Talanta. 115 (2013) 214–21.

[186] S. Kumar, S. Zou, Electrooxidation of carbon monoxide on gold nanoparticle ensemble electrodes: Effects of particle coverage, J. Phys. Chem. B. 109 (2005)

15707–15713.

[187] J. Kimling, M. Maier, B. Okenve, V. Kotaidis, H. Ballot, A. Plech, Turkevich method for gold nanoparticle synthesis revisited, J. Phys. Chem. B. 110 (2006) 15700–15707.

# Vitae


| | |
|---|---|
| Name: | Muhammad Azeem Akbar Rana |
| Nationality: | Pakistani |
| Date of Birth: | 3/23/1987 |
| Email: | azeem_goldenedge@yahoo.com |
| Current Address: | Department of Chemistry, King Fahd University of Petroleum & Minerals, Dhahran 31261, Saudi Arabia |
| Permanent Address: | House No. 3, Street No.2 Hameed Town opposite Peoples colony, Ferozwala, Sheikhupura 39350, Pakistan. |
| Academic Background: | Ph.D., King Fahd University for Petroleum & Minerals, Dhahran, Saudi Arabia. December 2017<br>M.Phil., University of Engineering and Technology, Lahore Pakistan. 2011<br>B.S.(Hons.) Institute of Chemistry, University of the Punjab, Lahore Pakistan. 2008 |

Published Work: Open-circuit electrochemical polymerization for the sensitive detection of phenols. (Electroanalysis: I.F. 2.851)

Novel electrochemically treated graphite pencil electrode surfaces for the determination of trace α-naphthol in water samples. (Journal of the Chinese Chemical Society: I.F. 0.935)